Contribution to the understanding of fresh and hardened state properties of low cement concrete

Mayra Tagliaferri de Grazia

A thesis submitted to the Faculty of Graduate and Postdoctoral Studies in partial fulfillment of the requirements for the degree of

MASTER OF APPLIED SCIENCE

in Civil Engineering

Department of Civil Engineering

Faculty of Engineering

University of Ottawa

Abstract

Concrete, the major construction material used in the civil industry worldwide, displays remarkable performance and economic benefits. Yet, it also presents a huge environmental impact producing about 7% of the global carbon dioxide (CO_2). Given the rise of global warming concerns, studies have been focusing on alternatives to reduce the amount of Portland cement (PC), which is the least sustainable ingredient of the mixture, for example by adopting particle packing model (PPM) techniques. Although a promising alternative, there is currently a lack of studies regarding the efficiently use of PPMs to reduce PC without compromising the fresh and hardened properties of the material. This work appraises the influence of PPMs and advanced mix-design techniques on the fresh (rheological behaviour) and hardened (compressive strength, modulus of elasticity, porosity, and permeability) state behaviours of systems with reduced amount of PC, the so-called low cement content (LCC) concrete. Results show that is possible to produce eco-efficient concrete maintaining and/or enhancing fresh and hardened properties of the material. Nevertheless, further durability and long-term behaviour must be performed on LCC systems.

Keywords: Low cement content; eco-efficient concrete; particle packing models; *Maximum Paste Thickness*; *Interparticle Separation Distance*; porosity; binder intensity; rheological model.

Acknowledgements

First of all, I am thankful for the opportunity God provided me with to fulfill my dream and conclude a Master of Applied Science in Civil Engineering at University of Ottawa.

I would like to acknowledge and express my deepest gratitude to my supervisor Dr. Leandro Sanchez, who helped and guided me not only throughout this research but also when teaching me how to become a researcher. Moreover, Dr. Sanchez has also become a friend who believed in my potential and with his effort and availability, he showed me that it is always possible to work smarter along with good mood despite being full of duties when we are doing what we love.

The support of my parents, Adalberto and Silvia, and my sister Thays, for their assistance at all times and being my base even far from home. To my father for making me be passionate about engineering, for teaching me how to become a hard worker and for supporting me to pursue my dreams regardless of distance. My mother for her support before final exams and my emotional base. My sister for being a great example, in which I followed most of her steps and all the advice.

My deepest thanks to my fiancee Gustavo Adami who helped me since the day one until the submission of this thesis. For all supporting, reviewing, and practicing presentations 24-7.

I would like to thank the financial support from the University of Ottawa for the international experience scholarship and Mitacs for the Mitacs Globalink Research Award. The opportunity to have an international experience at University of Sao Paulo in Brazil where I was able to work with amazing undergraduate and master students. In addition, I worked under the remarkable supervision of Dr. Cesar Romano and Dr. Pileggi, who has a significant amount of papers, a book, and a research group focused on packing models and characterization of concrete that will enhance my international experience.

The efforts of my colleagues and friends Diego Souza who always give me outstanding advice as a researcher and Marcelo Almeida who is always available to share his knowledge.

I would like to acknowledge the lab technician at University of Ottawa, Muslim Majeed and Gamal Elnabelsy, for teaching me the daily tasks. Additionally, Andre Demers from CANMET for his availability and passion for helping and teaching how to use the equipment.

Last but not least, I would like to extremely thank Natural Sciences and Engineering Research Council of Canada (NSERC) for the funding they provided for this research project and my dream.

Table of Contents

List of Figures

List of Tables

List of Symbols/Abbreviations

ΔP	Pressure Variation
μ	Fluid Viscosity
ACI	American Concrete Institute
a_i	Apparent Volume of the i^{th} Size Particle in a Monodisperse System
AP	Apparent Porosity
AV	Apparent Viscosity
BC	Binder Content
bi	Binder Intensity
c	Coarse
C_2S	Dicalcium Silicate
C_3A	Tricalcium Aluminate
$CaCO_3$	Limestone
CaO	Lime
CO_2	Carbon Dioxide
CPFT	Cumulative (Volume) Percent Finer Than D_p
C-S-H	Calcium Silicate Hydrate
D_L	Larger Particle Diameter
D_{max}	Maximum Aggregate Size
D_{min}	Minimum Aggregate Size
D_P	Particle Diameter
D_S	Smallest Particle Diameter
f	Fines
f'_c	Concrete Compressive Strength
f_r	Relationship between Compressive Strength and Cement Content
g	Aggregate Volume in a Unit Volume of Concrete
g*	Packing Density of the Aggregate
H_2O	Water Vapour
HA	Hysteresis Area
He	Helium Gas
HRWRA	High-Range Water-Reducing Admixtures
IF	Inert Fillers
IPS	*Interparticle Spacing*
k_1	Darcian Permeability Constant
K_1, K_2, K_3, K_4, K_5, K_6	Empirical Constants

k_2	non-Darcian Permeability Constant
k_B	Viscosity Constant of Bingham
k_{HB}	Viscosity Constant of Herschel-Bulkley
L	Specimen Thickness
LCC	Low Cement Content
m	Aggregate to Cement Ratio
MCO	Mortar Content Optimization
m_d	Dry Mass
m_i	Immersed Mass
MPT	*Maximum Paste Thickness*
MPT_{coarse}	Maximum Distance between the Coarse Aggregates
m_w	Wet Mass
n	Number of Particle Sizes
n	Flow Behaviour Factor
N_2	Nitrogen Gas
NMS	Nominal Maximum Size
$Ø_p$	Packing Density
$Ø_{p1}$	Packing Density of Large Particles
$Ø_{p2}$	Packing Density of Small Particles
P	Performance Requirement
PC	Portland Cement
PF	Packing Factor
P_{of}	Pore Fraction
P_{ofc}	Pore of Aggregate Fraction Assuming the Densest Packing
PPMs	Particle Packing Models
PSD	Particle Size Distribution
PUNDIT	Portable Ultrasound Non-Destructive Digital Indicating Tester
q	Distribution Coefficient
SCC	Self-Consolidating Concrete
SCMs	Supplementary Cementitious Materials
SSA	Specific Surface Area
TP	Total Porosity
UPV	Ultrasonic Pulse Velocity
V_1	Fraction of Small Particles Solid Volume
V_2	Fraction of Large Particles Solid Volume
V_a	Apparent Volume

V_{ai}	Apparent Volume of the Mixture with n Particle Sizes
v_s	Speed of Air-Percolation
Vs	Volume Fraction Solids
VSA	Volume Surface Area
VSA_c	Calculated Volume Surface Area of Aggregate Fraction
V_{sc}	Volumetric Aggregate Solid Fraction
V_{solid}	Solid Volume
V_{total}	Total Volume (Solids and Pores)
w/c	Water to Cement Ratio
w/f	Water to Fines Ratio
x_i	Mass Fraction of i^{th} Size Particle
γ	Rotation
ρ	Fluid Density
ρ_{rel}	Relative Density
τ	Torque
τ_o	Yield Torque
ρ_{part}	Particle Density

Chapter Two: Chapter One: Introduction

1.1. Portland Cement Production

Concrete is used in a variety of construction projects worldwide, from sidewalks and curvets to skyscrapers and bridges. Although other materials can be also selected in the construction industry (e.g. steel, timber, etc.), concrete remains the cheapest, most durable and common one. Yet, important concerns have risen in the technical society over the past decades regarding concrete's carbon footprint.

Concrete production is responsible for roughly 7% of global carbon dioxide (CO_2) emissions, wherein Portland cement (PC; the main concrete component) production accounts for almost 6.5% of the annual CO_2 emission (Limbachiya, Bostanci and Kew, 2014). Studies have shown that a ton of PC produces approximately one ton of CO_2 (Naik *et al.*, 1996; Hasanbeigi, Price and Lin, 2012; Gonçalves and Margarido, 2015). Moreover, the amount of CO_2 emitted during PC production depends on the ratio between clinker and PC, which is responsible for more than 50% of the total CO_2 released. A ton of clinker is responsible for releasing approximately 540 kilograms of CO_2 during the calcination[1] process, where limestone ($CaCO_3$) is transformed into lime (CaO), as described in the following chemical reaction (Hasanbeigi, Price and Lin, 2012).

$$CaCO_3 \xrightarrow{\Delta} CaO + CO_2$$

[1] Calcination is an English word derivated from the Latin word *calcinare* that means to burn lime. It is a thermal treatment process in which causes decomposition of carbonates and other compounds.

The thermal energy needed for the calcination process is responsible for the other 50% of CO_2 emissions during PC production. In order to achieve the required temperature (1400-1500 °C), fuel is burned in the kilns allowing calcination.

In 2012 and 2016, the global cement industry produced around 3.8 and 4.2 billion tons of PC, respectively (Statista, 2017a). The top ten PC producers are China, India, United States, Turkey, Vietnam, Brazil, Iran, Russia, Indonesia, and South Korea (Statista, 2017b, 2017a; Statistics Canada, 2017). Table 1.1 displays the cement production from 2012 to 2016 in the top ten countries, Canada, and worldwide. In Canada, PC production is steady and represents less than 0.5% of the total production over the last five years. China is the country that most produces PC, releasing more than 55% of the CO_2 globally emitted between 2012 and 2016.

Table 1.1. Cement production in million metric tons worldwide[2].

Year	China	India	United States	Turkey	Vietnam	Brazil
2012	2210.0	270.0	74.9	63.9	60.0	68.8
2013	2420.0	280.0	77.4	71.3	58.0	70.0
2014	2480.0	260.0	83.2	75.0	60.5	72.0
2015	2350.0	270.0	84.3	77.0	61.0	72.0
2016	2410.0	290.0	85.9	77.0	70.0	60.0
Year	**Iran**	**Russia**	**Indonesia**	**South Korea**	**Canada[3]**	**World[4]**
2012	70.0	61.5	32.0	48.0	12.5	3800.0
2013	72.0	66.4	56.0	47.3	11.6	4080.0
2014	65.0	68.4	65.0	63.2	11.9	4180.0
2015	65.0	69.0	65.0	63.0	12.2	4100.0
2016	53.0	56.0	63.0	55.0	11.9	4200.0

It is clear that PC production is higher in developing countries. Furthermore, Figure 1.1 highlights that the largest global cement producers are also major global CO_2 emitters (Statista, 2017b, 2018a).

[2] Information from (Statista, 2017b)

[3] Canada information from S A A M Fennis and J. C. Walraven, 'Using Particle Packing Technology for Sustainable Concrete Mixture Design', Heron, 57.2 (2012), 73–101.

[4] World information from (Statista, 2018b)

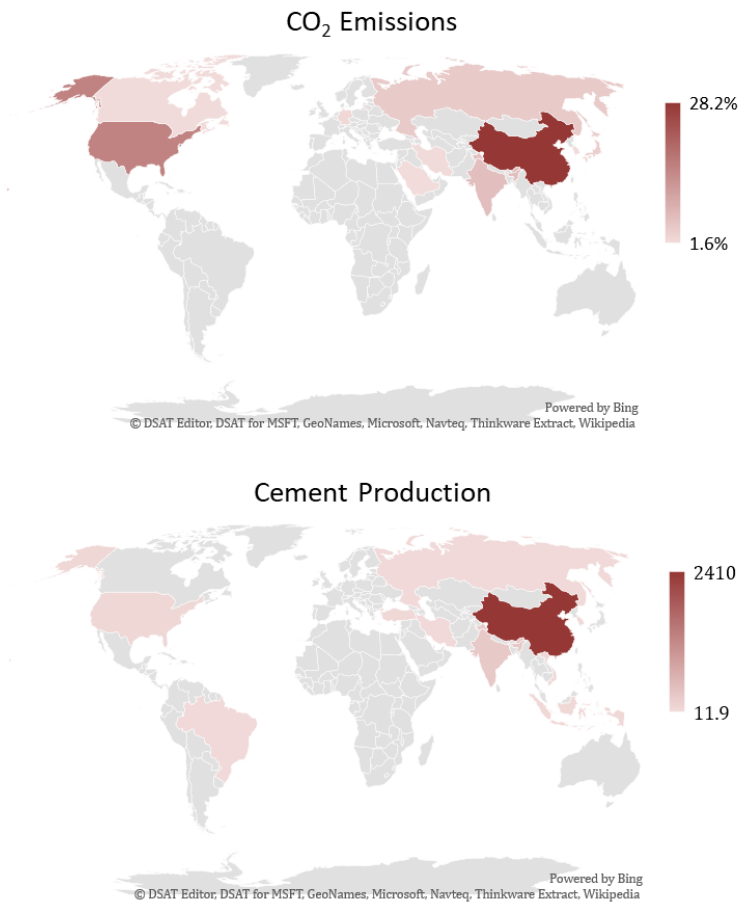

Figure 1.1 Map of global share of CO_2 emissions and cement production in million metric tons from the top 10 producers in 2016.

Although PC production presents considerable environmental impacts, it also comprises an economic concern since it is the most expensive component in concrete. As a result, recent studies have been focusing on three main approaches to reduce the carbon footprint of concrete: the first approach consists of reducing PC content by using supplementary cementitious materials (SCMs) and/or inert fillers (IF) as a partial replacement; the second one addresses more efficient technologies to produce PC releasing less CO_2; whereas the last approach is optimizing PC efficiency in concrete mixtures through the use of advanced mix-design techniques (e.g. particle packing models - PPMs) (Noël, Sanchez and Fathifazl, 2016). SCMs are considered outstanding PC replacements since they often improve concrete performance, durability, and sustainability; however, their availability does not increase at the same rate as PC demand. Conversely, studies shows that IF can be used as a partial PC

replacement and/or as an addition to PC resulting in benefits to concrete mechanical properties, besides reducing its environmental impact (Damineli *et al.*, 2016; Knop and Peled, 2016b, 2016a; Varhen *et al.*, 2016; Shadkam *et al.*, 2017). The second technique, while important, cannot match the rapid annual growth of cement demand (Zachar and Asce, 2011; Juenger and Siddique, 2015). The third approach has been shown to reduce effectively (by more than 50%) PC content in concrete mixtures (Fennis and Walraven, 2012). However, there is currently a lack of studies regarding the best way to implement PPMs to design concrete mixtures with reduced amount of PC, along with a lack of understanding on how they may affect the fresh (e.g. rheology) and hardened properties of concrete.

1.2. Research Objectives

The main objective of this research project is to evaluate two distinct advanced techniques to mix-design concrete mixtures (i.e. PPMs and mobility parameters) and evaluate their influence on the fresh and hardened state properties of mixes with reduced amount of PC, the so-called low cement content (LCC) concrete. It is worth noting that the concrete mixtures researched over this Thesis are considered for structural applications and thus minimum mechanical properties and durability-related criteria are imperative.

In this research program, different types of low cement content (LCC) concrete were mix-proportioned and evaluated through rheometry, physical (i.e. permeability and porosity) and mechanical testing (i.e. compressive strength and modulus of elasticity). Comparison amongst the different techniques used and results obtained are then performed and considerations for future research in the area are proposed.

1.3. Thesis Organization

This thesis is divided into five chapters. Chapter 1 shows the concerns related to concrete's carbon footprint, discussed throughout the Introduction. Moreover, Chapter 1 consists of the following items: introduction, research objectives, and thesis organization.

Chapter 2 presents a detailed literature review on the use of LCC concrete as a new eco-efficient alternative for the construction industry. This section discusses on the following topics: mix-design methods, PPMs, binder efficiency, particle and particle's distance effects, limestone fillers effect and the influence of PPMs on the fresh, hardened and durability related properties of concrete designed through PPMs.

Chapter 3 consists of a journal paper which evaluates the effect of Alfred model with two different approaches on the fresh and hardened properties of concrete.

Chapter 4 is based on a journal paper which focuses on the effect of two mobility parameters (*Interparticle Spacing* and *Maximum Paste Thickness*) the fresh and hardened properties of concrete.

Chapter 5 brings forward the conclusion obtained throughout this project and proposes suggestions for future research in the area.

1.4. References

Damineli, B. L. et al. (2016) 'Viscosity prediction of cement-filler suspensions using interference model: A route for binder efficiency enhancement', Cement and Concrete Research, 84, pp. 8–19.

Fennis, S. A. A. M. and Walraven, J. C. (2012) 'Using particle packing technology for sustainable concrete mixture design', Heron, 57(2), pp. 73–101.

Gonçalves, M. C. and Margarido, F. (2015) Materials for Construction And Civil Engineering : Science, Processing, And Design. Springer International Publishing.

Hasanbeigi, A., Price, L. and Lin, E. (2012) 'Emerging Energy-Efficiency and CO2 Emission-Reduction Technologies for Cement and Concrete Production: A Technical Review', Renewable and Sustainable Energy Reviews. Elsevier, 16(8), pp. 6220–6238.

Juenger, M. C. G. and Siddique, R. (2015) 'Recent advances in understanding the role of supplementary cementitious materials in concrete', Cement and Concrete Research, 78, pp. 71–80.

Knop, Y. and Peled, A. (2016a) 'Packing density modeling of blended cement with limestone having different particle sizes', Construction and Building Materials. Elsevier Ltd, 102, pp. 44–50.

Knop, Y. and Peled, A. (2016b) 'Setting behavior of blended cement with limestone: influence of particle size and content', Materials and Structures, 49, pp. 439–452.

Limbachiya, M., Bostanci, S. C. and Kew, H. (2014) 'Suitability of BS EN 197-1 CEM II and CEM V cement for production of low carbon concrete', Construction and Building Materials, 71, pp. 397–405.

Naik, T. R. et al. (1996) 'Permeability of high-strength concrete containing low cement factor', Journal of Energy Engineering, 122(1), pp. 21–39.

Noël, M., Sanchez, L. and Fathifazl, G. (2016) 'Recent Advances in Sustainable Concrete for Structural Applications', in Sustainable Construction Materials & Technologies 4, p. 10.

Shadkam, H. R. et al. (2017) 'An investigation of the effects of limestone powder and Viscosity Modifying Agent in durability related parameters of self-consolidating concrete (SCC)'.

Statista (2017a) Cement production globally and in the U.S. from 2010 to 2017 (in million metric tons). Available at: https://www.statista.com/statistics/219343/cement-production-worldwide/ (Accessed: 28 March 2018).

Statista (2017b) Major Countries in Worldwide Cement Production from 2011 to 2017. Available at: https://www.statista.com/statistics/267364/world-cement-production-by-country/ (Accessed: 28 March 2018).

Statista (2018a) Largest producers of CO2 emissions worldwide in 2016, based on their share of global CO2 emissions. Available at: https://www.statista.com/statistics/271748/the-largest-emitters-of-co2-in-the-world/ (Accessed: 8 March 2018).

Statista (2018b) U.S. and world cement production 2017, Statista. Available at: https://www.statista.com/statistics/219343/cement-production-worldwide/ (Accessed: 2 May 2018).

Statistics Canada (2017) Production of Building Materials (Cement). Available at: http://www.statcan.gc.ca/tables-tableaux/sum-som/l01/cst01/manuf31c-eng.htm (Accessed: 15 June 2017).

Varhen, C. et al. (2016) 'Effect of the substitution of cement by limestone filler on the rheological behaviour and shrinkage of microconcretes', Construction and Building Materials, 125, pp. 375–386.

Chapter Two: Background and Literature Review

2.1. Design Methods

In order to achieve a more eco-efficient concrete by reducing the amount of PC, a proper mix-design technique should be selected. However, only reducing PC in concrete is not enough. A proper mix-design approach must proportion a mixture with suitable fresh and hardened state properties, as shown in Figure 2.1. In terms of fresh properties, flowability is the main feature to be evaluated. Yet, concrete compressive strength, modulus of elasticity and durability-related characteristics should also be investigated in order to appraise the hardened state properties of the material.

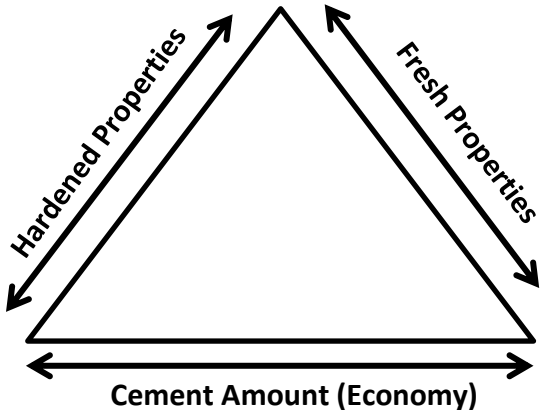

Figure 2.1. Qualitative triangle for a proper mix-design.

2.1.1. American Concrete Institute (ACI) Method

The ACI method is the most common concrete mix-design method used in North America. Although it is an easy technique, the method is governed by the slump and water to cement ration selection according to the construction application and durability aspects, as illustrated in Figure 2.2. The exposure condition is also an important factor which must be

considered in this design process. However, this approach often results in non-eco-friendly mixtures with moderate to high amounts of PC (e.g. 350 to 450 kg/m^3).

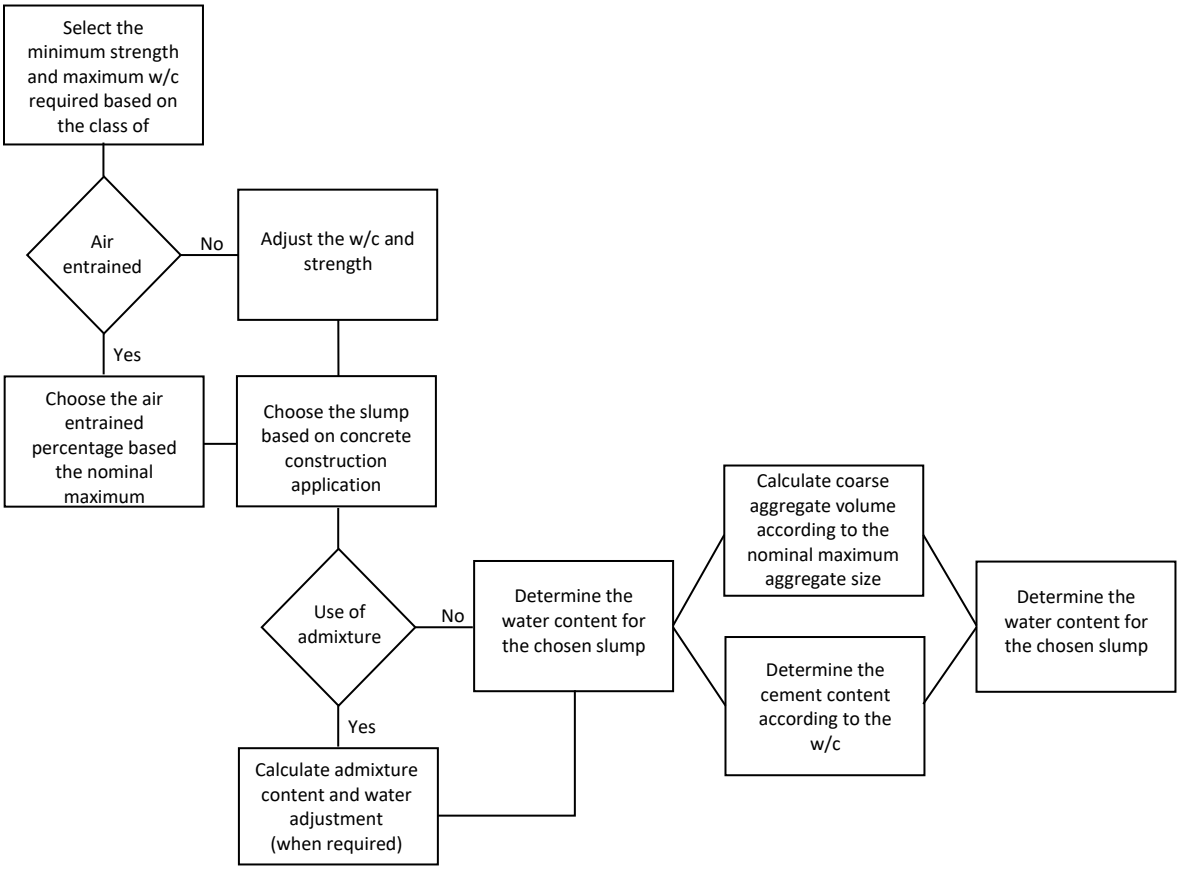

Figure 2.2. ACI method flowchart.

Additionally, the ACI method disregards some important features of the mixture components such as the particle size distribution (PSD) of the binder and aggregates, the aggregate lithotype, shape and texture, etc.; all parameters that definitely impact on the fresh (e.g. flowability) and hardened (e.g. stiffness, etc.) state of concrete mixtures (Shilstone, 1990; Neville, 2011; Polat *et al.*, 2013).

2.1.2. Mortar Content Optimization (MCO)

There are several methods able to optimize the mortar content and thus PC use in concrete. One of those methods is the so-called Mortar Content Optimization (MCO) method. In this procedure, a concrete mix is optimized through 3 experimental steps: a) mechanical

properties (Abram's law); b) consistency requirements (Lyse's law) and; c) eco-efficient (Molinari's law) aspects.

It is well known that the compressive strength of conventional concrete (well compacted) is inversely proportional to the w/c (Monteiro, Helene and Kang, 1993; Kosmatka, Kerkhoff and Panarese, 2002; ßat, Alyamaç and Ince, 2008; Helene and Tutikian, 2011; Neville, 2011). This relationship (Equation 2.1) was created by Abrams in 1918.

$$f'_c = \frac{K_1}{K_2{}^{w/c}} \qquad \textit{Equation 2.1}$$

Where f'_c is the concrete compressive strength at 28-days, w/c is the water to cement ratio, and K_1 and K_2 are empirical constants.

Compaction is an extremely important factor that directly affects the compressive strength of concrete since the presence of segregation, voids and honeycombs due to the lack of compaction may reduce the concrete strength, as illustrated in Figure 2.3.

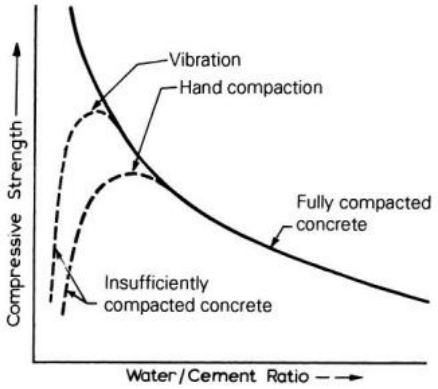

Figure 2.3. Relationship between the w/c and the compressive strength accounting the compaction (Neville, 2011).

Lyse's law (Equation 2.2) demonstrates the relationship between w/c and aggregates for a specific concrete consistency measured by the slump test (Monteiro, Helene and Kang, 1993; ßat, Alyamaç and Ince, 2008). The latter is the link between Abrams's and Molinari's law. Lyse's law states that for a given slump, it is possible to enhance concrete compressive strength by decreasing the aggregate's and water content. However, the PC content required increases along with the decrease of aggregate's content.

$$m = k_3\left(\frac{w}{c}\right) + k_4 \qquad \textit{Equation 2.2}$$

Where m is the relationship between aggregates and cement (i.e. sum of fine and coarse aggregate mass divided by PC mass), k_3 and k_4 are constants which depend on the materials, and w/c is the water to cement ratio.

The third and last law, Molinari's law (Monteiro, Helene and Kang, 1993; ßat, Alyamaç and Ince, 2008), correlates the aggregate to cement ratio (a/c) and cement content for different concrete mix-designs with same slump, as shown in Equation 2.3.

$$Cement\ Content = \frac{1000}{K_5 * m + K_6} \qquad \textit{Equation 2.3}$$

Where K_5 and K_6 are empirical constants and m is the relationship between aggregates and PC.

A four-quadrant mix-design diagram (Figure 2.4) can be drawn with the combination of the above three laws. Hence, it is possible to predict the fresh and hardened state behaviours of concrete mixtures with distinct amounts of PC. Yet, the drawback of the current method is the need of important amount of experimental data using the same raw materials than the given concrete to be able to plot the below curves. Furthermore, MCO does not account either for the PSD along with the features (lithotype, shape and texture) of the coarse and fine aggregates used.

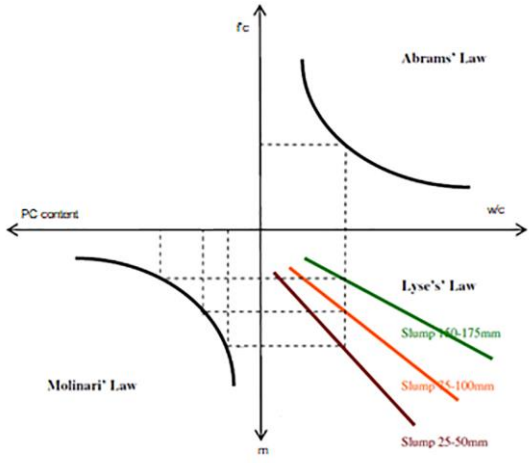

Figure 2.4. A mix-design monogram sample adapted from (Hu, Wang and Gaunt, 2013).

2.2. Packing Models

Aggregates PSD can be optimized through the use of PPMs, resulting in a system with high packing density and low porosity. Packing density ($Ø_p$) is defined by the ratio of the aggregate's bulk density to the total density (i.e. the percentage of solid volume that fills the total volume; Equation 2.4).

$$Ø_p = \frac{V_{solid}}{V_{total}} \qquad \textit{Equation 2.4}$$

Therefore, $Ø_p$ is inversely proportional to the voids fraction. The packing density of a granular system such as concrete may be affected by a number of factors; however, the most important parameters are the size, shape and volume of the particles, along with the distance among them and their electrostatic interactions (Kawashima *et al.*, 2012; Kwan and Li, 2012; Aïssoun, Hwang and Khayat, 2016; Mehdipour and Khayat, 2017). Thus, packing density can be enhanced by a clever selection of aggregates size and portion, where the voids/pores formed amongst coarser particles are filled by finer particles. Then, these particles create new and smaller voids that are next filled by even finer particles, resulting in a very low porosity system. It is worth noting that high densely packing systems may be achieved by adding particles to the mix that are smaller than the voids between the current components; otherwise, the existing particles would be disturbed and displaced resulting in increased porosity. This phenomenon is known as "loosening effect" and it is illustrated in Figure 2.5 (Mangulkar and Jamkar, 2013). Besides, a second and also important phenomenon, the so-called "wall effect", may take place whenever fine particles get trapped around much coarser particles due to an improper selection of PSD, increasing the system porosity, as illustrated in Figure 2.5.

Kawashima et al. (2012) explain mathematically how voids can be created in the binary system considering a cement paste matrix. The cement paste $Ø_p$ is primarily affected by flocculation or agglomeration of the particles (i.e. the stage where a single cement particle becomes a floc of higher volume). Therefore, two possible states can be considered: flocculation and dispersion. The former takes place when large particles (flocs) have the

maximum $\emptyset_p$ and their voids are filled with smaller particles. The system $\emptyset_p$ can be calculated by Equation 2.5.

$$\emptyset_p = \frac{\emptyset_{p1}}{1-V_2} \qquad \textit{Equation 2.5}$$

Where $\emptyset_{p1}$ is the packing density of large particles, V_2 is the fraction of small particles solid volume.

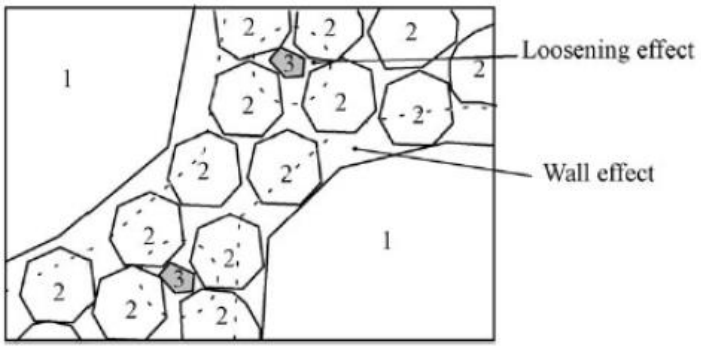

Figure 2.5. Wall and Loosening effect (Mangulkar and Jamkar, 2013)**.**

If one increases the volume of small particles (V_2), the packing density is governed by the second state: dispersion. In this case, the system $\emptyset_p$ can be calculated by Equation 2.6 (Kawashima *et al.*, 2012).

$$\emptyset_p = \frac{\emptyset_{p2}}{1-(1-\emptyset_{p2})\,V_1} \qquad \textit{Equation 2.6}$$

Where $\emptyset_{p2}$ is the packing density of small particles, V_1 is the fraction of large particles solid volume.

The packing density of flocculated or dispersed systems is presented in Figure 2.6. It is important to emphasize that the packing density of a granular system changes as a function of the casting process. Whenever particles are placed one by one, the maximum packing density is easily achieved, and it is called virtual packing density. However, in real casting scenarios, the aggregates are placed randomly and with different energies, which may change their shape, resulting in a much lower packing density than the virtual packing (Kawashima *et al.*, 2012).

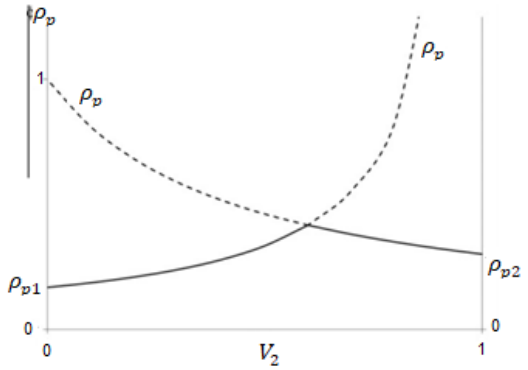

Figure 2.6. Cement paste packing density as a function of small particles volume adapted from (Kawashima *et al.*, 2012).

Su, Hsu and Chai (2001) studied a new mix-design for self-consolidating concrete (SCC) based on the packing factor (PF), which is the relationship between the compacted bulk density and the loose bulk density of aggregates. PF can be increased with the rise of fine and coarse aggregates in the mix (i.e. the volume of voids is reduced by adding finer particles). Consequently, it requires fewer binders to fill the voids, producing a more economical and eco-efficient concrete. Analyzing Figure 2.7, when the PF is increased from 1.16 to 1.18, the passing ability evaluated throughout the L-box test and the flowability evaluated throughout the V-funnel is decreased by 16% and 36%, respectively.

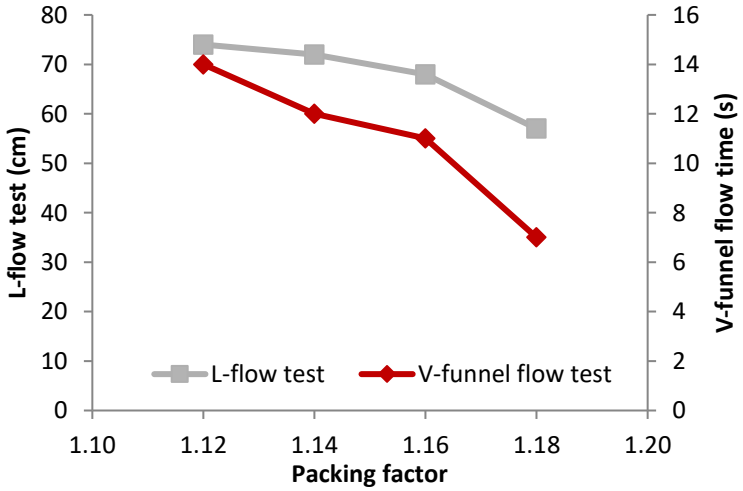

Figure 2.7. Relationship between packing factor, flowability, and passing ability based on (Su, Hsu and Chai, 2001).

Normally, the voids formed between the aggregates are filled with cement paste; therefore, reducing the system porosity results in a lower need for cement paste (Goltermann, Johansen and Palbøl, 1997). In the 30s, Westman and Hugill developed an algorithm (Equation 2.7) to calculate the PF based on packing theories (Dinger and Funk, 1994).

$$V_{a1} = a_1 x_1 \qquad \textit{Equation 2.7}$$

$$V_{a2} = x_1 + a_2 x_2$$

$$V_{a3} = x_1 + x_2 + a_3 x_3$$

$$\dots$$

$$V_{ai} = \sum_{j=1}^{i-1} x_j \quad {}_1 + a_i x_i$$

Where a_i is the apparent volume of the i^{th} size particle in a monodisperse system, x_i is the mass fraction of i^{th} size particle, V_{ai} is the apparent volume of the mixture with n particle sizes, n is the number of particle sizes.

It is considered that the maximum apparent volume (V_a) is directly proportional to the porosity and inversely proportional to the PF, as shown in Equation 2.8 (Dinger and Funk, 1994).

$$V_a = \frac{1}{PF} \qquad \textit{Equation 2.8}$$

Although fine and coarse aggregate particles are non-spherical, considering monodisperse[1] spherical particles filling a given volume (e.g. bucket), it would result in a total of approximately one-fourth of empty spaces. This packing density, around 75%, is only theoretical where the particles are ordered. In real scenarios, it would result in a $Ø_p$ between 60% and 64% (Oliveira *et al.*, 2000). For that reason, monodisperse distributions have a porosity equal to 40% considering maximum packing. Therefore, the porosity of real distributions can be calculated with the modified Westman and Hugill algorithm - Equation 2.9 (Dinger and Funk, 1994).

[1]Mix of same sized particles.

$$Porosity\ (\%) = \left(1 - \frac{1}{V_{amax}}\right) * 40\% \qquad \textit{Equation 2.9}$$

The main advantage of packing models is the reduction of the system porosity in which also reduce the amount of cement paste required to fill the voids among the particles (De Larrard, 2009; Fowler and Rached, 2011; Fennis and Walraven, 2012; Mangulkar and Jamkar, 2013; Noël, Sanchez and Fathifazl, 2016). It also presents an economic benefit since the PC is more expensive (and less sustainable) than the aggregates. Additionally, it is more eco-efficient than conventional concrete, stronger and more durable than natural rocks (De Larrard, 2009).

PPMs can generally be divided into two types: discrete and continuous. Discrete models are numerical approaches developed from specified multimodal (also known as gap-graded) distributions containing "n" discrete size classes of particles based on the assumption that each class of particle will be rearranged to achieve the maximum $Ø_p$ possible (Fennis and Walraven, 2012; Mangulkar and Jamkar, 2013). Continuous models are numerical procedures developed considering particles with continuous size distribution (i.e. no gaps throughout the whole PSD) (Fennis and Walraven, 2012).

Discrete models aim to achieve the highest $Ø_p$ by adding the maximum amount of coarse aggregate in a specified volume and then complete the voids with finer particles (Dinger and Funk, 1994). One of the first discrete models developed was Furnas model for binary mixtures (Mangulkar and Jamkar, 2013). However, this model was only valid whenever the fine particle size was much smaller compared to the coarse particle size. If the ratio between the fine and coarse particle sizes is approximately equal to one, there can be two negative interaction effects: wall and loosening, as previously mentioned in Figure 2.5.

One of the first and well-known continuous models was presented by Fuller in 1907, where the gradation curves for maximum $Ø_p$ were proposed, known as Fuller-Thompson equation. This optimum PSD can be calculated by Equation 2.10 using a distribution coefficient equal to 0.5 (Fennis and Walraven, 2012; Mangulkar and Jamkar, 2013).

$$CPFT = 100 * \left(\frac{D_P}{D_L}\right)^q \qquad \textit{Equation 2.10}$$

Where CPFT is the cumulative (volume) percent finer than D_P, D_P is the particle diameter, D_L is the larger particle diameter, and q is the distribution coefficient.

Studies were performed based on Fuller-Thompson equation to achieve an ideal packing through continuous PPMs. According to Andreasen, the ideal packing occurs when there is a similarity in the particles distribution and arrangements even whether comparing particles with different sizes, as illustrated in Figure 2.8, the so-called granulation image (Oliveira *et al.*, 2000). Besides, Andreasen determined experimentally that the distribution coefficient should be between a third and a half (Oliveira *et al.*, 2000; Fennis and Walraven, 2012).

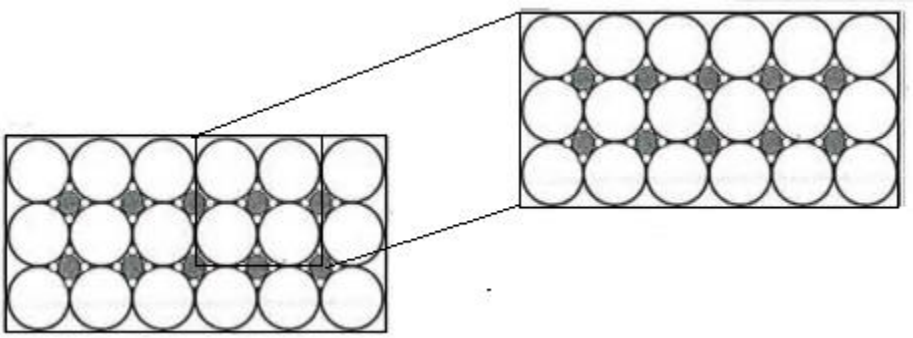

Figure 2.8. Ideal packing showed through granulation image.

One of the drawbacks of using Fuller-Thompson curve is the disregard of the smallest particle size of the PSD, which in reality is different from 0. Therefore, in 1980, Funk and Dinger enhanced Fuller-Thompson equation accounting not only for the largest particle diameter but also for the smallest particle diameter (D_S), as displayed in Equation 2.11, known as Alfred model.

$$CPFT = 100 * \left(\frac{{D_P}^q - {D_S}^q}{{D_L}^q - {D_S}^q}\right) \qquad \textit{Equation 2.11}$$

Based on computational analysis, it was determined that the optimum packing is achieved when the distribution factor is equal to 0.37 (Dinger and Funk, 1994; Fennis and Walraven, 2012). Conversely, the optimum q-factor reduces concrete flowability as the concrete presents less porosity and thus PC content. Aiming to improve concrete flowability, a q-factor of 0.21 is often suggested since it results in a higher amount of fines and lower amount of coarse aggregates producing a suitable amount of powder to liquid ratio, helping the

coarse aggregate particles slippage. The difference between the q-factors of 0.21 and 0.37 can be seen in Figure 2.9, which presents the CPFT using Alfred model.

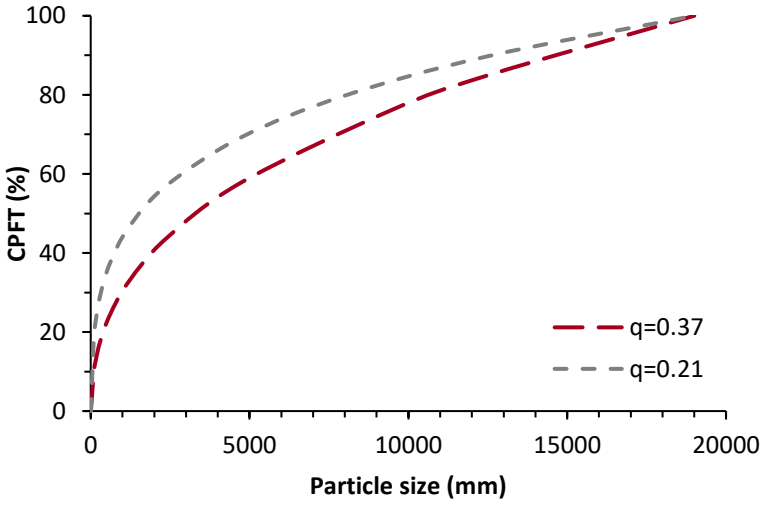

Figure 2.9. Particle size distribution of different q-factors using Alfred model.

Applying the Westman and Hugill concepts to Alfred Model, the porosity of different systems using distinct coefficient of distribution is calculated and presented in Figure 2.10.

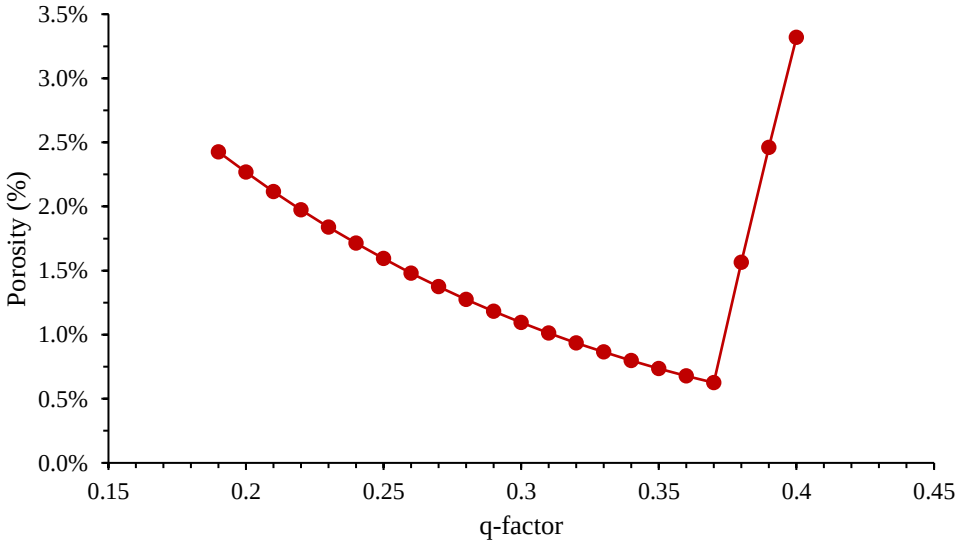

Figure 2.10. Relationship between porosity and Alfred model q-factor.

Modifying the distribution factor of concrete mixtures based on experimental results can improve their behaviour in the fresh or hardened states. However, one of the negative

points of using continuous PPMs (i.e. Alfred model) is that the latter only accounts for the dry system (i.e. water and PC hydration are disregarded in the design). Moreover, the aggregates features (i.e. shape, texture and lithotype) are only accounted indirectly (through changes in the distribution factors). Finally, there are no variables able to quantify and or forecast the fresh properties of concrete mixtures designed through the use of PPMs. Therefore other techniques (section 2.5), accounting for mobility parameters such as *Interparticle Spacing* (IPS) and the *Maximum Paste Thickness* (MPT) were developed and are currently used in combination with PPMs (Dinger and Funk, 1994).

Although recent research using PPMs have been conducted to produce LCC systems, there is still a gap concerning the fresh and mechanical properties of this type of concrete, particularly, its suitability for structural applications considering durability and long-term aspects.

2.3. Binder Efficiency

Compressive strength at 28-days is the main parameter for structural design. Although PC is responsible for generating calcium silicate hydrate (C-S-H) in the mix and thus strength, there is a misconception in concrete industry that the higher the PC content the higher the concrete strength. Popovics (1990) was the first researcher that presented a study correlating the compressive strength development of a given concrete mix to its binder content (i.e. PC amount) (Equation 2.12).

$$f_r = \frac{f'_c}{BC} \qquad \textit{Equation 2.12}$$

Where f_r is the relationship between compressive strength and PC content, f'_c is the concrete compressive strength, and BC is the binder content.

Considering the environmental impact of concrete, Damineli et al. (2010) proposed an index correlating the amount of binder required to develop one unit of concrete property, for instance, the compressive strength. They called it as binder intensity index (bi; Equation 2.13) and it quantifies the eco-efficiency of concrete mixtures.

$$bi = \frac{BC}{P}$$ Equation 2.13

Where bi is the binder intensity index, BC is the binder content (kg/m^3), and P is the performance requirement (e.g. compressive strength – MPa).

This calculation does not require additional information and may facilitate the analysis of the environmental effects caused by different types of concrete. Moreover, to evaluate bi outcomes worldwide, Damineli et al. (2010) selected 156 random Brazilian and international concrete mix-designs used for distinct applications from 1988 to 2009, resulting in a total of 1585 data points, as displayed in

Figure 2.11. This study clearly demonstrated that high strength concrete mixtures are "naturally" more optimized since they incorporated lower bi factors compared to conventional concrete. On the other hand, conventional concrete mixes (i.e. 20-40 MPa) showed to be often designed with moderate to high PC contents, which clearly demonstrates the need for techniques to improve their eco-efficiency. Data below shows that the majority of concrete produced worldwide presents PC contents ranging from 250 to 500 kg/m³ and the vast majority of bi found in conventional concrete are close to or higher than 10 kg.m^{-3}.MPa^{-1}. Finally, it is important to note that only roughly 2% of the concrete mixtures commonly used worldwide present PC contents lower than 250 kg/m³ of concrete.

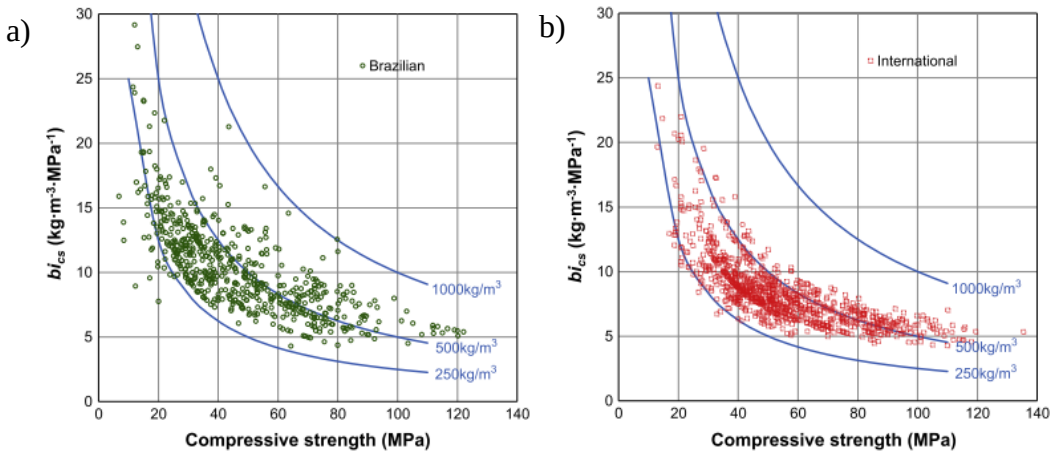

Figure 2.11. Relationship between binder intensity and compressive strength at 28-days a) Brazilian records b) international records (Damineli et al., 2010).

2.4. Particles Effects

2.4.1. Aggregate Interlock

The capacity of aggregate particles of transferring loads from one side of a narrow crack to the other is called aggregate interlock. It is affected by some aggregate features such as their shape and texture. For instance, self-consolidating concrete, which has a higher fine to coarse aggregate ratio compared to conventional concrete may result in a reduction of aggregate interlock. The latter may produce a negative impact on the shear capacity of reinforced concrete members (Neville, 2011).

2.4.2. Aggregate Bond

The aggregates bond may also affect the hardened state properties of concrete. The bond between aggregates and cement paste depends on the quality of the cement paste itself, but also on some features of the aggregates (especially the coarse aggregates) such as hardness, shape and texture. Coarse aggregates are classified by shape and texture. Aggregate shapes can be described as following: rounded, angular, flaky, elongated, or flaky and elongated (Figure 2.12). Moreover, aggregates are also classified as rough or smooth regarding their texture. Generally, gravels are considered round and smooth, whereas crushed stones are angular and rough; therefore, crushed stones have the potential of providing the mixture with better aggregate/paste bond in the hardened state,

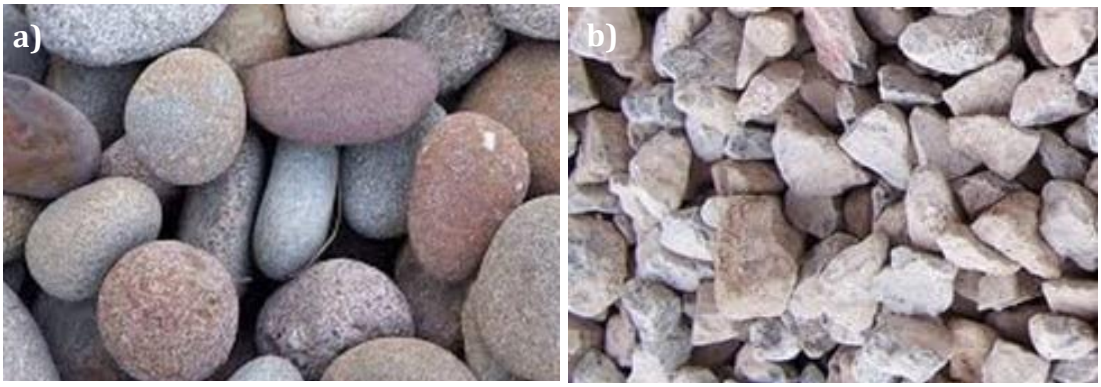

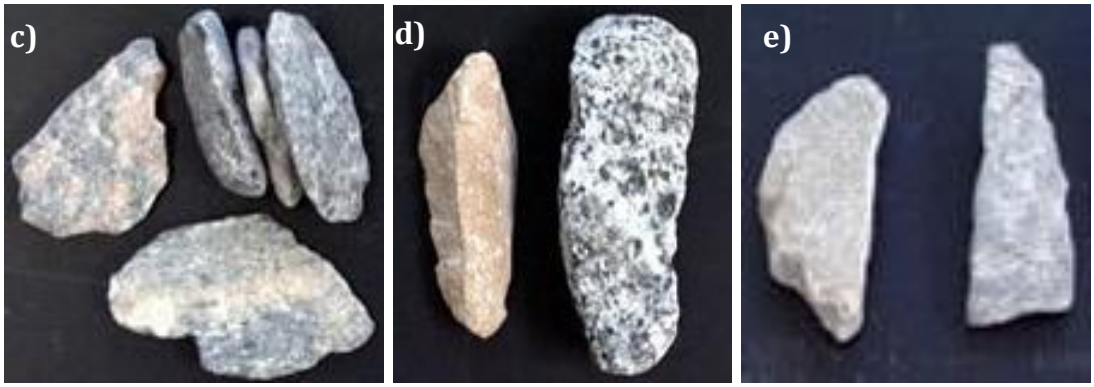

Figure 2.12. Types of coarse aggregates: a) rounded, b) angular, c) flaky, d) elongated, and e) flaky and elongated (The Constructor, 2017).

2.5. Particle Distance Effects

Concrete is made of aggregates (i.e. fine and coarse: particles greater than 125 µm), water, and reactive or inert fines (particles smaller than 125 µm; e.g. cement and limestone fillers, respectively) (Hunger and Brouwers, 2009). It is known that the w/c must be suitable to provide sufficient amount of water for the PC hydration process. Yet, the water is not only important regarding strength aspects, but it also plays an important role concerning the suspension flowability. Before concrete sets, water is responsible for moving the granular particles and thus has a direct impact on the overall flowability of the suspension. Therefore, one may conclude that a minimum amount of water is required to enable the material's flow in the fresh state (Damineli, 2013). It has been found that the minimum amount of water may be considered as the average distance that separates two adjacent fine particles, assuming that all the particles are not agglomerated (Oliveira *et al.*, 2000). The latter is called *Interparticle Spacing* (IPS).

On the other hand, the minimum amount of cement paste to enable flow in a mix is considered as the maximum distance between two coarse aggregate adjacent particles and is called *Maximum Paste Thickness* (MPT) (Dinger and Funk, 1994; Oliveira *et al.*, 2000; Damineli, 2013; Varhen *et al.*, 2016). These two above parameters are called "mobility parameters" and have demonstrated to be promising while the mix-design of highly packed systems.

2.5.1. *Interparticle Spacing* (IPS) & *Maximum Paste Thickness* (MPT)

IPS is the average distance of adjacent fine particles. Figure 2.14 shows that IPS is directly proportional to the water content in the mix. IPS can be calculated by Equation 2.14 (Dinger and Funk, 1994).

$$IPS = \frac{2}{VSA}\left[\frac{1}{V_s} - \frac{1}{(1-P_{of})}\right] \qquad \textit{Equation 2.14}$$

Where IPS is the *Interparticle Spacing* in a slip, VSA is the calculated volume surface area per cubic centimetre of powder, V_s is the volume fraction solids, P_{of} is the pore fraction assuming the densest packing.

It is worth noting that PPMs consider all particles are spherical. Since this is not a reality, the IPS is calculated based on the VSA to account for the different particle shapes. VSA can be calculated from the SSA as follows (Equation 2.15).

$$VSA = SSA * \rho_{part} \qquad \textit{Equation 2.15}$$

Where VSA is the volume surface area (m^2/g), SSA is the specific surface area (m^2/g), and ρ_{part} is the particle density (g/cm^3).

Likewise, MPT is the *Maximum Paste Thickness* among adjacent aggregate particles greater than 100-125 μm. It can be calculated by Equation 2.156 (Oliveira *et al.*, 2000)

$$MPT = \frac{2}{VSA_c}\left[\frac{1}{V_{sc}} - \frac{1}{(1-P_{ofc})}\right] \qquad \textit{Equation 2.16}$$

Where MPT is the distance between aggregates, VSA_c is the calculated volume surface area of aggregate fraction, V_{sc} is the volumetric aggregate solid fraction, P_{ofc} is the pores of aggregate fraction assuming the densest packing.

Previous studies highlight that the greater the IPS and MPT, the higher the flowability of the mixes (Varhen *et al.*, 2016; Silva, Segadães and Lopes, 2017). It occurs as a result of the decrease of friction among the particles without changing the water content. Moreover, these two mobility parameters are directly proportional to the concrete microstructure (e.g. permeability) (Innocentini *et al.*, 2003).

De Larrard and Belloc (1997) proposed a different approach for MPT. The authors introduced a *Maximum Paste Thickness* accounting for only the coarse aggregates (i.e. particles greater than 5 mm), as illustrated in Figure 3.13 and called it MPT_{coarse} Equation 2.17.

$$MPT_{coarse} = D_{max}\left(\sqrt[3]{\frac{g^*}{g}} - 1\right) \qquad \textit{Equation 2.17}$$

Where MPT_{coarse} is the maximum distance between the coarse aggregates, D_{max} is the maximum aggregate size, g is the aggregate volume in a unit volume of concrete, and g* is the packing density of the aggregate (assuming a granular mix).

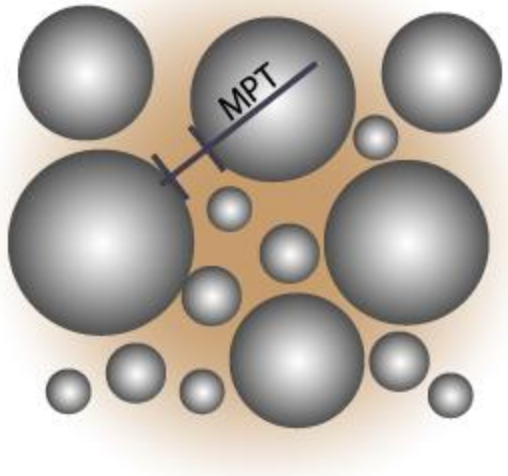

Figure 2.13. *Maximum Paste Thickness* of coarse aggregates.

The packing density of the aggregate can be calculated by three different methods: solid suspension model (Equation 2.18), refined version for rounded aggregate (Equation 2.19), and for crushed aggregate (Equation 2.19) (De Larrard and Belloc, 1997).

$$g^* = 1 - 0.47\sqrt[5]{\frac{D_{min}}{D_{max}}} \qquad \textit{Equation 2.18}$$

$$g^* = 1 - 0.39\left(\frac{D_{min}}{D_{max}}\right)^{0.22} \qquad \textit{Equation 2.19}$$

$$g^* = 1 - 0.45\left(\frac{D_{min}}{D_{max}}\right)^{0.19} \qquad \textit{Equation 2.20}$$

Where g* is the packing density of the aggregate, D_{max} is the maximum aggregate size (90% passing), and D_{min} is the minimum aggregate size (10% passing).

According to the authors, MPT_{coarse} can be seen as a "small-scale" compressive strength test where the cement paste is the concrete specimen and the two adjacent aggregates are the test machine plattens (De Larrard and Belloc, 1997). Results have shown that the lower the MPT_{coarse}, the higher the mechanical properties of PPM mix-designed mixtures (De Larrard and Belloc, 1997; Chen et al., 2013; Le et al., 2017; Shadkam et al., 2017). Furthermore, the MPT_{coarse} was found to influence the durability-related parameters of densely packed systems, especially the ones governed by transport mechanisms (Shadkam et al., 2017).

2.5.2 Dispersion Force

Aggregates are concrete components with low specific surface area[2] (SSA), which results in higher gravitational forces (i.e. mass forces). Therefore, these heavy particles tend to be deposited due to gravity. Yet, fines have higher superficial forces due to their high SSA and low mass. Particles with less than 125 µm tend to agglomerate and to act as bigger particles when mixed with water as a result of Van der Waals attraction forces (Oliveira *et al.*, 2000; Adamczyk, 2006; Castro and Pandolfelli, 2009). Van der Waals interactions take place among molecules and/or atoms of the same material through oscillations in their charges; therefore, the particles are not constantly in equilibrium (Oliveira *et al.*, 2000; Adamczyk, 2006). Besides acting as bigger particles, the distance between particles is reduced by the agglomeration effect, resulting in flowability challenges: increase of particle collision, rise of the system's viscosity and water getting stuck among agglomerated particles (Figure 2.14). The latter may reduce PC hydration which emphasized the need for controlling the distance among the particles and thus the mobility parameters previously presented.

[2] SSA is measured in m^2/g

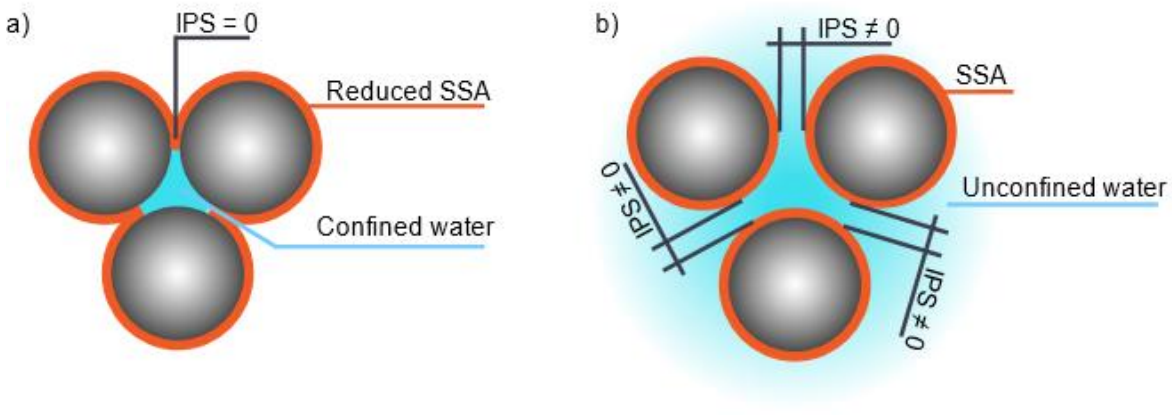

Figure 2.14. Particles a) agglomerated with IPS = 0 b) deagglomerated with IPS ≠ 0.

2.6. Limestone fillers effects

A number of studies have been focusing on PC reduction in the past decades. Most of the research performed evaluated PC replacement in percentage by SCMs. However, increased attention to the use of limestone fillers as mineral admixtures and/or partial replacement of PC has been demonstrated in the recent years. Results found in literature have shown that limestone fillers are a promising alternative to PC reduction for several reasons highlighted hereafter:

- Limestone fillers are by-products from aggregate quarries and thus constitute an economic and sustainable alternative to civil construction (Ingram and Daugherty, 1991; Knop and Peled, 2016a);
- They present considerable ecological benefits due to the reduction of CO_2 emission compared to PC production (Knop and Peled, 2016a; Varhen *et al.*, 2016);
- Limestone fillers may improve the rheological performance of cementitious materials (i.e. cement paste, mortar and concrete made by PC) (Knop and Peled, 2016a, 2016b);
- Fillers may improve the microstructure of concrete and thus reduce porosity and shrinkage. Moreover, they may improve durability-related properties of the

material, especially the ones linked to transport mechanisms (Shadkam *et al.*, 2017), (Varhen *et al.*, 2016);

- Limestone filler enhances the hydration process, especially at early ages, due to the increase of nucleation sites for hydration products and which raises the amount of space available for hydration products precipitation (Lothenbach, Scrivener and Hooton, 2011).

2.7. Influence of PPMs on the fresh state properties of concrete

Developing a mixture design through PPMs significantly modifies the fresh properties of concrete due to the variation of aggregates PSD. As mentioned before, PPMs can reduce the voids volume between the aggregates particles. Since these voids are normally filled by cement paste, lessening the voids means also reducing PC content. For example, increasing the aggregate packing density and maintaining the paste content constant results in the enhancement of concrete flowability (Mehdipour and Khayat, 2017).

Besides packing density, the rheological behaviour of cementitious materials is also affected by the amount of water and the shape of the particles, as mentioned in section 2.2 (Kawashima et al., 2012; Kwan and Li, 2012; Aïssoun, Hwang and Khayat, 2016; Mehdipour and Khayat, 2017). The latter can be evaluated through the particle SSA. Angular aggregate particles (i.e. higher SSA) require more IPS than a spherical aggregate (i.e. lower SSA) to have the same flowability (Kwan and Li, 2012; Mehdipour and Khayat, 2017). It is important to note that any loss in the rheological behaviour of concrete mixtures can also be adjusted with the selection of higher water to cement ratios and/or the use of chemical admixtures in the mix, especially the so-called high range water reducers (i.e. superplasticizers). However, concerns were raised in literature while the use of high amounts of superplasticizers since they may decrease significantly the viscosity of the mixture and thus cause segregation (Golaszewski and Szwabowski, 2004).

A series of studies have been performed to evaluate the influence of packing density and PSD on the rheological behaviour of concrete. Aïssoun et al. (2016) concluded that for super

flowable concrete with a given sand to aggregate ratio, increasing aggregate particles smaller than 315 µm reduces the inter-particle friction; hence, the yield stress and consistency.

Pacheco-Torgal et al. (2013) developed a comprehensive study on the use of fillers for improving concrete eco-efficiency. As displayed in Figure 2.15 on the darker dots, concrete mixtures with lower bi factor may be produced whenever inert fillers are added to the mix. However, the PSD of fillers also plays an important role in the system packing density and rheological properties. Knop & Peled (2016) evaluated the packing density of blended cement with limestone, which was composed of particles larger than, smaller than or equal to PC particles. It was concluded that the loosening and wall effects calculated by different models, such as developed by de Larrard (1999) and Yu, Zou, & Standish (1996), are not accurate for all types of blended cement with limestone studied.

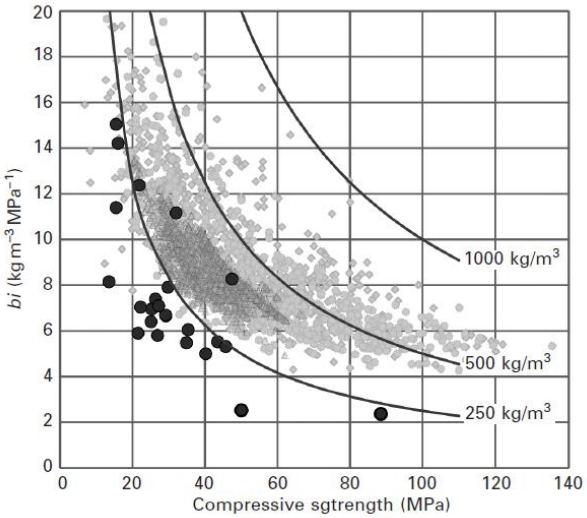

Figure 2.15. Eco-efficient concrete mixtures produced with fillers (Pacheco-Torgal et al., 2013).

Therefore, one may conclude that the optimized packing system is the one that provides the highest packing (i.e. the lowest PC content) without harming the mobility of particles and thus flowability of the mix in the fresh state.

2.8. Influence of PPMs on the compressive strength of concrete

It is known that compressive strength of cementitious materials is associated with the water/binder ratio of the system, where the higher the latter, the lower the compressive strength of the material (Abrams law). However, whenever PPMs are used to improve the system packing density, the compressive strength cannot only be predicted by Abrams law and thus new parameters are needed to fully explain the hardened properties of these systems.

Fennis, Walraven, & den Uijl (2013) studied 50 mortar mixtures designed with PPMs and concluded that although the compressive strength could not be predicted only by the w/c, it could be correlated with the cement-spacing factor, which accounted for the volumetric distance between the cement particles. Therefore, an increase in the w/c would reduce the system packing density and thus decrease its compressive strength.

John *et al.* (2018) verified the effect of high inert filler content on highly packed concrete mixtures. It was verified that the relationship between w/c and compressive strength (Abrams law) cannot be applied on these concrete mixtures, instead, the use of the water to fines ratio is suggested in this respect.

2.9. Durability and long-term properties of concrete designed through PPMs

Although LCC concrete may result in lower carbon footprint, its long-term behaviour and volumetric stability is still unknown and should be further evaluated. A few studies have been reported in the literature on permeability and shrinkage of highly packed systems and the main conclusions are presented in the following sub-sections.

2.9.1. Permeability

Concrete permeability is one of the main concrete characteristics that must be evaluated to predict concrete durability (Stroeven *et al.*, 2015), especially while dealing with problems caused by transport mechanisms.

Studies appraise the permeability of high-strength LCC concrete containing fly ash using three methods: air permeability, water permeability and chloride ion permeability (Naik *et al.*, 1996). Regardless of the test method, the permeability decreased with time due to the pozzolanic effect and thus increase of C-S-H in the concrete microstructure. This study showed that increasing the percentage of SCMs (e.g. fly ash) and decreasing PC content may result in a reduction of the air permeability up to 55% of replacement. However, concrete mixtures with high amounts of SCMs (e.g. 74% of fly ash replacement) presented a significant increase on permeability because of the lower amount of C-S-H products formed when compared to mixes with higher PC content. Similarly to air permeability, mixtures with 74% of fly ash presented higher permeability. This study concluded that the optimum fly ash replacement must be between 35-55% considering the performed tests and pozzolanic contributions.

Nonetheless, to analyze the influence of PPMs on concrete permeability, it is necessary to understand the packing density influence on the concrete mixture and not only account for the PC replacement by SCMs. Innocentini et al. (2001) verified that there are two main types of pores that affect concrete permeability. The first type refers to pores resulted from gaps among the particles within the cementitious system whereas the second type refers to the gaps among the particles in the granular system. As mentioned in section 2.2, there is a lower packing density in the fine particles (i.e. matrix) due to flaws in the interface paste aggregates and also due to secondary phenomena such as loosening or wall effects, which results in higher porosity. These flaws (i.e. pores) proportion lower permeability resistance to the matrix.

2.9.2. Shrinkage

It is well established that concrete shrinkage is one of the most important volumetric instability issues in concrete. Although all types of shrinkage are associated with the variation of moisture content in concrete and/or internal pore pressure, it is worth understanding the different types of shrinkage (Idiart, López and Carol, 2011). Literature shows that there are six types of concrete shrinkage: chemical, autogenous, plastic, drying, carbonation, and thermal.

Regarding the effect of LCC on concrete shrinkage, it can be verified that the chemical shrinkage may be directly decreased with PC reduction (Tazawa, Miyazawa and Kasai, 1995; Khairallah, 2009; Fu, 2011). Moreover, according to Mehta & Monteiro (2006), autogenous shrinkage, and consequently drying shrinkage increase with the rise of PC content.

Therefore, LCC mixtures may have a positive effect on the distinct types of shrinkage. Yet, there is a lack of literature results supporting the latter and thus further studies are still needed in the area.

2.10. References

Adamczyk, Z. (2017) Particles at interfaces : interactions, deposition, structure. Second, Potential Interactions Among Particles. Second. London : Academic Press.

Aïssoun, B. M., Hwang, S. D. and Khayat, K. H. (2016) 'Influence of aggregate characteristics on workability of superworkable concrete', Materials and Structures/Materiaux et Constructions, 49(1–2), pp. 597–609.

Castro, A. K. and Pandolfelli, V. C. (2009) 'Review: Concepts of particle dispersion and packing for special concretes production', 18 Cerâmica, 55, pp. 18–32.

Damineli, B. (2013) Consumo de ligantes: controle reologico, empacotamento e dispersao de particulas. University of Sao Paulo.

Damineli, B. L. et al. (2010) 'Measuring the eco-efficiency of cement use', Cement and Concrete Composites, 32, pp. 555–562.

Dinger, D. and Funk, J. (1994) Predictive process control of crowded particulate suspensions. 1st edn. Edited by S. S. + B. M. LLC. New York.

Fennis, S. A. A. M. and Walraven, J. C. (2012) 'Using particle packing technology for sustainable concrete mixture design', Heron, 57(2), pp. 73–101.

Fennis, S. A. A. M., Walraven, J. C. and den Uijl, J. A. (2013) 'Compaction-Interaction Packing Model: Regarding The Effect Of Fillers In Concrete Mixture Design', Materials and Structures, 46(3), pp. 463–478.

Fowler, D. and Rached, M. (2011) 'Optimizing Aggregates to Reduce Cement in Concrete Without Reducing Quality', Transportation Research Record: Journal of the Transportation Research Board, 2240, pp. 89–95.

Fu, T. (2011) Autogenous Deformation and Chemical Shrinkage of High Performance Cementitious Systems. Oregon State University.

Golaszewski, J. and Szwabowski, J. (2004) 'Influence of superplasticizers on rheological behaviour of fresh cement mortars', Cement and Concrete Research, 34, pp. 235–248.

Goltermann, P., Johansen, V. and Palbøl, L. (1997) 'Packing of Aggregates : An Alternative Tool to Determine the Optimal Aggregate Mix', ACI Materials Journal, (94), pp. 435–442.

Helene, P. and Tutikian, B. F. (2011) 'Dosagem dos Concretos de Cimento Portland', in Cechella Isaia, G. (ed.) Concreto: Ciência e Tecnologia. 1st edn. São Paulo: Ibracon, pp. 415–451.

Hu, J., Wang, K. and Gaunt, J. A. (2013) 'Behavior and mix design development of concrete made with recycled aggregate from deconstructed lead-contaminated masonry materials', Construction and Building Materials, 40(January), pp. 1184–1192.

Hunger, M. and Brouwers, H. J. H. (2009) 'Flow Analysis of Water–Powder Mixtures: Application to Specific Surface Area and Shape Factor', Cement and Concrete Composites, 1(31), pp. 39–59.

Idiart, A. E., López, C. M. and Carol, I. (2011) 'Modeling of drying shrinkage of concrete specimens at the meso-level', Materials and Structures, 44, pp. 415–435.

Ingram, K. D. and Daugherty, K. E. (1991) 'A Review of Limestone Additions to Portland Cement and Concrete', Cement & Concrete Composites, 13, pp. 165–170.

Innocentini, M. et al. (2001) 'Effect of particle size distribution on the drying behavior of refractory castables', Ceramica, 47(304).

Innocentini, M. D. M. et al. (2003) 'PSD-Designed refractory castables', Am. Ceram. Soc. Bull., 82(7), p. 9401–9406.

Kawashima, S. et al. (2012) 'Study of the mechanisms underlying the fresh-state response of cementitious materials modified with nanoclays'.

Khairallah, R. S. (2009) Analysis of autogenous and drying shrinkage of concrete. McMaster University.

Knop, Y. and Peled, A. (2016a) 'Packing density modeling of blended cement with limestone having different particle sizes', Construction and Building Materials. Elsevier Ltd, 102, pp. 44–50.

Knop, Y. and Peled, A. (2016b) 'Setting behavior of blended cement with limestone: influence of particle size and content', Materials and Structures, 49, pp. 439–452.

Kosmatka, S. H., Kerkhoff, B. and Panarese, W. C. (2002) 'Designing and Proportioning Normal Concrete Mixtures', in Design and Control of Concrete Mixtures. Portland Cement Association, pp. 151–172.

Kwan, A. K. H. and Li, L. G. (2012) 'Combined effects of water film thickness and paste film thickness on rheology of mortar', Materials and Structures, 45, pp. 1359–1374.

De Larrard, F. (1999) Concrete Mixture Proportioning: A Scientific Approach. London and New York: Scientific Approach, E&FN SPON.

De Larrard, F. (2009) 'Concrete optimisation with regard to packing density and rheology', in 3rd RILEM international symposium on rheology of cement suspensions such as fresh concrete. France, p. 8.

De Larrard, F. and Belloc, A. (1997) 'The influence of aggregate on the compressive strength of normal and high-strength concrete', ACI Materials Journal, 94(5), pp. 417–426.

Lothenbach, B., Scrivener, K. and Hooton, R. D. (2011) 'Supplementary cementitious materials', Cement and Concrete Research, 41, pp. 217–229.

Mangulkar, M. N. and Jamkar, S. S. (2013) 'Review of Particle Packing Theories Used For Concrete Mix Proportioning', International Journal Of Scientific & Engineering Research, 4(5).

Mehdipour, I. and Khayat, K. H. (2017) 'Effect of particle-size distribution and specific surface area of different binder systems on packing density and flow characteristics of cement paste', Cement and Concrete Composites. Elsevier Ltd, 78, pp. 120–131.

Mehta, P. K. and Monteiro, P. J. M. (2006) Concrete: Microstructure, Properties, and Materials. McGraw-Hill.

Monteiro, P. J. M., Helene, P. R. L. and Kang, S. (1993) 'Designing concrete mixtures for strength, elastic modulus and fracture energy', Materials and Structures, 26, pp. 443–452.

Naik, T. R. et al. (1996) 'Permeability of high-strength concrete containing low cement factor', Journal of Energy Engineering, 122(1), pp. 21–39.

Neville, A. M. (2011) Properties of Concrete. Pearson Education Limited.

Noël, M., Sanchez, L. and Fathifazl, G. (2016) 'Recent Advances in Sustainable Concrete for Structural Applications', in Sustainable Construction Materials & Technologies 4, p. 10.

Oliveira, I. R. et al. (2000) Dispersão e Empacotamento de Partículas. São Paulo: Fazendo Arte Editorial.

Pacheco-Torgal, F. et al. (2013) Eco-Efficient Concrete. Woodhead Publishing Limited.

Polat, R. et al. (2013) 'The Correlation Between Aggregate Shape And Compressive Strength Of Concrete: Digital Image Processing Approach', International Journal of Structructural and Civil Engineering Research, 2(3), pp. 2319–6009.

Popovics, S. (1990) 'Analysis of the concrete strength versus water-cement ratio relationship', ACI Materials Journal, 87(5), pp. 517–529.

Shadkam, H. R. et al. (2017) 'An investigation of the effects of limestone powder and Viscosity Modifying Agent in durability related parameters of self-consolidating concrete (SCC)'.

Shilstone, J. M. (1990) 'Concrete Mixture Optimization', Concrete International: Design and Construction, 12(6), pp. 33–40.

Silva, A. P., Segadães, A. M. and Lopes, R. A. (2017) 'Castable systems designed with powders reclaimed from dismantled steel induction furnace refractory linings', Ceramics International, 43, pp. 5020–5031. doi: 10.1016/j.ceramint.2017.01.012.

ßat, K., Alyamaç, E. and Ince, R. (2008) 'A preliminary concrete mix design for SCC with marble powders', Construction and Building Materials, 23, pp. 1201–1210.

Stroeven, P. et al. (2015) 'Capabilities for property assessment on different levels of the micro-structure of DEM-simulated cementitious materials', Construction and Building Materials, 88, pp. 105–117.

Su, N., Hsu, K.-C. and Chai, H.-W. (2001) 'A simple mix design method for self-compacting concrete', Cement and Concrete Research, 31, pp. 1799–1807.

Tazawa, E., Miyazawa, S. and Kasai, T. (1995) 'Chemical shrinkage and autogenous shrinkage of hydrating cement paste', Cement and Concrete Research, 25(2), pp. 288–292.

The Constructor (2017) Classification of aggregates based on size and shape -coarse and fine, The Constructor. Available at: https://theconstructor.org/building/classification-of-aggregates-size-shape/12339/ (Accessed: 25 February 2017).

Varhen, C. et al. (2016) 'Effect of the substitution of cement by limestone filler on the rheological behaviour and shrinkage of microconcretes', Construction and Building Materials, 125, pp. 375–386.

Yu, A. B., Zou, R. P. and Standish, N. (1996) 'Modifying the Linear Packing Model for Predicting the Porosity of Nonspherical Particle Mixtures', Ind. Eng. Chem. Res., 35, pp. 3730–3741.

Chapter Three: Investigation of Alfred Model Effect on the Fresh and Hardened State Properties of Low-Cement Content (LCC) Systems

Mayra T. de Grazia[1*], Leandro Sanchez[1], Roberto C. O. Romano[2], Rafael G. Pileggi[2]

[1]Department of Civil Engineering, University of Ottawa, Ottawa, CANADA

[2]Department of Civil Engineering, Polytechnic School, University of São Paulo, São Paulo, BRAZIL

3.1. Abstract

Concrete, the major construction material used in the civil industry worldwide, presents a huge environmental impact producing about 7% of the global carbon dioxide (CO_2). Given the concerns related to global warming, studies have been focusing on distinct approaches aiming to reduce the amount of Portland cement (PC) which is the least sustainable ingredient of the mixture, by adopting alternative mix-design strategies such as the use of particle packing models (PPMs). However, there is currently a lack of literature results on the efficiency of the use of PPMs to reduce PC while maintaining or improving concrete properties in the fresh and/or hardened states. This work aims to investigate the influence of continuous PPMs on the fresh (rheological behaviour) and hardened (compressive strength, modulus of elasticity, porosity, and permeability) state of mixtures designed with approximately 150, 200, and 270 kg/m^3 PC contents. Results show that is possible to produce eco-efficient concrete without compromising the fresh and hardened properties of the material. Nevertheless, further durability and long-term investigations must be performed on systems with low cement content (LCC).

Keywords: Eco-efficient concrete; low cement content; particle packing models; *Interparticle Separation Distance*; *Maximum Paste Thickness*.

3.2. Introduction

Nowadays, the construction industry is not only focusing on the performance and economic benefits of the materials used but rather on their environmental impact. Concrete is the most important construction material used worldwide especially due to its interesting mechanical and durability-related properties, relatively low cost along with its ability to mould any given geometry type in the fresh state (Imbabi, Carrigan and Mckenna, 2012). However, concrete presents a significant non-sustainable impact regarding carbon dioxide (CO_2) emissions that may reach up to 7% of the global CO_2 release. Portland cement (PC) production is the main responsible for concrete carbon footprint accounting for 6.5% of the annual CO_2 production (Limbachiya, Bostanci and Kew, 2014). From 2010 to 2017, the global PC production increased approximately 24%; i.e. a growth of around 113 million metric tons on average per year (Statista, 2018). Reducing PC content of concrete mixtures impacts directly on CO_2 emissions since a ton of PC produces approximately one ton of CO_2 (Naik *et al.*, 1996; Hasanbeigi, Price and Lin, 2012; Gonçalves and Margarido, 2015). Moreover, a number of different issues may be raised by the use of moderate to high amounts of PC in concrete such as temperature rise and volumetric instability (Shabab *et al.*, 2016; Wen *et al.*, 2016; Makul and Sua-Iam, 2018). Therefore, new strategies have been studied aiming to reduce PC's usage in concrete. It has been found that the partial PC replacement by supplementary cementitious materials (SCMs) could not only increase cement efficiency but also concrete performance (Zachar and Asce, 2011; Juenger and Siddique, 2015). However, the availability of SCMs worldwide is not enough to match the demand of PC. Moreover, some SCMs types are depleting over the years due to the closure of industries responsible for producing these residues (Damineli and John, 2012; Noël, Sanchez and Fathifazl, 2016). Inert fillers, which are normally by-products of the aggregates industry, can also be used as a partial replacement of PC, improving concrete eco-efficiency (Damineli *et al.*, 2016; Knop and Peled, 2016b, 2016a; Varhen *et al.*, 2016). For example, the addition of limestone fillers results in the reduction of total porosity of the material due to the so-called filler effect (Romano *et al.*, 2008; Castro and Pandolfelli, 2009) as well as in the enhancement of

nucleation sites for hydration products, which increases the total space available for the precipitation of hydration products (Lothenbach, Scrivener and Hooton, 2011).

Another alternative to decrease PC usage is adopting advanced mix-design techniques, such as particle packing models (PPMs), which is the method selected for this research. PPMs may enhance the granular system reducing the materials porosity and consequently minimizing the amount of cementitious materials required to fill the voids among the aggregate particles (Romano *et al.*, 2008; Castro and Pandolfelli, 2009; Noël, Sanchez and Fathifazl, 2016). Although different PPM approaches may be found in the literature able to improve eco-efficiency of concrete, there is still a scientific gap on the most suitable technique capable of producing low cement content (LCC) systems without impacting the fresh and hardened state properties of concrete.

3.3. Background

3.3.1. Particle Packing Models (PPMs)

PPMs may enhance the particle size distribution (PSD) of granular systems, reducing the materials porosity and consequently increasing the system packing density ($Ø_p$). The main factors that affect the system packing density are size, shape and volume of the particles, along with the distance between them and their electrostatic interactions (Damineli *et al.*, 2016; Knop and Peled, 2016b, 2016a; Varhen *et al.*, 2016). PPMs studies are divided into two main types: discrete and continuous. Discrete models consider that the multimodal (also known as gap-graded) distributions containing “n” discrete size classes of particles rearrange by-itself to reach the maximum packing possible (Fennis and Walraven, 2012; Mangulkar and Jamkar, 2013). Conversely, continuous PPMs consider continuously sized particles, that is, no gaps throughout the total particle size distribution (PSD). Moreover, it considers the so-called “granulation image”, where the particles matrix around each particle must be the same, regardless of the size of the particle (Fennis and Walraven, 2012).

In 1907, Fuller and Thompson presented one of the first continuous PPMs, the so-called Fuller-Thompson curve, which is a power curve that accounts for two variables: the distribution factor (q) and the largest particle size (D_L). Studies performed based on the Fuller-Thompson curve concluded that besides the above two parameters, the smallest particle size would also influence the packing density of granular systems. Therefore, in 1980, Funk and Dinger improved Fuller-Thompson's approach by accounting for the smallest particle diameter (D_S). The latter was defined as Alfred model and is presented by Equation 3.1 (Oliveira *et al.*, 2000).

$$CPFT = 100 * \left(\frac{{D_P}^q - {D_S}^q}{{D_L}^q - {D_S}^q}\right) \qquad \textit{Equation 3.1}$$

Where CPFT is the cumulative (volume) percent finer than D_P, D_P is the particle diameter, D_L is the larger particle diameter, D_s is the smaller particle diameter, and q is the distribution coefficient.

A number of studies were conducted with Alfred's model over time, especially in ceramics, and it has been found that the distribution factor that brings the highest packing density and lowest porosity, requiring thus the least water and PC demands to granular systems is 0.37 (Dinger and Funk, 1994; Fennis and Walraven, 2012). Otherwise, the fresh state behaviour of mixtures with high packing density was found to be a challenge; hence lower distribution factors ranging from 0.20-0.22 were suggested for high flowability mixes such as self-consolidating concrete.

3.3.2. Fresh state mobility parameters

PPMs are normally used to decrease the porosity of granular systems, resulting in highly packed mixtures that may present important issues in the fresh state. In order to understand the fresh properties of high packing density systems, there is a need for studying the mobility among the particles throughout the whole PSD. Previous research shows that the *Interparticle Separation Distance* (IPS) and *Maximum Paste Thickness* (MPT) are two mobilities parameters that are essential to understanding the concrete behaviour in the

fresh state (De Larrard and Belloc, 1997; Bonadia *et al.*, 1999; Innocentini *et al.*, 2003; Varhen *et al.*, 2016). IPS is considered the average distance of two adjacent fines particles (smaller than 100-125 µm), assuming non-agglomerated particles (Oliveira *et al.*, 2000). Therefore, IPS can be considered equal to the total amount of fluid (water) that separates fine particles, as illustrated in Figure 3.1. IPS can be calculated by Equation 3.2 (Dinger and Funk, 1994). It is worth noting that fine particles tend to agglomerate due to Van der Waals attraction forces (Oliveira *et al.*, 2000; Adamczyk, 2006; Castro and Pandolfelli, 2009). Hence, the agglomeration makes fine particles to act as bigger particles likely causing flowability issues (i.e. increasing of particle collision, friction, and overall viscosity). Besides fresh state challenges, low IPS values may result in poor hydration degree, since water can become trapped among fine particles and thus not be able to percolate and hydrate all binder particles, as shown in Figure 3.1a.

$$IPS = \frac{2}{VSA}\left[\frac{1}{V_s} - \frac{1}{(1-P_{of})}\right] \qquad \textit{Equation 3.2}$$

Where IPS is the *Interparticle Spacing* in a slip, VSA is the calculated volume surface area per cubic centimetre of powder, V_s is the volume fraction solids, P_{of} is the pore fraction assuming the densest packing.

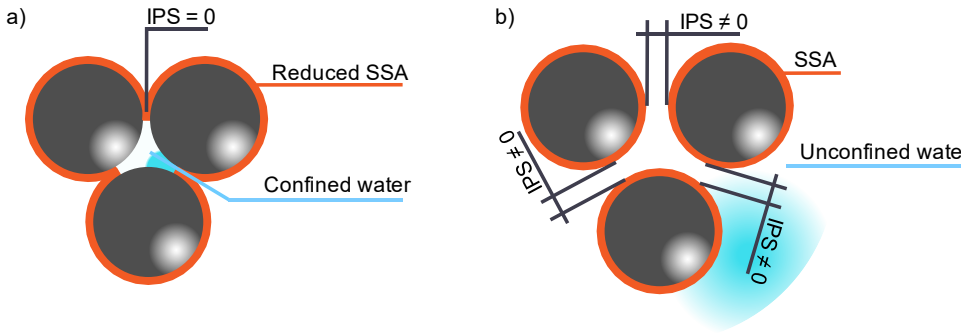

Figure 3.1. Particles a) agglomerated with IPS = 0 b) deagglomerated with IPS ≠ 0.

Additionally, MPT measures the maximum distance amongst coarser particles (greater than 125 µm) (De Larrard and Belloc, 1997; Bonadia *et al.*, 1999; Innocentini *et al.*, 2003; Shadkam *et al.*, 2017). It is considered as the thickness of paste (fine particles and water) that separates the aggregates and can be calculated by Equation 3.3.

$$MPT = \frac{2}{VSA_c}\left[\frac{1}{V_{sc}} - \frac{1}{(1-P_{ofc})}\right] \qquad \textit{Equation 3.3}$$

Where MPT is the distance between aggregates, VSA_c is the calculated volume surface area of aggregate fraction, V_{sc} is the volumetric aggregate solid fraction, P_{ofc} is the pore of aggregate fraction assuming the densest packing.

3.3.3. Hardened state mechanical properties

The short and long-term hardened state properties of concrete can be affected by a number of factors such as the water to cement ratio (w/c), packing density, amount of fine particles (i.e. filler effect), etc. Abrams law is a widely well-known equation, developed in 1918, that correlates the compressive strength of conventional concrete mixtures (completely compacted) with the w/c (Monteiro, Helene and Kang, 1993; Kosmatka, Kerkhoff and Panarese, 2002; ßat, Alyamaç and Ince, 2008; Helene and Tutikian, 2011; Neville, 2011). However, the sole use of Abrams' law is not precise enough to predict the behaviour of highly packed systems designed through the use of advanced techniques such as PPMs (De Larrard and Belloc, 1997). As a result, De Larrard & Belloc (1997) proposed a new parameter able to characterize the mechanical properties (and thus the compressive strength) of densely packed concrete mixtures and also named it as MPT (i.e. *Maximum Paste Thickness*). In this case, MPT represents the maximum distance between adjacent "coarse aggregate particles", as highlighted in Figure 3.2. In order to facilitate the nomenclature, from now on, the MPT according to De Larrard & Belloc (1997) will be presented as MPT_{coarse} and will be calculated by Equation 3.4. According to the authors, MPT_{coarse} can be seen as a "small-scale" compressive strength test where the cement paste is the concrete specimen and the two adjacent aggregates are the test machine plattens (De Larrard and Belloc, 1997). Results have shown that the lower the MPT_{coarse}, the higher the mechanical properties of PPM mix-designed mixtures (De Larrard and Belloc, 1997; Chen *et al.*, 2013; Le *et al.*, 2017; Shadkam *et al.*, 2017). Furthermore, the MPT_{coarse} was found to influence the durability-related parameters of densely packed systems, especially the ones governed by transport mechanisms (Shadkam *et al.*, 2017).

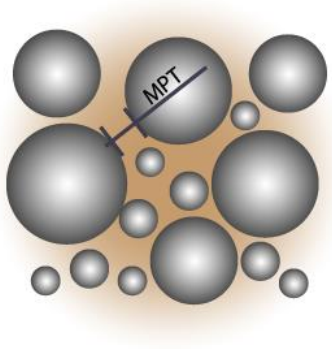

Figure 3.2. *Maximum Paste Thickness* of coarse aggregates.

$$MPT_{coarse} = D_{max}\left(\sqrt[3]{\frac{g^*}{g}} - 1\right) \qquad \textit{Equation 3.4}$$

Where MPT_{coarse} is the maximum distance between the coarse aggregates, D_{max} is the maximum aggregate size; g is the aggregate volume in a unit volume of concrete, which can be easily derived from the mixture proportioning; and g* is the packing density of the aggregates (assuming a granular mix) which can be calculated by Equation 3.5.

$$g^* = 1 - 0.45\left(\frac{D_{min}}{D_{max}}\right)^{0.19} \qquad \textit{Equation 3.5}$$

Where D_{min} is the minimum aggregate size corresponding to 10% passing, and D_{max} is the maximum aggregate size corresponding to 90% passing.

3.3.4. Eco-Efficiency in concrete

Regardless the mix-design adopted and the PC content, it is important to consider not only strength but also environmental impact. As a result, Damineli et al. (2010) developed an index, the so-called binder intensity (bi) factor, that evaluates PC efficiency. This index measures the eco-efficiency of a given mix by accounting for the amount of PC or binder required (BC in kg/m^3) to obtain 1 MPa of desired property such as compressive strength (f'c) (Equation 3.6).

$$bi = \frac{BC}{f'c} \qquad \textit{Equation 3.6}$$

Where BC is the amount of binder content and f'c is the compressive strength at a specific date (i.e. 28-day).

3.4. Scope of the Work

The main objective of this work is to evaluate the influence of continuous PPMs on the fresh and hardened state properties of low cement content (LCC) systems designed with different amounts of inert fillers and PC. A total of six concrete mixtures with PC contents equal to 282, 261, 214, 197, 161, and 149 kg per m^3 were mix-designed with distinct PPM approaches (i.e. Alfred model with one and two distribution factors - q). Fresh (i.e. slump, mixing energy, and rheological behaviour) and hardened (compressive strength, modulus of elasticity, porosity, and permeability) state properties were analyzed and a comparison among the distinct mixes is performed.

3.5. Materials and methods

3.5.1. Raw materials characterization

Six concrete mixtures were mix-designed through Alfred's model to achieve eco-efficient systems. Two types of sand (one natural sand with nominal maximum size (NMS) of 500 µm and another manufactured limestone sand with NMS of 4.75 mm) and a limestone coarse aggregate (NMS of 19mm) from Sao Paulo, Brazil were used in the research. ASTM C33 (ASTM C33, 2016a) was used to classify the different aggregate particles according to the selected Alfred's curves. First, the materials were sieved and quartered (ensuring a representative sampling). Then, the particle-size distribution (PSD) of particles smaller than 350 µm were determined through the use of laser diffraction analysis while particles greater than 350 µm were characterized through dynamic image techniques. The PSD of all the materials mentioned above is shown in Figure 3.3.

The final size fractions, based on ASTM C33, of the granular materials used presented the following ranges: cement and inert fillers (smaller than 100 µm), fine aggregates (100-150

µm; 150-300 µm, 300-600 µm, 600-1180 µm, 1180-2360 µm, 2360-4750 µm), and coarse aggregates (4750-9500 µm, 9500-12500 µm, and 12500-19000 µm) (ASTM C33, 2016b). A high early strength (type HE) PC from the Brazilian market (i.e. CPV-ARI) according to the National Brazilian Standard (NBR) 5733 was selected for the research (ABNT, 1991). The latter is similar to ASTM C150 type III CP (ASTM C150, 2018). A limestone filler was used as a partial replacement of PC for the mixes. Table 3.1 displays the chemical composition of the PC and inert filler used.

Table 3.1. PC chemical composition.

Material	Contents (%)								Loss on Ignition (%)
	Na_2O	MgO	Al_2O_3	SiO_2	Fe_2O_3	SO_3	K_2O	CaO	
Cement	0.33	2.63	5.01	21.1	2.64	2.86	0.85	60.1	3.36
Filler	-	5.64	0.4	4.16	<0.10	<0.10	<0.10	47.5	41.2

The specific gravity was determined through the helium gas (He) pycnometry test at a Multipicnometer equipment. The superficial surface area (SSA) was analyzed through BET method using nitrogen gas (N_2) and water vapour (H_2O).

Table 3.2 presents the results of the prior described procedures.

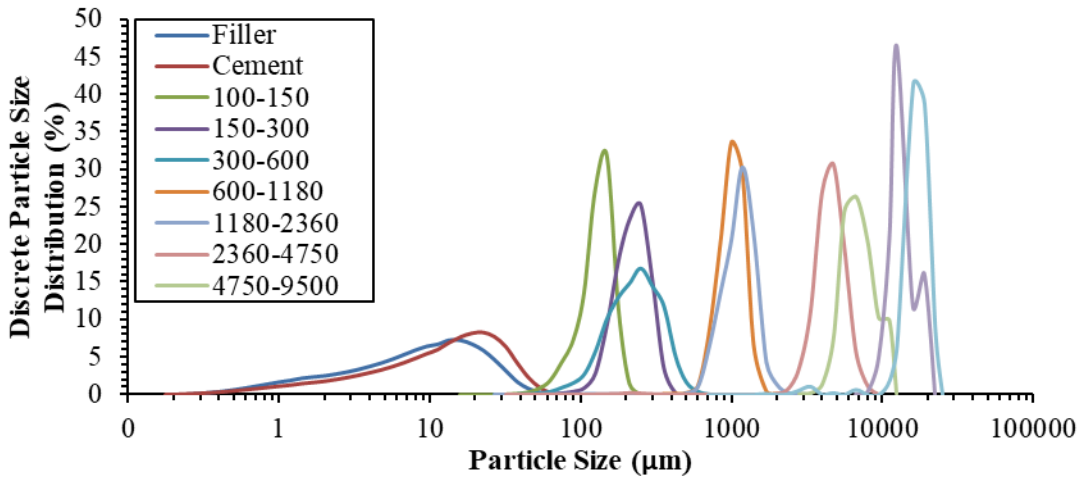

Note: F.A. = fine aggregate, C.A. = coarse aggregate

Figure 3.3. Particle size distribution of raw materials.

Table 3.2. Physical Materials Characterization.

Material (μm)		Mass (g)	Volume (cm^3)	Standard Deviation	Specific Gravity (g/cm^3)	Standard Deviation	SSA (m^2/g)
Filler D	<100	3.98	1.48	0.003	2.70	0.005	1.16
Cement	<100	16.49	5.31	0.003	3.11	0.001	1.30
Natural Sand	100-150	20.37	7.58	0.004	2.69	0.001	0.47
	150-300	21.49	8.07	0.002	2.66	0.001	0.23
	300-600	23.36	8.76	0.005	2.67	0.001	0.25
Man. Sand	600-1180	21.89	7.63	0.005	2.87	0.002	0.27
	1180-2360	22.52	7.85	0.007	2.87	0.003	0.25
Coarse Aggregate 1	2360-4750	146.68	53.74	0.063	2.73	0.003	0.12
	4750-9500	159.23	58.78	0.017	2.71	0.001	0.09
Coarse Aggregate 2	9500-12500	138.12	51.40	0.035	2.69	0.002	0.01
	12500-19000	161.11	59.87	0.037	2.69	0.002	0.01

3.5.2. Mix-design procedure

The mix-design techniques used in this research may be divided into two phases: a) first, three concrete mixtures were proportioned through Alfred's model using a coefficient of distribution (q) equal to 0.37. The smallest and largest size fractions considered were 5 μm and 19 mm, respectively. The binder content (i.e. PC in this work) selected for the mixes were equal to 149, 197, and 261kg/m^3, while the water to fines (w/f) ratio was kept constant as 0.5 aiming for a desirable fresh state performance as suggested in previous studies (John *et al.*, 2018). Fillers were used as a PC partial replacement by percentage since the PSD of the fillers and PC were quite similar. The amount of coarse and fine aggregates of the three mixtures was kept almost the same in volume; b) second, three concrete mixtures were mix-proportioned with a modified version of Alfred's model; i.e. breaking the PSD in two parts (i.e. the first from DS to 100 μm and the second from 100 μm to DL). Then two distinct distribution factors were selected: 0.37 for the coarser particles (greater than 100 μm) and 0.21 for the finer particles (smaller than 100 μm). The lower coefficient factor (0.21) selected for the first part of the PSD (i.e. fines fraction) aimed to improve the fresh state properties of the mixture. The PC content was kept the same as close to phase 1 as possible; however,

the amount of inert filler used this time is higher due to the low distribution factor adopted which brings more fines to the mix. In order to compare the concrete mixtures from the two phases, the same water to cement ratio was selected for phase 2 mixtures with similar PC contents. Otherwise, the w/f was kept constant equal to 0.3. The final CPFT calculated by Alfred's model is illustrated in Figure 3.4, while the mix-design proportioned of the six concrete mixtures are detailed in Table 3.3. It is worth noting that acronyms were given to the distinct mixes based on the PC content, coefficient of distribution coarse (c), and coefficient of distribution fine (f). For example, the concrete mixture with 282 kg/m^3 of the binder, 0.37 and 0.21 of distribution coefficient of coarse and fine, respectively, was labelled as C282-0.37c-0.21f.

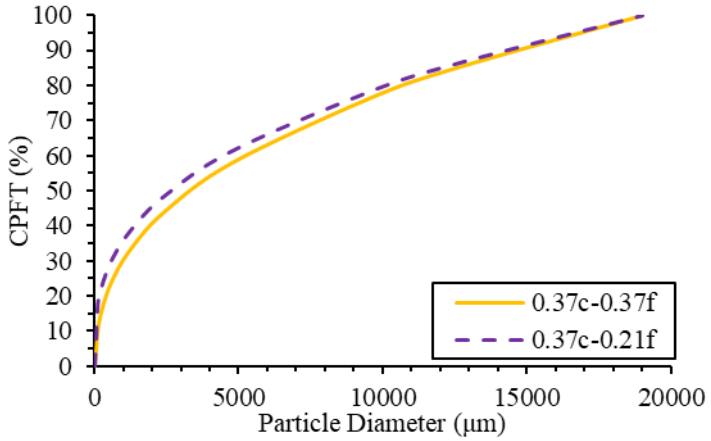

Figure 3.4. CPFT versus particle size for phase 1 and 2 concrete mixtures.

Table 3.3. Mix-design for the eco-efficient concrete mixtures.

Mixture Name	Cement (kg/m³)	Fine Aggregate (kg/m³)	Coarse Aggregate (kg/m³)	Filler (kg/m³)	Water (kg/m³)	Admixture (kg/m³)	W/F	W/C
C261-0.37c-0.37f	261	777	1275	0	140	1.35	0.5	0.5
C197-0.37c-0.37f	197	795	1304	61	120	1.31	0.5	0.6
C149-0.37c-0.37f	149	797	1308	104	118	1.28	0.5	0.8
C282-0.37c-0.21f	282	703	1153	143	152	2.03	0.3	0.5
C214-0.37c-0.21f	214	721	1182	212	131	1.99	0.3	0.6
C161-0.37c-0.21f	161	723	1186	259	128	1.95	0.3	0.8

Note: F.A. = fine aggregate, C.A. = coarse aggregate, w/c = water to cement ratio, and w/f = water to fines ratio.

Additionally, a polycarboxylate-based high range water reducer was used to increase the flowability of the mixtures in the fresh state. The amount of admixture used in all mixes was 0.5% of the mass of fines (i.e. particles smaller than 100 μm), as recommended by the supplier.

3.5.3. Fabrication and testing methods

Fifteen litres of all mixtures were mixed to evaluate the fresh state properties through rheological analysis. Eight 100 by 200 mm cylinders were then fabricated according to ASTM C 39 (ASTM C39, 1999). The specimens were demoulded after 24 hours, ground and cured in saturated limewater in a controlled room temperature of 25 ± 2 °C for 3 weeks. Then, the cylinders were moved to a dry controlled chamber with a temperature of 23 ± 2 °C and humidity of 50 ± 4% prior to testing.

3.5.4. Fresh state assessment

All the concrete ingredients were weighed and mixed using a planetary rheometer (Figure 3.5). The fresh state analyzes were divided into two measurements: mixing energy and viscosity as a function of the torque applied. Time dependence of the mixtures was also evaluated in all mixes. For the first measurements, six different concrete mixtures were mixed and assessed in the rheometer according to the stages described in Table 3.4. Thus, the maximum and final torque required to enable flow for each mixture was determined.

The second fresh state analysis appraises the whole rheological behaviour and profile of the six distinct concrete mixtures. The test protocol consists of shear-controlled time-step cycles that are applied to the mixtures until a shear rate of 1380 rpm (acceleration process) is reached and decreases at the same stepwise down to a shear rate of 35 rpm (deceleration process) as highlighted in Figure 3.6. The rotation speed was maintained constant for eight seconds in each step and the torque was determined at the average point of each of them. The main rheological parameters (i.e. viscosity, yield stress, and shear rate) were determined as a function of the shear stress applied.

Figure 3.5. Planetary rheometer used to evaluate the fresh state properties, an example for C-161-0.37c-0.21f.

Table 3.4. Stages of mixing eco-efficient concrete mixtures.

Step	Start (s)	End (s)	Duration (s)	Description	Rotation (rpm)
1	0	1	1	Initiation of the rheometer	
2	2	240	238	Mixing initiation - cement, filler, and F.A. added	127
3	241	301	60	Water and admixture (30s) added and mixing (30s)	127
4	302	452	150	Homogenization and mixing of mortar	127
5	453	603	150	Stop analysis: ensure that no powder is lost and stuck	0
6	604	854	250	Homogenization and mixing of mortar	127
7	855	985	130	Mortar cycle	6-253
8	986	1306	320	Concrete mixing	127

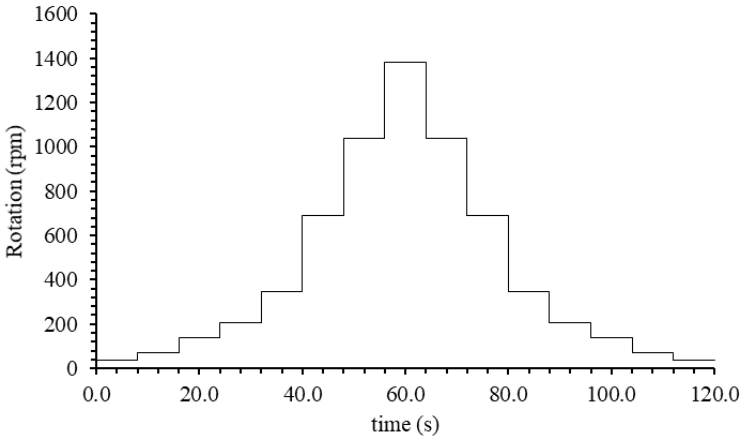

Figure 3.6. Shear history used to evaluate the fresh properties after the mixing stage.

3.5.5. Hardened state assessment

Compressive strength, dynamic modulus of elasticity, air permeability and porosity were the test procedures performed at 28 days on all samples. The compressive strength test was carried out on three specimens of each of the six concrete mixtures according to ASTM C 39 (ASTM C39, 1999).

The dynamic modulus of elasticity was determined by the ultrasonic pulse velocity (UPV) test using the Portable Ultrasound Non-Destructive Digital Indicating Tester (PUNDIT) aiming to evaluate the potential stiffness differences amongst the mixtures.

The air permeability test was carried out according to the vacuum-decay method (Innocentini *et al.*, 2001, 2003, 2009; Romano *et al.*, 2015). To allow a uniaxial air flux, the specimens were axially wrapped with plastic film (Figure 3.7). Then, a suction cup was connected to the specimen's ends in which a caulk mass was added to prevent air leakage during the test. The whole apparatus was connected to a data acquisition system and the results were monitored during the test. After the fixation of the suction cup, the air pump was turned on until negative pressure stabilization. Next, the pump was switched off and the pressure drop was monitored and recorded as a function of time. The permeability constant (Darcian - k_1) was determined from the Forchheimer model (Equation 3.7), considering negligible air-compressibility and only accounting the linear portion ($\mu.v_s/ k_1$).

$$\frac{\Delta P}{L} = \frac{\mu}{k_1} v_s + \frac{\rho}{k_2} {v_s}^2 \qquad \textit{Equation 3.7}$$

Where L is the specimen thickness, ΔP is the pressure variation, μ is the fluid viscosity, ρ is the fluid density, v_s is the speed of air-percolation, k_1 and k_2 is the Darcian and non-Darcian permeability, respectively.

It is worth noting that the first term ($\mu.v_s/ k_1$) represents the viscous effects of the fluid-solid interaction, while the second term ($\rho.v_s/ k_2$) accounts for the inertial effects.

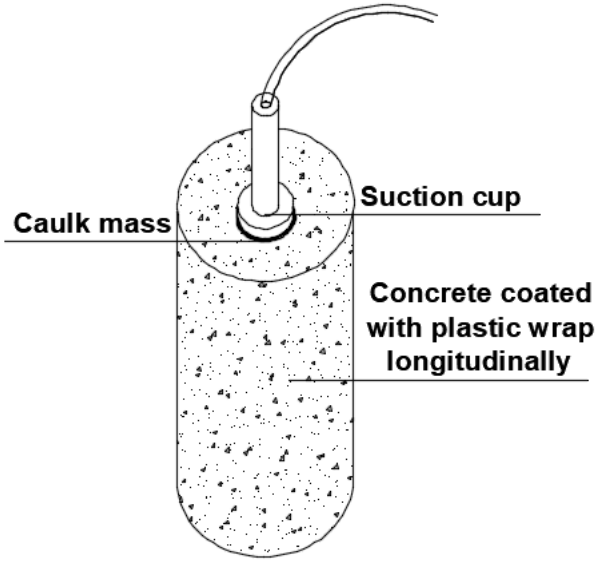

Figure 3.7. Air permeability test setup.

The porosity test was performed to compare the different properties of each concrete mixture. It was determined based on Archimedes immersion method (Romano *et al.*, 2015). First, specimens dry mass (m_d) was determined. Then, they were immersed in water and subjected to vacuum for the first two hours to ensure water penetration into the samples. After 24 hours of immersion, the immersed (m_i) and wet (m_w) mass values were determined. The apparent porosity (AP) was calculated by Equation 3.8.

$$\mathrm{AP}\ (\%) = \frac{m_w - m_i}{m_w - m_d} * 100\% \qquad \textit{Equation 3.8}$$

3.6. Results

3.6.1. Concrete mixing energy

Figure 3.8 presents the mixing energy of all concrete mixtures analyzed. It can be seen that before the addition of water (i.e. first half of the Fines region), the homogenization and mixing of fines resulted in the same torque. Nevertheless, when water was added, the concrete mixtures from phase 2 required higher torque than phase 1 mixtures. Moreover, all mixtures within the same phase presented the same torque; consequently, mixing energies until the concrete analysis. The maximum and final torque measured in the concrete analysis ranged from 12.65 to 8.21 (N.m), 9.34 to 9.72 (N.m), and constant 10.31 (N.m) for the phase 1 mixtures, C-261-0.37c-0.37f, C-197-0.37c-0.37f, and C-149-0.37c-0.37f, respectively. In phase 2, the torque results ranged from 12.65 to 4.59 (N.m), 12.74 to 12.06 (N.m), and 14.38 to 12.93 (N.m) for the mixtures C-282-0.37c-0.21f, C-214-0.37c-0.21f, and C-161-0.37c-0.21f, respectively. The mix-energy of these six distinct mixtures was equal to 5145, 5633, 5883, 6241, 8865, 9408 (N.m.s), respectively.

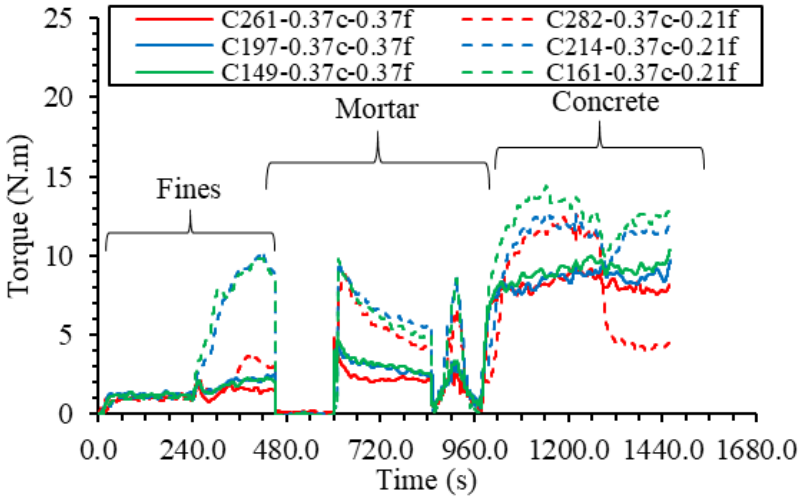

Figure 3.8. Rheological analysis of mortar and concrete mixture.

Analyzing the data above, one verifies that although a number of studies in the literature show that the "optimum packing" often results in negative effects on the fresh state properties (Dinger and Funk, 1994; Fennis and Walraven, 2012), it is clear that the energy

consumed during phase 1 mixtures (q=0.37) is considerably lower than phase 2 mixtures. Moreover, for phase 1 mixtures, the energy consumes did not seem to be impacted by PC content. Otherwise, for phase 2 mixtures, the higher the PC content, the lower the maximum and final torques, as expected.

Figure 3.9 displays the results obtained from the planetary rheometer during the shear test described in 4.4. All concrete mixtures from phase 1 presented an initial torque between 6 and 7.5 N.m indicating the presence of important yield stress. Two of the phase 2 mixtures showed a similar behaviour and thus slightly higher initial torques of around 7.3 and 8.5 N.m were found. Otherwise, C-282-0.37c-0.21f presented the lowest initial torque obtained (1.5 N.m). Furthermore, the phase 1 mixes presented a quite linear torque vs rotation behaviour and thus did not present important viscosity change as a function of the torque applied. Conversely, phase 2 mixtures presented a viscosity decrease as a function of the torque applied, behaving similarly to a shear thinning (pseudoplastic) material.

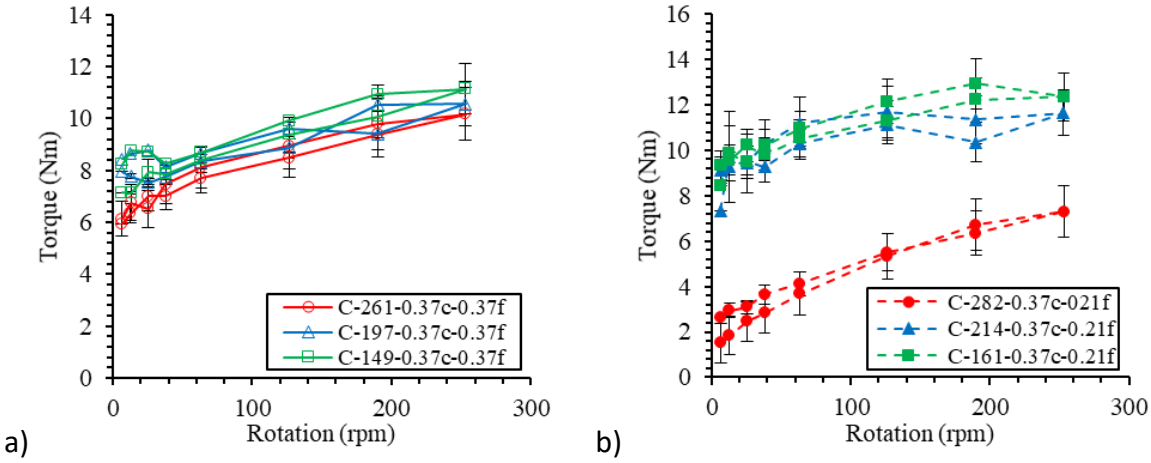

Figure 3.9. ***Hysteresis loop a) phase 1 b) phase 2***

The time dependence study of the mixtures is presented in Table 3.5. It is worth noting that time dependence evaluation is the search for “thixotropy” and/or “rheopexy” behaviours of suspensions. Thixotropy is a shear thinning time-dependent behaviour defined by the viscosity decrease as a function of the torque applied over time. Conversely, rheopexy mixtures present a shear thickening time-dependent behaviour defined by the viscosity

increase as a function of the torque applied over time (Han and Ferron, 2016; Ferraris *et al.*, 2017). Thus, tests were performed to evaluate the reversibility of viscosity variation over time with an increase of applied torque (Rubio-Hernández, Velázquez-Navarro and Ordóñez-Belloc, 2013).

Analyzing Table 3.5 results, one notices that all mixtures from phase 1 presented negative hysteresis area (HA) values, while mixtures from phase 2 showed positive HA results. The latter means that phase 1 mixtures presented a rheopexy behaviour since the HA is lower than zero, while phase 2 concrete mixtures presented a thixotropic behaviour since the HA is greater than zero (Filho *et al.*, 2016; Chauhan *et al.*, 2018).

Table 3.5. Concrete mixtures rheological properties

Concrete Name	Hysteresis Area (N.m.rpm)	Minimum Torque (N.m)	Apparent Viscosity (N.m/rpm)
C-261-0.37c-0.37f	-80.11	5.94	0.052
C-197-0.37c-0.37f	-21.87	7.55	0.049
C-149-0.37c-0.37f	-137.09	7.12	0.057
C-282-0.37c-0.21f	42.34	1.50	0.035
C-214-0.37c-0.21f	155.38	7.35	0.054
C-161-0.37c-0.21f	116.64	8.44	0.064

Moreover, Table 3.5 highlights the ratio between torque and rotation and the first deceleration point, known as apparent viscosity (AV). In phase 1, AV was maintained almost constant, while phase 2 mixtures showed an increase of AV with the decrease of PC, as expected.

3.6.2. Air-Permeability

Figure 3.10a and b display the effect of PC content and w/c on permeability, respectively. From Figure 3.10a, it can be seen that phase 1 concrete mixtures presented lower permeability responses than phase 2 mixes. The latter is likely found due to the higher amount of fillers used in mixtures from phase 2. Comparing phase 1 mixtures results, the higher the PC content, the higher the permeability found. On the other hand, phase 2

presented a downward trend, indicating the higher PC contents resulted in lower permeability.

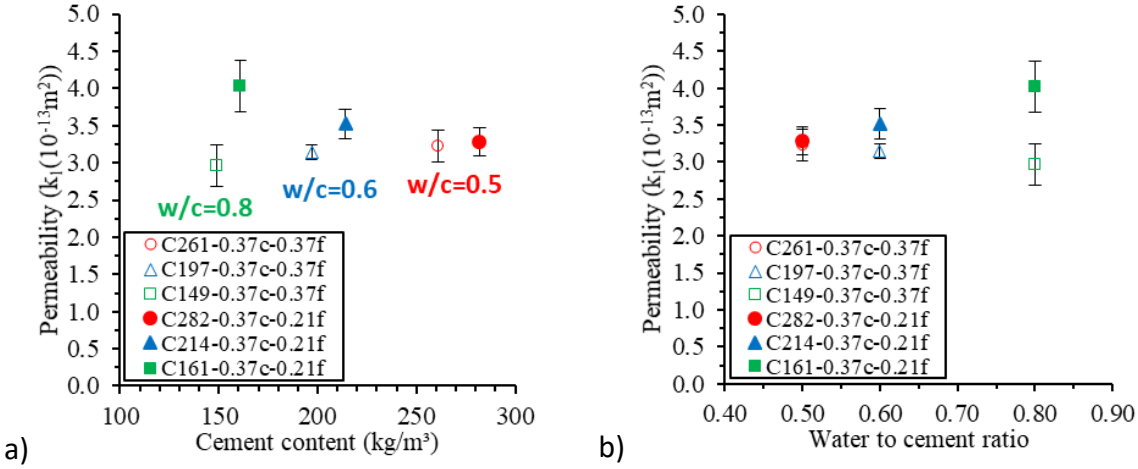

Figure 3.10. ***Relationship between permeability and a) cement content and b) w/c.***

It is well-known that w/c and pore size affects the matrix permeability (Innocentini *et al.*, 2001; Mehta and Paulo J M Monteiro, 2006; Lothenbach, Scrivener and Hooton, 2011). However, from Figure 3.10b one notices that phase 1 mixtures presented an almost constant permeability (3.1 x 10^{-13} m^2 ± 0.15) as a function of the w/c ratio. However, for phase 2 mixtures, the higher the w/c, the higher the permeability measured, as expected.

3.6.3. Porosity

Figure 3.11a and b display the comparison between AP vs PC and AP vs w/c, respectively, of the six different concrete mixtures studied. It can be seen that the reduction of PC content (hydration products) resulted in an increase of AP. Moreover, similarly to the permeability, the higher the w/c, the higher the porosity of the mixtures, as expected. Analyzing both phases, phase 2 mixtures displayed on average AP values 1.35 times higher than phase 1 mixtures. The two mixtures that presented higher porosity were C-149-0.37c-0.37f and C-161-0.37c-0.21f, which is equal to approximately 6.7 and 8%, respectively. Furthermore, mixes C-197-0.37c-0.37f and C-261-0.37c-0.37f achieved similar APs of around 3.5%, while mixes C-214-0.37c-0.21f and C-282-0.37c-0.21f showed identical APs of 5.3%.

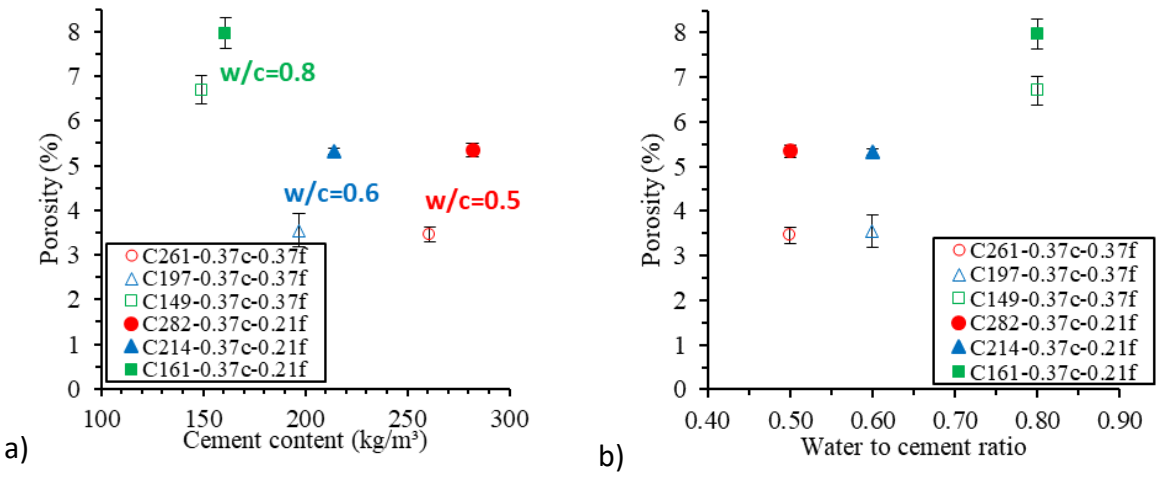

Figure 3.11. ***Comparison between apparent porosity and a) cement content and b) w/c.***

3.6.4. Compressive Strength

Figure 3.12 highlights the 28-day compressive strength results of the six concrete mixtures evaluated as a function of the cement content and the water to cement ratio. The compressive strength values of phase 1 mixtures ranged from 43 MPa for C-149-0.37c-0.37f mixture to 66 MPa for the C-261-0.37c-0.37f mix, whereas phase 2 mixtures displayed a compressive strength ranging from 49 MPa to 70 MPa for mixtures C-161-0.37c-0.21f and C-282-0.37c-0.21f, respectively.

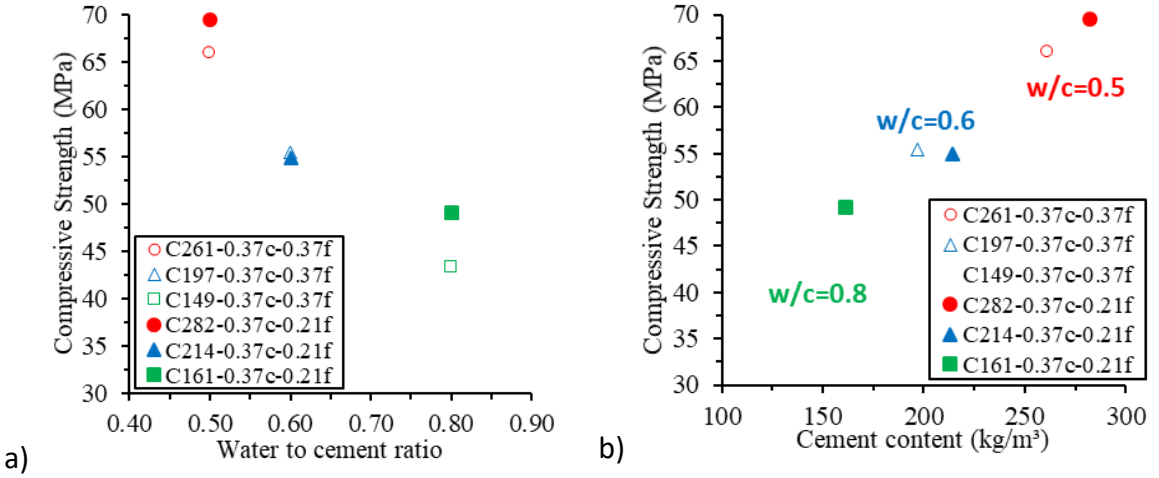

Figure 3.12. ***Correlation of compressive strength with a) w/c and b) cement content.***

Figure 3.12a shows that the higher the water to cement ratio, the lower the compressive strength for all mixes, as expected and according to Abrams law (Mehta and Paulo J M Monteiro, 2006; Helene and Tutikian, 2011; Han and Ferron, 2016; Ferraris *et al.*, 2017; Shadkam *et al.*, 2017). Furthermore, analyzing Figure 3.12b one verifies that higher compressive strength results were reached while the use of higher amounts of PC for both phases 1 and 2 mixes. However, as previously mentioned, a full comparison among the distinct mixes cannot be directly made since they were proportioned with different water to cement ratios. Therefore, proper comparison is only performed between phase 1 and 2 mixes with the same PC amount. Hence, whether the latter is performed, one notices that phase 2 mixtures, the ones presenting higher amounts of inert fillers, showed greater compressive strength when compared to phase 1 mixes (i.e. 5% on average).

3.6.5. Dynamic modulus of elasticity

Figure 3.13a and b display the correlation of dynamic modulus of elasticity with cement content and w/c, respectively. The modulus of elasticity values of phase 1 mixtures ranged from 46.5 GPa for C-149-0.37c-0.37f and C-197-0.37c-0.37f mixtures to 54.7 GPa for the mix C-261-0.37c-0.37f, whereas phase 2 mixtures displayed a modulus of elasticity ranging from 51.9 GPa to 53.5 GPa for mixtures C-161-0.37c-0.21f and C-282-0.37c-0.21f, respectively.

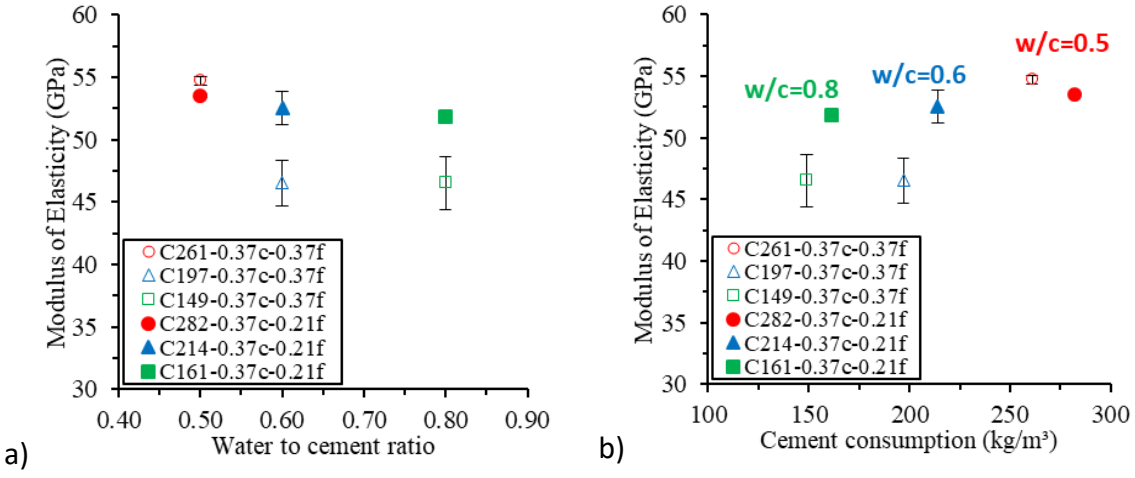

Figure 3.13. ***Correlation of Modulus of Elasticity with a) w/c and b) cement content.***

Figure 3.13a displays the modulus of elasticity results as a function of the water to cement ratio. Looking the data gathered, one verifies that the higher the w/c the lower the modulus of elasticity of all mixtures, as expected. However, this pattern was found to be more evident in phase 1 mixtures. Otherwise, the higher the PC amount, the higher the modulus of elasticity found for all mixtures. Nonetheless, as for the compressive strength results, the comparison among all the distinct mixtures cannot be directly made due to their different microstructure brought by the use of different water to cement ratios. Therefore, comparing only phases 1 and 2 mixtures with the same PC content (and thus same w/c) one attests that phase 2 mixtures, presenting higher amounts of inert fillers showed higher stiffness when compared to phase 1 mixes.

3.7. DISCUSSION

3.7.1. Packing density, MPT, and IPS

Studies show that using Alfred's model, the optimum packing density is achieved when the distribution factor is equal to 0.37 (Dinger and Funk, 1994; Fennis and Walraven, 2012). Figure 3.14 shows the correlation between the coefficient of distribution q and the packing density of granular systems calculated according to Westman and Hugill model (Dinger and Funk, 1994). Considering an ideal continuous model (i.e. no gap within the PSD and considering all particles completely spherical) with a coefficient of distribution equal to 0.37, the interparticle porosity obtained by Westman and Hugill model is about 0.63%. Moreover, the mobility parameters MPT and IPS calculated are equal to 1.57 µm and 0.82 µm, respectively. However, the PSD of a "real" system does not represent a uniform ideal continuous model and for that reason, the system presents much greater porosity and different MPT and IPS values. The two mobility parameters and packing densities of all mixtures are presented in Table 3.6.

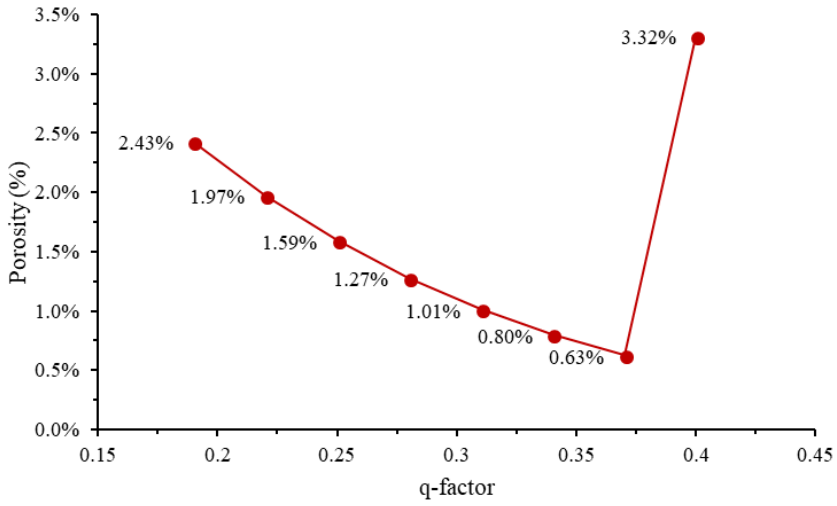

Figure 3.14. ***Relationship between Alfred q-factor and porosity.***

Analyzing Table 3.6 data, it is possible to notice that the higher the PC content, the higher the MPT and IPS values, as expected since there is a higher amount of cement paste and water to separate the fine and coarse particles. Moreover, lower IPS results were obtained in phase 2 mixes when compared to phase 1 due to the higher amounts of fillers used in the second type of mixtures. MPT showed an opposite behaviour and thus higher values were obtained for phase 2 mixtures likely due to the higher amount of fines and thus higher paste thickness between coarser particles.

Table 3.6. Mobility parameters, porosity and fresh state properties concrete mixtures.

Parameters	**C-261-0.37c-0.37f**	**C-197-0.37c-0.37f**	**C-149-0.37c-0.37f**
Calculated Porosity (%)	17.9%	17.9%	17.9%
IPS (µm)	0.81	0.76	0.74
MPT (µm)	0.45	0.29	0.26
Slump (mm)	13.0	11.0	6.0
Parameters	**C-282-0.37c-0.21f**	**C-214-0.37c-0.21f**	**C-161-0.37c-0.21f**
Calculated Porosity (%)	15.9%	15.2%	14.7%
IPS (µm)	0.55	0.40	0.36
MPT (µm)	1.38	1.43	1.58
Slump (mm)	155.0	0.0	0.0

The consistency of all mixtures measured through slump tests, which measure indirectly their yield stress, was also assessed. Lower consistency values were obtained with higher PC

contents, which seems to demonstrate that PC acted as a lubricant to the materials studied in this work. Conversely, the porosity of the system did not vary as a function of PC for phase 1 mixtures whereas slightly decreased with the PC decrease in phase 2 mixes. Furthermore, phase 2 mixes presented slightly less porosity than phase 1 mixtures, which could be linked at least partially to the use of fillers as a PC replacement. Figure 3.15 illustrates the volumetric fractions of the different components of all six mixtures for a better visualization of the above discussion.

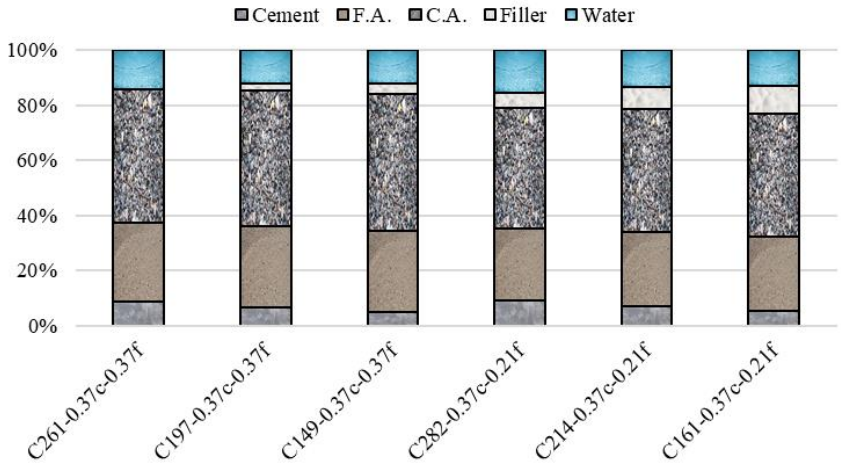

Figure 3.15. Volume of each material on eco-efficient concrete mixtures.

3.7.2. Fresh state

A number of literature works consider that cement based-materials often follow a Bingham rheological model, in which a linear shear stress vs shear rate relationship is found (Bao, Lavrov and Møll Nilsen, 2017; Ferraris *et al.*, 2017). In other words, the viscosity of Bingham mixtures does not change as a function of the torque applied (Bao, Lavrov and Møll Nilsen, 2017; Ferraris *et al.*, 2017). However, granular suspensions such as concrete can also present different rheological behaviours where the viscosity changes according to the torque applied; examples of the latter are shear thinning and shear thickening behaviours. Shear thinning mixtures have their viscosity decreased with the increase in shear stress whereas shear thickening mixes have their viscosity increased by the increase in shear stress.

Normally in concrete technology, the Ostwald-de Waele model, also known as the power-law model (Equation 3.9), is the model used to evaluate nonlinear suspensions (Alfani *et al.*, 2007; Bao, Lavrov and Møll Nilsen, 2017).

$$\tau = \tau_0 + \gamma^n \qquad \textit{Equation 3.9}$$

Where: τ is the torque, τ_o is the yield torque, γ is the rotation, and n is flow behaviour factor. The flow behaviour factor (n) is lower than 1 for shear thinning (pseudoplastic) suspensions while greater than 1 for shear thickening (dilatant) suspensions (Bao, Lavrov and Møll Nilsen, 2017).

Figure 3.16 shows the comparison between the six shear stress vs shear rate behaviours obtained for the distinct mixes. Looking at the below data, one verifies that all the mixtures present a shear thinning behaviour where the viscosity (slope of the curve) decreases as a function of the shear stress. Shear thinning or pseudoplastic mixtures are often recommended for applications under high torque regimes such as pumping and or vibrating processes (Pileggi and Pandolfelli, 2002).

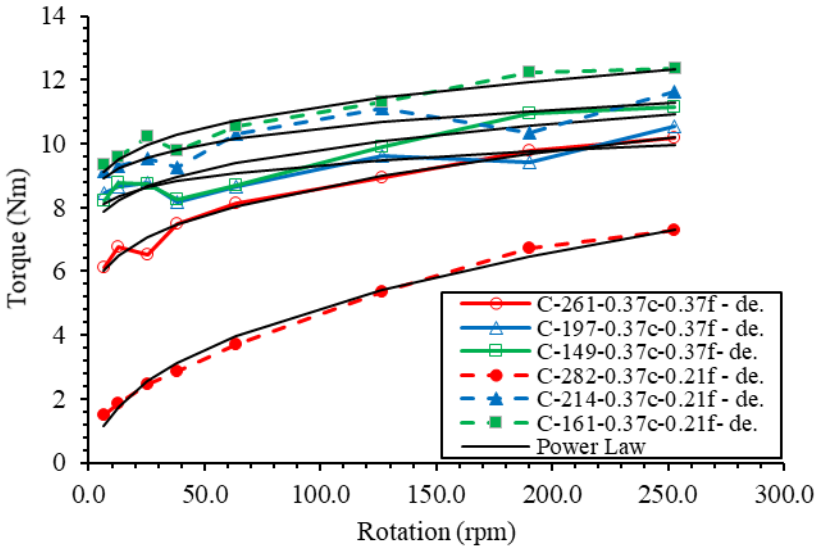

Figure 3.16. ***Rheological behaviour of eco-efficient concrete compared to power law.***

Yield stress is defined as the minimum and initial torque enabling flow. As previously mentioned the slump test is an indirect qualitative measurement of the yield stress of

concrete mixtures since it measures the flow of mixes under their self-weight. Thus, if a given mix is self-levelling, it means that its yield stress is zero. Otherwise, the latter is different from zero.

Considering Figure 3.16 data, all mixtures resulted in a yield stress of around 8N.m, except C-282-0.37c-0.21f which presented yield stress close to zero. Likewise, the prior mix presented the highest slump measured among the mixtures studied (i.e. 155 mm) which is likely linked to its PC amount that acted as a lubricant.

Figure 3.17 gives a plot on the correlation between the mixing energy and mobility parameters calculated from the six different mixtures.

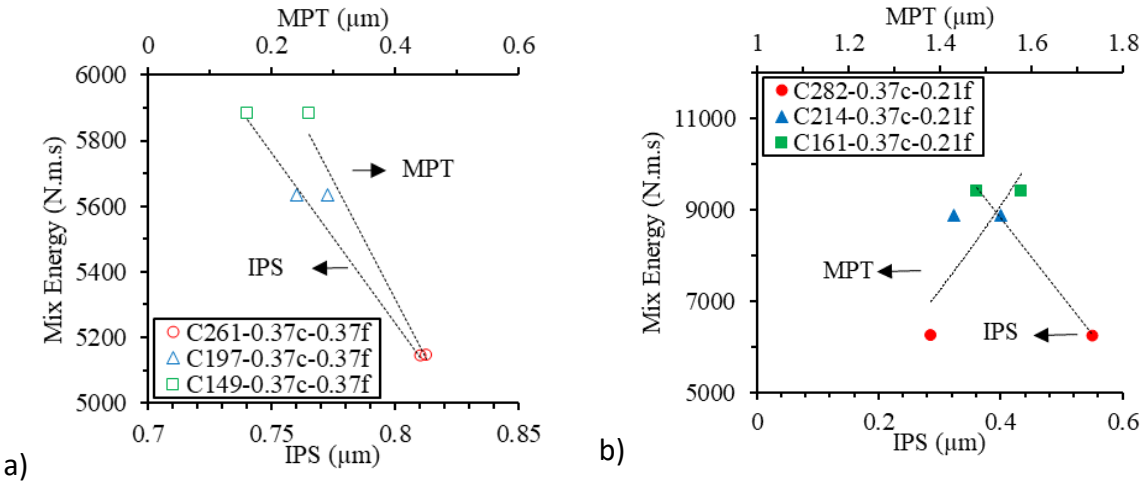

Figure 3.17. ***Correlation of mix energy and mobility parameters a) phase 1, b) phase 2.***

Evaluating the plot, one verifies that the higher the IPS and MPT, the lower the mixing energy implemented in the system to enable flow. The latter is intuitive since greater IPS and MPT provide more space and improve mobility amongst the particles, leading to less energy required to enable flow. The mixing energy results obtained for phase 2 mixtures were higher than phase 1, which may be explained by the lower IPS values of those mixtures and seems to demonstrate that the overall fresh state behaviour of the six studies concrete mixes was more governed by IPS than MPT. Finally, the greater the PC content the lower the mixing energy required for all, as expected.

3.7.3. Hardened state behaviour

It is well established that the mechanical properties (particularly the compressive strength) of conventional concrete is directly affected by w/c (Abram's law), since the latter influences the porosity and microstructure of the hardened material (Mehta and Paulo J M Monteiro, 2006; Helene and Tutikian, 2011; Han and Ferron, 2016; Ferraris *et al.*, 2017; Shadkam *et al.*, 2017). However, in this research, advanced PPM techniques were adopted to mix-proportion densely packed systems with a reduced amount of PC and high amount of inert fillers. Thus, one may think that the sole use of Abrams law would not be enough to explain the distinct behaviour found in the hardened state, as reported in previous studies (John *et al.*, 2018).

Figure 3.18a and b give a plot on the correlation between the hardened properties studied (i.e. permeability, apparent porosity, compressive strength and modulus of elasticity) and some parameters selected for analysis (i.e. MPT_{coarse}, w/f and w/c).

Analyzing Figure 3.18, one verifies that although previous research had pointed out the influence of the MPT_{coarse} on the mechanical properties of concrete (i.e. compressive strength and modulus of elasticity (De Larrard and Belloc, 1997), this relationship could not be captured in this work and it seems that the hardened state properties varied almost independently of the MPT_{coarse} results.

On the other hand, John *et al.* (2018) verified that in concrete mixtures mix-proportioned with moderate to high amounts of inert fillers, Abrams law is not directly applied and thus the correlation between compressive strength and w/c is not clear anymore; instead the authors suggested the use of the water to fines ratio in this regard (John *et al.*, 2018). If one evaluates the w/f values for the different mixtures studied in this research one may notice that phase 2 mixes (w/f = 0.3) presented slightly higher compressive strengths and stiffness than phase 1 mixtures (w/c = 0.5), which seems to demonstrate the importance of this variable. Nevertheless, Abrams law seemed to keep governing the systems evaluated since the higher the w/c, the lower the compressive strength and stiffness of all mixes. Therefore,

it seems that w/c and w/f are the most promising variables to assess the mechanical properties of densely packed LCC systems.

Conversely, the measured values of porosity and permeability of phase 1 mixtures were lower (and thus better) than the results obtained for phase 2 mixes. The latter seems to be related to the better pack density of phase 1 systems which were obtained through the use of optimum distribution factors of 0.37. Moreover, the MPT_{coarse} results for phase 2 mixtures are higher than phase 1 mixes which demonstrate that the higher paste thickness among the coarse aggregate particles may result in high permeable and porous media. Therefore, one may claim that the phase 1 mixtures would present improved durability-related properties when compared to phase 2 mixes, especially in cases related to transport mechanisms

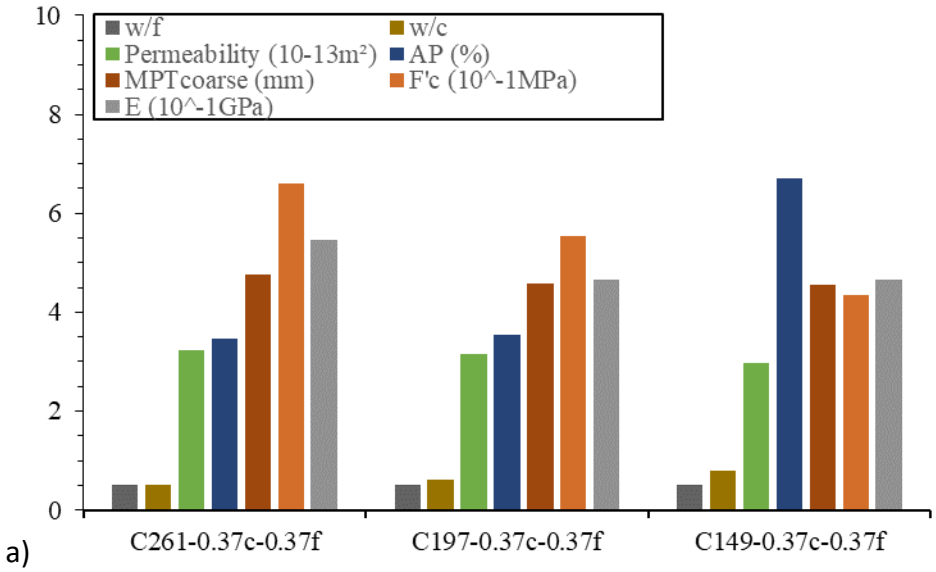

a)

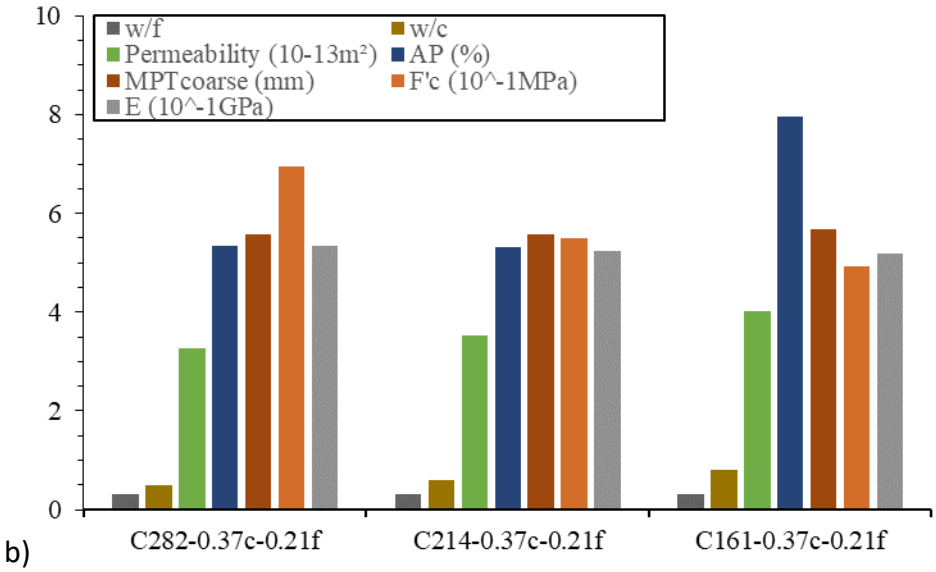

Figure 3.18. Comparison between several properties studied a) phase 1 and b) phase 2.

3.7.4. Binder Intensity

Figure 3.19 shows a summary of international records correlating bi with compressive strength. It is important to note that most of the conventional concrete (20-40 MPa) produced worldwide are proportioned with moderate to high amounts of cement (i.e. higher than the 250 kg/m^3 bottom line), presenting higher bi factors than the values considered as eco-efficient (i.e. 10 kg/m^3. MPa^{-1} (Damineli *et al.*, 2010; Damineli and John, 2012). Considering the concrete mixes investigated in this work and plotting them against the international record, one notices that all of them may be considered eco-efficient, with bi values lower than 5 kg/m^3. MPa$^{-1.}$ The latter highlights the importance of using high amount of fines in the mix (i.e. fillers) along with the importance of a proper mix-design technique such as PPMs. Moreover, these values might have been even lower while the use of supplementary cementing materials (SCMs) and or different types of fillers.

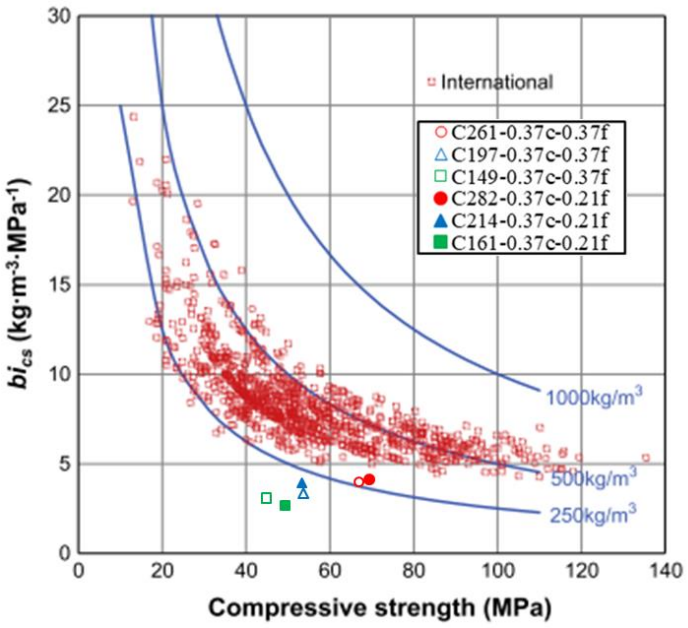

Figure 3.19. Relationship between binder intensity and compressive strength at 28-days with international records adapted from (Damineli et al., 2010).

3.8. CONCLUSION

The main goal of the current research was to better understand the effect of PPMs on the fresh and hardened properties of LCC systems. The primary conclusions of the work are presented hereafter:

- PPM is a successful technique that may be used to mix-proportion high densely packed and eco-efficient systems.
- All the LCC mixtures studied in this work presented a shear thinning behaviour and thus might be used in applications under high torque regimes such as pumped and/or vibrated concrete. However, the consistency values obtained throughout this research program can be considered high in the market, except for the mix C-282-0.37c-0.21f. Yet, the latter means the inefficiency of the slump test to forecast the rheological behaviour of concrete under different torque regimes.

- It has been found that the sole use of Abrams law is not enough to explain the hardened state behaviour of densely packed mixtures with a reduced amount of cement. However, the water to fines ratio (w/f) looks a promising alternative to be combined with the w/c while the mechanical properties evaluation of LCC systems.
- Densely packed systems through the use of PPMs and distribution factor of 0.37 seem to present the best durability-related properties (in regard to transport mechanisms) among the mixes studied. The latter is likely due to the overall lower porosity, permeability along with lower MPT_{coarse} of these mixtures.
- The fresh state, mechanical properties and eco-efficiency of PPMs mix-designed concrete seems quite interesting. However, the long-term behaviour of LCC systems with high amounts of filler and reduced PC content is still unknown and should be further investigated.

3.9. ACKNOWLEDGMENTS

The authors gratefully acknowledge the financial support from the University of Ottawa for the international experience scholarship, Mitacs for the Mitacs Globalink, Research Award Natural Sciences and Engineering Research Council of Canada (NSERC), and Laboratory of Microstructure and Material Eco-efficiency – LME.

3.10. REFERENCES

ABNT (1991) NBR 5733: Cimento Portland com Alta Resistencia Inicial. Rio de Janeiro, Brazil.

Adamczyk, Z. (2017) Particles at interfaces : interactions, deposition, structure. Second, Potential Interactions Among Particles. Second. London : Academic Press.

Alfani, R. et al. (2007) 'The use of the capillary rheometer for the rheological evaluation of extrudable cement-based materials'.

ASTM C150 (2018) 'Standard Specification for Portland Cement'. West Conshohocken.

ASTM C33 (2016) 'Standard Specification for Concrete Aggregates'. United States.

ASTM C39 (1999) ‘Standard Test Method for Compressive Strength of Cylindrical Concrete Specimens’, ASTM C39, American Society for Testing and Materials.

Bao, K., Lavrov, A. and Møll Nilsen, H. (2017) ‘Numerical modeling of non-Newtonian fluid flow in fractures and porous media’, Comput Geosci, 21, pp. 1313–1324.

Bonadia, P. et al. (1999) ‘Maximum paste thickness (MPT) principle applied to high alumina refractory castables’, Cerâmica. Associação Brasileira de Cerâmica, 45(291), pp. 24–28.

Castro, A. K. and Pandolfelli, V. C. (2009) ‘Review: Concepts of particle dispersion and packing for special concretes production’, 18 Cerâmica, 55, pp. 18–32.

Cesar De Oliveira Romano, R. et al. (2015) ‘Impact of aggregate grading and air-entrainment on the properties of fresh and hardened mortars’.

Chauhan, G. et al. (2018) ‘Rheological studies and optimization of Herschel-Bulkley flow parameters of viscous karaya polymer suspensions using GA and PSO algorithms’, Rheologica Acta, 57, pp. 267–285.

Chen, Y.-Y. et al. (2013) ‘Effect of paste amount on the properties of self-consolidating concrete containing fly ash and slag’, Construction and Building Materials, 47, pp. 340–346.

Damineli, B. L. et al. (2010) ‘Measuring the eco-efficiency of cement use’, Cement and Concrete Composites, 32, pp. 555–562.

Damineli, B. L. et al. (2016) ‘Viscosity prediction of cement-filler suspensions using interference model: A route for binder efficiency enhancement’, Cement and Concrete Research, 84, pp. 8–19.

Damineli, B. L. and John, V. M. (2012) ‘Developing Low CO2 Concretes: Is Clinker Replacement Sufficient? The Need of Cement Use Efficiency Improvement’, in Key Engineering Materials. Trans Tech Publications, pp. 342–351.

Dinger, D. and Funk, J. (1994) Predictive process control of crowded particulate suspensions. 1st edn. Edited by S. S. + B. M. LLC. New York.

Fennis, S. A. A. M. and Walraven, J. C. (2012) ‘Using particle packing technology for sustainable concrete mixture design’, Heron, 57(2), pp. 73–101.

Ferraris, C. F. et al. (2017) ‘Role of Rheology in Achieving Successful Concrete Performance’, (June), pp. 43–51.

Filho, R. S. A. et al. (2016) ‘Evaluating the applicability of rheometry in steel fiber reinforced self-compacting concretes’, Ibracon structures and materials journal, 9(6), pp. 969–988.

Gonçalves, M. C. and Margarido, F. (2015) Materials for Construction And Civil Engineering : Science, Processing, And Design. Springer International Publishing.

Han, D. and Ferron, R. D. (2016) 'Influence of high mixing intensity on rheology, hydration, and microstructure of fresh state cement paste', Cement and Concrete Research, 84, pp. 95–106.

Hasanbeigi, A., Price, L. and Lin, E. (2012) 'Emerging Energy-Efficiency and CO2 Emission-Reduction Technologies for Cement and Concrete Production: A Technical Review', Renewable and Sustainable Energy Reviews. Elsevier, 16(8), pp. 6220–6238.

Helene, P. and Tutikian, B. F. (2011) 'Dosagem dos Concretos de Cimento Portland', in Cechella Isaia, G. (ed.) Concreto: Ciência e Tecnologia. 1st edn. São Paulo: Ibracon, pp. 415–451.

Imbabi, M. S., Carrigan, C. and Mckenna, S. (2012) 'Trends and developments in green cement and concrete technology', International Journal of Sustainable Built Environment, 1, pp. 194–216.

Innocentini, M. et al. (2001) 'Effect of particle size distribution on the drying behavior of refractory castables', Ceramica, 47(304).

Innocentini, M. D. et al. (2009) 'Permeability optimization and performance evaluation of hot aerosol filters made using foam incorporated alumina suspension', Journal of Hazardous Materials, 162, pp. 212–221.

Innocentini, M. D. M. et al. (2003) 'PSD-Designed refractory castables', Am. Ceram. Soc. Bull., 82(7), p. 9401–9406.

John, V. M. et al. (2018) 'Fillers in cementitious materials — Experience, recent advances and future potential', Cement and Concrete Research, in press.

Juenger, M. C. G. and Siddique, R. (2015) 'Recent advances in understanding the role of supplementary cementitious materials in concrete', Cement and Concrete Research, 78, pp. 71–80.

Knop, Y. and Peled, A. (2016a) 'Packing density modeling of blended cement with limestone having different particle sizes', Construction and Building Materials. Elsevier Ltd, 102, pp. 44–50.

Knop, Y. and Peled, A. (2016b) 'Setting behavior of blended cement with limestone: influence of particle size and content', Materials and Structures, 49, pp. 439–452.

Kosmatka, S. H., Kerkhoff, B. and Panarese, W. C. (2002) 'Designing and Proportioning Normal Concrete Mixtures', in Design and Control of Concrete Mixtures. Portland Cement Association, pp. 151–172.

De Larrard, F. and Belloc, A. (1997) 'The influence of aggregate on the compressive strength of normal and high-strength concrete', ACI Materials Journal, 94(5), pp. 417–426.

Le, T. et al. (2017) 'Hardened behavior of mortar based on recycled aggregate: Influence of saturation state at macro- and microscopic scales'.

Limbachiya, M., Bostanci, S. C. and Kew, H. (2014) 'Suitability of BS EN 197-1 CEM II and CEM V cement for production of low carbon concrete', Construction and Building Materials, 71, pp. 397–405.

Lothenbach, B., Scrivener, K. and Hooton, R. D. (2011) 'Supplementary cementitious materials', Cement and Concrete Research, 41, pp. 217–229.

Makul, N. and Sua-Iam, G. (2018) 'Effect of granular urea on the properties of self-consolidating concrete incorporating untreated rice husk ash: Flowability, compressive strength and temperature rise', Construction and Building Materials, 162, pp. 489–502.

Mangulkar, M. N. and Jamkar, S. S. (2013) 'Review of Particle Packing Theories Used For Concrete Mix Proportioning', International Journal Of Scientific & Engineering Research, 4(5).

Mehta, P. K. and Monteiro, P. J. M. (2006) Concrete: microstructure, properties, and materials, Concrete.

Monteiro, P. J. M., Helene, P. R. L. and Kang, S. (1993) 'Designing concrete mixtures for strength, elastic modulus and fracture energy', Materials and Structures, 26, pp. 443–452.

Naik, T. R. et al. (1996) 'Permeability of high-strength concrete containing low cement factor', Journal of Energy Engineering, 122(1), pp. 21–39.

Neville, A. M. (2011) Properties of Concrete. Pearson Education Limited.

Noël, M., Sanchez, L. and Fathifazl, G. (2016) 'Recent Advances in Sustainable Concrete for Structural Applications', in Sustainable Construction Materials & Technologies 4, p. 10.

Oliveira, I. R. et al. (2000) Dispersão e Empacotamento de Partículas. São Paulo: Fazendo Arte Editorial.

Pileggi, R. G. and Pandolfelli, V. C. (2002) 'Rheology and particle size distribution of pumpable refractory castables', Cerâmica, 48(305), pp. 11–16.

Romano, R. C. O. et al. (2008) 'Influence of the dispersion process in the silica fume properties', Cerâmica, 54, pp. 456–461.

Rubio-Hernández, F. J., Velázquez-Navarro, J. F. and Ordóñez-Belloc, L. M. (2013) 'Rheology of concrete: a study case based upon the use of the concrete equivalent mortar', Materials and Structures, 46, pp. 587–605.

Shabab, M. E. et al. (2016) 'Synergistic Effect of Fly Ash and Bentonite as Partial Replacement of Cement in Mass Concrete', Korean Society of Civil Engineers, 20(5), pp. 1987–1995.

Shadkam, H. R. et al. (2017) ‘An investigation of the effects of limestone powder and Viscosity Modifying Agent in durability related parameters of self-consolidating concrete (SCC)’, Construction and Building Materials, 156, pp. 152–160.

ßat, K., Alyamaç, E. and Ince, R. (2008) ‘A preliminary concrete mix design for SCC with marble powders’, Construction and Building Materials, 23, pp. 1201–1210.

Statista (2018) U.S. and world cement production 2017, Statista. Available at: https://www.statista.com/statistics/219343/cement-production-worldwide/ (Accessed: 2 May 2018).

Varhen, C. et al. (2016) ‘Effect of the substitution of cement by limestone filler on the rheological behaviour and shrinkage of microconcretes’, Construction and Building Materials, 125, pp. 375–386.

Wen, Z. et al. (2016) ‘Design and Preparation of High Elastic Modulus Self-compacting Concrete for Pre-stressed Mass Concrete Structures’, Journal of Wuhan University of Technology.

Zachar, J. and Asce, M. (2011) ‘Sustainable and Economical Precast and Prestressed Concrete Using Fly Ash as a Cement Replacement’, J. Mat. in Civil Engineering, 23(6), pp. 789–792.

Chapter Four: Influence of the Amount of Cement on the Fresh and Hardened State Properties of Low-Cement Content (LCC) Systems

Mayra Grazia[1*], Leandro Sanchez[1], Roberto Romano[2], Rafael Pileggi[2]

[1]Department of Civil Engineering, University of Ottawa, CANADA

[2]Department of Civil Engineering, Polytechnic School, University of São Paulo, BRAZIL

4.1. Abstract

Portland cement (PC), likely the major concrete constituent, is responsible for about 6.5% of the total carbon dioxide (CO_2) emissions worldwide. Therefore, recent studies have been focusing on alternatives to decrease PC content and thus reduce the carbon footprint of concrete construction. Although guidelines suggest a minimum cement content of approximately 250-300 kg/m³, depending on the type of the structure/structural member, there is currently a lack of information on the impact of the amount of cement on the overall behaviour of concrete. This work evaluates the influence of the cement content on the fresh (i.e. rheological behaviour) and hardened (i.e. compressive strength, dynamic and static modulus of elasticity, porosity and permeability) properties of concrete mixtures produced with low to moderate (i.e. 54, 159, and 260 kg/m³) PC amounts. Results show that is possible to produce eco-efficient concrete without compromising the fresh and hardened states of the material. Yet, the durability and long-term properties of the low-cement content (LCC) systems still need to be further appraised.

Keywords: Low cement content; eco-efficient concrete; particle size distribution; *Maximum Paste Thickness*; permeability; modulus of elasticity; binder intensity; rheological model.

4.2. Introduction

Concrete is likely one of the most energy-efficient construction materials currently used in the construction industry. However, it produces approximately 7% of carbon dioxide (CO_2) released annually, wherein Portland cement (PC) production is already responsible for about 6.5% (Limbachiya, Bostanci and Kew, 2014). Therefore, reducing PC in concrete mixtures impacts directly on CO_2 emissions since a ton of PC produces approximately one ton of CO_2 [4]–[6]. Moreover, a number of different issues may be raised by the use of moderate to high amounts of PC in concrete such as temperature rise and volumetric instability (Shabab *et al.*, 2016; Wen *et al.*, 2016; Makul and Sua-Iam, 2018).

The environmental impact caused by concrete can be mitigated by a number of different strategies such as the use of supplementary cementing materials (SCMs; e.g. silica fume, fly ash, blast furnace slag, natural pozzolans, etc.) and or inert fillers. Using SCMs as a partial replacement of PC often results in improvements on the fresh and hardened states of concrete (Zachar and Asce, 2011; Juenger and Siddique, 2015). However, the availability of SCMs worldwide is not enough to match the demand of PC. Moreover, some SCMs types are depleting over the years due to the closure of industries responsible for producing these residues (Damineli and John, 2012; Noël, Sanchez and Fathifazl, 2016). Likewise, it has been found that the use of inert fillers (IF) either as a partial PC replacement or in addition to PC (or both) may provide mechanical and chemical benefits to concrete, besides reducing its environmental impact (Damineli *et al.*, 2016; Knop and Peled, 2016b, 2016a; Varhen *et al.*, 2016; Shadkam *et al.*, 2017).

Another possibility to reduce PC in concrete is through the use of advanced mix-design techniques, such as particle packing models (PPMs). Studies have shown that the higher the packing density of granular systems such as concrete, the lower the material's porosity and thus cementitious materials required to fill the voids among the aggregate particles (Romano *et al.*, 2008; Castro and Pandolfelli, 2009; Noël, Sanchez and Fathifazl, 2016). Furthermore, the use of particles finer than cement (i.e. SCMs and or IF), may result in the reduction of the total porosity of the concrete due to the so-called filler effect (Romano *et al.*, 2008;

Castro and Pandolfelli, 2009) along with their contribution to the overall PC hydration due to the increase of nucleation sites (Lothenbach, Scrivener and Hooton, 2011). However, although the above strategies are widely known, eco-efficient concrete with a reduced amount of PC is currently not used for important structural applications, especially due to the lack of information on the fresh and hardened properties of low cement content (LCC) systems.

4.3. Background

4.3.1. Particle Packing Models (PPMs)

PPMs are used to optimize the particle size distribution (PSD) of granular systems such as concrete, resulting in the increase of the packing density ($Ø_p$) and reduction of the material's porosity. A number of factors may affect the packing density and porosity of concrete; however, the most important parameters are the size, shape and volume of the particles, along with the distance among them and their electrostatic interactions (Kawashima *et al.*, 2012; Kwan and Li, 2012; Aïssoun, Hwang and Khayat, 2016; Mehdipour and Khayat, 2017). The latter can be mostly controlled by a suitable selection of the PSD of the mixture.

There are two main types of PPMs: discrete and continuous. Discrete models consider "narrowly defined size classes of particles such as monodisperse, bimodal or even narrow size cuts of multimodal particles" (Brouwers and Radix, 2005). Therefore, discrete approaches refer to the packing of multimodal distributions containing "n" discrete size classes of particles, the so-called gap-graded systems. Continuous PPMs consider continuously sized particles available in the mixture (i.e. no gaps throughout the entire PSD). Furthermore, it assumes a similarity condition for particle packing, which means that the array of particles (i.e. "granulation image") surrounding every particle in the distribution should be similar, regardless the size of the particle(Mangulkar and Jamkar, 2013). The latter approach is considered compelling in concrete technology since most of the concrete components designed for conventional applications might be treated as continuous PSDs, at least in theory (Kwan, Chan and Wong, 2013).

4.3.2. Packing porosity

Cement content is directly proportional to the porosity found amongst the aggregates particles. Westman and Hugill developed an algorithm (Equation 4.1) to calculate the packing factor (PF) of granular systems based on PPM theories (Dinger and Funk, 1994). The PF is calculated according to Equation 4.2 and is considered the ratio between tightly packed and loosely packed systems (Dinger and Funk, 1994; Su, Hsu and Chai, 2001; Sebaibi *et al.*, 2013). According to the authors (Dinger and Funk, 1994), the PF is inversely proportional to the maximum apparent volume (V_a; true volume of particles) since V_a is directly proportional to the system porosity (Dinger and Funk, 1994).

$$V_{a1} = a_1 x_1 \qquad \textit{Equation 4.1}$$

$$V_{a2} = x_1 + a_2 x_2$$

$$V_{a3} = x_1 + x_2 + a_3 x_3$$

…

$$V_{ai} = \sum_{j=1}^{i-1} x_j \quad {}_1 + a_i x_i$$

Where a_i is the apparent volume of the i^{th} size particle in a monodisperse system, x_i is the mass fraction of i^{th} size particle, V_{ai} is the apparent volume of the mixture with n particle sizes, and n is the number of particle sizes.

$$PF = 1 - \left(\frac{1}{CSR}\right)^{0.37} \qquad \textit{Equation 4.2}$$

Where CSR is the class size ratio between two consecutive classes.

It is well-established that filling a volumetric space with monodisperse spherical particles results in approximately one-fourth of empty spaces (i.e. packing density around 75%). However, the latter approach is mainly theoretical since, in real life, granular systems rarely are made by completely spherical particles. Hence, in practice, $\emptyset_p$ lies between 60% and 64%

(Oliveira *et al.*, 2000). For that reason, the porosity of real granular systems can be calculated with the modified Westman and Hugill algorithm - Equation 4.3 (Dinger and Funk, 1994).

$$Porosity\ (\%) = \left(1 - \frac{1}{V_{a\ max}}\right) * 40\% \qquad \textit{Equation 4.3}$$

4.3.3. Mobility Parameters

Although the use of PPMs aims to increase the packing density and reduce the overall porosity of concrete mixtures, highly packed and low porosity systems may present some issues in the fresh state. For that reason, the sole use of PPMs is not enough while the mix-proportioning of low porosity systems and a discussion on the mobility of the particles is needed.

Two parameters have been proposed with the aim of explaining the mobility of granular systems: the *Interparticle Separation Distance* (IPS) and the *Maximum Paste Thickness* (MPT) (De Larrard and Belloc, 1997; Bonadia *et al.*, 1999; Innocentini *et al.*, 2003; Shadkam *et al.*, 2017). IPS is considered as the average distance between two adjacent particles smaller than 100-125 µm (Oliveira *et al.*, 2000). These small particles are normally separated by water and thus IPS can be understood as the thickness of the fluid amongst them. IPS can be calculated by Equation 4.4 (Dinger and Funk, 1994; Bonadia *et al.*, 1999; Innocentini *et al.*, 2003; Romano *et al.*, 2015; Shadkam *et al.*, 2017). It has been found that the lower the IPS, the lower the flowability of granular systems (i.e. the higher the viscosity and particles collisions). Conversely, high IPS yields less viscous, more flowable mixes (Oliveira *et al.*, 2000; Adamczyk, 2006; Castro and Pandolfelli, 2009).

$$IPS = \frac{2}{VSA}\left[\frac{1}{V_S} - \frac{1}{(1-P_{of})}\right] \qquad \textit{Equation 4.4}$$

Where IPS is the interparticle spacing, VSA is the calculated volume surface area per cubic centimetre of powder, V_s is the volume fraction fine solids (particles smaller than 125 µm), and P_{of} is the pore fraction assuming the densest packing of the fine particles.

MPT measures the maximum distance amongst aggregate particles greater than 125 µm (De Larrard and Belloc, 1997; Bonadia *et al.*, 1999; Innocentini *et al.*, 2003; Shadkam *et al.*, 2017). In MPT's case, particles greater than 125 µm are separated by the cement paste and it can be calculated by Equation 4.5. Likewise IPS, the higher the MPT the higher the flowability and the lower the viscosity of concrete mixtures.

$$MPT = \frac{2}{VSA_c}\left[\frac{1}{V_{sc}} - \frac{1}{(1-P_{ofc})}\right] \qquad \textit{Equation 4.5}$$

Where MPT is the distance between aggregates, VSA_c is the calculated volume surface area of aggregate (particles greater than 125 µm) fraction, V_{sc} is the volumetric aggregate solid fraction, and P_{ofc} is the pore of aggregate fraction assuming the densest packing.

4.3.4. Eco-efficiency in concrete

Although many studies investigate the mechanical properties of concrete, there is a lack of information regarding the eco-efficiency of the material. It is well known that PC is the main component responsible for most of greenhouse gases emitted during concrete production. Therefore, Damineli et al. (Damineli *et al.*, 2010) proposed the use of the binder intensity (bi) index, which is a parameter that classifies the eco-efficiency of concrete through the relationship between the amount of PC used (BC) to achieve one unit of targeted property (P), such as the 28-day compressive strength as highlighted in Equation 4.6.

$$bi = \frac{BC}{P} \qquad \textit{Equation 4.6}$$

Considering P as the compressive strength at 28 days, bi represents the amount of binder required to obtain 1 MPa of compressive strength.

4.4. Scope of the Work

The main objective of this work is to evaluate the influence of the amount of PC on the overall behaviour (i.e. fresh and hardened states) of low cement content (LCC) systems designed with different types and amounts of inert fillers. Three concrete mixtures

containing the same flow (i.e. 615 ± 5 mm) and with distinct cement contents (i.e., 54, 159 and 260 kg/m³) were designed and evaluated in the fresh (i.e. slump, mixing energy, and rheological behaviour) and hardened states (i.e. compressive strength, dynamic and static modulus of elasticity, porosity, and permeability). Comparison among the different results obtained from the distinct mixes is then performed.

4.5. Materials and Methods

4.5.1. Raw materials characterization

Three different LCC concrete mixtures were mix-designed for this research. The PC used in all mixes was a type HE "high early strength" from the Brazilian market (i.e. CPV-ARI) according to the National Brazilian Standard (NBR) 5733. The latter is similar to ASTM C150 type III cement (ASTM C150, 2018). Table 4.1. Chemical composition of the HE cement and fillers used.displays the chemical composition of the PC and inert fillers used.

Table 4.1. Chemical composition of the HE cement and fillers used.

Material	Contents (%)								Loss on Ignition (%)
	Na_2O	MgO	Al_2O_3	SiO_2	Fe_2O_3	SO_3	K_2O	CaO	
Cement	0.33	3.36	5.01	21.1	2.64	2.86	0.85	60.1	3.36
Filler Performance	-	43.1	0.59	1.94	<0.10	<0.10	<0.10	47.7	43.1
Filler Replacement	-	41.2	0.4	4.16	<0.10	<0.10	<0.10	47.5	41.2

Two types of limestone fillers (performance – P, composed by particles smaller than PC and; replacement – R, composed by particles similar to PC), two types of sand (natural sand with nominal maximum size (NMS) of 500 μm and manufactured limestone sand with NMS of 4.75 mm), and a limestone coarse aggregate from Sao Paulo, Brazil were used in the research. The materials were first quartered, ensuring a representative sampling, and then were fully characterized through specific gravity and superficial surface area (SSA) tests.

The specific gravity test was conducted through the helium gas (He) pycnometry test at a multipicnometer equipment, whereas the SSA was determined through BET method using

nitrogen gas (N_2) and water vapour (H_2O). The results of the above methods of each material are displayed in Table 4.2.

Table 4.2. Physical Materials Characterization.

Material	Mass (g)	Volume (cm^3)	Standard Deviation	Specific Gravity (g/cm^3)	Standard Deviation	SSA (m^2/g)
Cement	4.03	1.37	0.011	2.96	0.023	1.19
Filler P	3.76	1.38	0.006	2.72	0.013	3.48
Filler R	3.98	1.48	0.003	2.70	0.005	1.16
Fine Aggregate 1	6.63	2.51	0.007	2.64	0.007	0.26
Fine Aggregate 2	209.81	78.34	0.044	2.68	0.002	0.28
Coarse Aggregate 1	154.17	57.77	0.031	2.67	0.001	0.06
Coarse Aggregate 2	167.25	62.71	0.024	2.67	0.001	0.01

The particle size distribution (PSD) of all the materials mentioned above is shown in Table 4.3. The PSD of particles smaller than 350 µm were determined through the use of laser diffraction analysis while particles greater than 350 µm were characterized through dynamic image techniques.

Table 4.3. Materials Particle Size Characterization.

Material	D10	D50	D90	unit
Cement	2.27	13.01	30.44	µm
Filler P	0.89	3.6	9.5	µm
Filler R	1.58	9.76	27.43	µm
Fine Aggregate 1	0.18	0.3	0.5	mm
Fine Aggregate 2	0.03	1.11	4.33	mm
Coarse Aggregate 1	5.54	9.62	15.16	mm
Coarse Aggregate 2	17.58	26.4	35.44	mm

Two types of commercial chemical admixtures were also used in all mixes to guarantee an initial flow of 615 ± 5 mm: a lignosulfonate-based mid-range plasticizer and a polycarboxylate-based superplasticizer.

4.5.2. Mix-design procedure and calculations

Preliminary experimental works were performed to evaluate the optimum ratios between the two fine and coarse aggregates considering mobility aspects (i.e. increase of flowability

and decrease of friction among the particles for the same water demand). The best flowability found was through the use of 25:75 and 60:40 ratios for coarse (coarse 1 to coarse 2) and fine (fine 1 to fine 2) aggregates, respectively.

Three distinct LCC mixtures (i.e. 54, 159 and 260 kg/m^3) were mix-proportioned through the use of the mobility concepts prior presented in 2.3 (i.e. IPS and MPT). IPS and MPT were targeted to present minimum results of 0.13 µm and 1.6 µm, respectively. Prior preliminary studies using the same raw materials of the current research have demonstrated interesting flowability behaviour of mixtures designed with the targeted mobility parameters. No further mix-design techniques (i.e. PPMs, distribution factors) or considerations were used to proportion the present mixes. Furthermore, 1% of the fines mass of admixture was used in all tested mixtures, wherein 50% of it was a midrange plasticizer, and 50% of it was a polycarboxylate-based plasticizer.

Table 4.4 presents the final mix-design proportioned. It is worth noting that acronyms were given to the distinct mixes based on their cement contents (e.g. C54 means a mixture with 54 kg/m^3).

Table 4.4. Mix-design for the eco-efficient concrete mixtures.

Mixture Name	Cement (kg/m³)	F.A. (kg/m³)	C.A. (kg/m³)	Filler (kg/m³)	Water (kg/m³)
C54	54	833	1059	356	115
C159	159	820	1041	244	133
C260	260	810	1029	138	146
Mixture Name	**Mix-design (c : a : b : f)**		**Admixtures (kg/m³)**	**W/C**	**W/F**
C54	1 : 15.4 : 19.6 : 6.6		4	2.13	0.28
C159	1 : 5.1 : 6.5 : 1.5		4	0.84	0.33
C260	1 : 3.1 : 4.0 : 0.5		4	0.56	0.37

Note: c = cement, a = fine aggregate (F.A.), b = coarse aggregate (C.A.), f = filler, w/c = water to cement ratio, and w/f = water to fines ratio.

Table 4.5 presents the calculated porosity (section 2.2) and mobility parameters (section 2.3) of the concrete mixtures studied in this research program. It is worth noting that for every increase of 100 kg/m^3 of PC, IPS increased 0.04 µm while MPT increased 0.15 µm.

Table 4.5. Packing porosity and mobility properties of eco-efficient concrete mixtures.

Parameters	C54	C159	C260
Calculated porosity (%)	9.6	9.9	10.3
Specific surface area (m^2/g)	0.49	0.49	0.50
Volumetric surface area (m^2/cm^3)	1.32	1.34	1.36
Interparticle Separation Distance (μm)	0.13	0.17	0.20
Maximum Paste Thickness (μm)	1.6	1.7	1.9

4.5.3. Fabrication and testing methods

Fifteen litres of the three distinct concrete mixtures presented in 3.2 were mixed and their fresh state properties were then evaluated through rheological measurements. Moreover, ten 100 by 200 mm cylinders were fabricated from each mix. The specimens were demoulded after three days, ground and cured in saturated limewater at a controlled room temperature of 25 ± 2 °C. A week before the physical and or mechanical testing, the specimens were moved to a dry controlled chamber with a temperature of 23 ± 2 °C and humidity of 50 ± 4%.

4.5.4. Fresh state measurements

The fresh state properties of the three different mixes were assessed through rheological measurements using a planetary rheometer (Figure 4.1). The fresh state analyzes were divided into two parts. First, the mixing energy of the different mixes was evaluated. Therefore, the fine aggregates, inert fillers and PC were initially homogenized in the rheometer over 4 minutes. Then, water was added to the system and the materials were mixed for thirteen more minutes. Finally, the coarse aggregate was added to the system and the final mixture was mixed for another four minutes. Second, the viscosity of the different mixtures was assessed as a function of the torque applied. Thus, a stepwise increase/decrease in shear rate (in which the rotation speed increased from 35 rpm to 1380 rpm within a time lapse of 8 seconds and then decreased back to the original point within the same time period) was used according to Figure 4.2.

Figure 4.1. Planetary rheometer used to evaluate the fresh state properties.

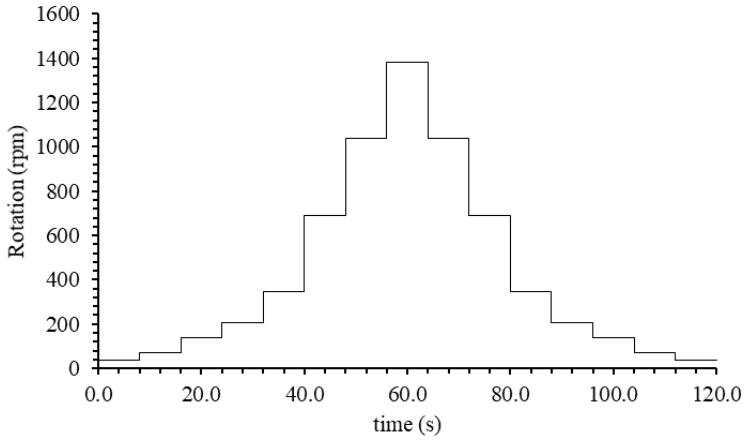

Figure 4.2. Shear history used to evaluate the fresh properties after the mixing stage.

4.5.5. Hardened state assessment

The hardened state analyses consisted of air permeability, dynamic and static modulus of elasticity, compressive strength and porosity. The test procedures were conducted at 14 and 28 days, except for the static modulus of elasticity, evaluated only at 28 days.

The air permeability test was performed according to the vacuum-decay method (Innocentini *et al.*, 2001, 2003, 2009; Romano *et al.*, 2015). First, the specimens were wrapped with a plastic film, except the top and bottom ends, to allow the uniaxial flux of air.

A suction cup was then attached to the top surface of the specimens with a caulk mass to prevent air leakage during the test. Next, an air pump was turned on until negative pressure stabilization. Finally, the pump was switched off, and the pressure drop was monitored and recorded as a function of time on the data acquisition (Figure 4.3).

a)  b) 

Figure 4.3. Air permeability test: a) Setup; b) Suction cup and surface of the specimen.

The results of the Darcian permeability constant (k_1) were determined from the Forchheimer equation (Equation 4.7), assuming negligible air-compressibility. The term $\mu.v_s/ k_1$ accounts for the viscous effects of the fluid-solid interaction, while the term $\rho.v_s/ k_2$ characterizes the inertial effects. It is worth noting that the Darcian permeability constant (k_1) accounts only for the linear portion ($\frac{\mu}{k_1} v_s$).

$$\frac{\Delta P}{L} = \frac{\mu}{k_1} v_s + \frac{\rho}{k_2} {v_s}^2 \qquad \textit{Equation 4.7}$$

Where L is the specimen thickness, ΔP is the pressure variation, μ is the fluid viscosity, ρ is the fluid density, v_s is the speed of air-percolation, k_1 and k_2 is the Darcian and non-Darcian permeability, respectively.

The dynamic modulus of elasticity was determined using the Portable Ultrasound Non-Destructive Digital Indicating Tester (PUNDIT). Transducers were placed on the ends of the specimens and the velocity of the ultrasonic wave was recorded from the average of four longitudinal measures per specimen. Then, the dynamic modulus of elasticity was calculated

from the velocity of the ultrasonic wave (m/s), specific mass of the concrete (kg/m³) and the dynamic Poisson coefficient.

The compressive strength test and modulus of elasticity were performed according to ASTM C 39 (ASTM C39, 1999) and ASTM C469 (ASTM C469, 2017), respectively.

The porosity of the specimens was determined from the Archimedes immersion method (Romano *et al.*, 2015). Ten slices of each specimen were cut, separated, weighed (dry mass - m_d) and classified according to their location (i.e. top, middle and bottom). Then, they were immersed in water and subjected to vacuum for the first two hours to ensure water penetration into the samples. After 24 hours, the values of immersed (m_i) and wet (m_w) mass were determined. The apparent porosity (AP) of each location was calculated by Equation 4.8.

$$\mathrm{AP}\ (\%) = \frac{m_w - m_i}{m_w - m_d} * 100\% \qquad \textit{Equation 4.8}$$

After that, the total porosity (TP) was calculated by *Equation 4.9*, considering the relative density (ρ_{rel}) of the concrete (Romano *et al.*, 2015).

$$\mathrm{TP}\ (\%) = (1 - \rho_{rel}) * 100\% \qquad \textit{Equation 4.9}$$

4.6. Results

4.6.1. Concrete mixing energy

It is worth noting that prior to the rheological evaluation, the flow test was performed in all mixtures to ensure the same initial consistency (i.e. 615 ± 5 mm). Then, rheological measurements were conducted in each of the mixtures with the aim of evaluating the mixing energy of each concrete mixture (Figure 4.4). Analyzing Figure 4.4 data one may notice that before adding water (i.e. fines mixing), all mixtures presented the same torque or mixing energy. Nevertheless, the addition of water (i.e. mortar phase) and also coarse aggregate (i.e. concrete phase) resulted in a much higher energy required to mix the mixtures. Moreover, one verifies that the lower the cement content, the higher the maximum and

final torques achieved while mixing, thus requiring higher mixing energy. The mix-energy obtained for C54, C159, and C260 were thus equal to 15824, 7455, and 3620 (N.m.s), respectively.

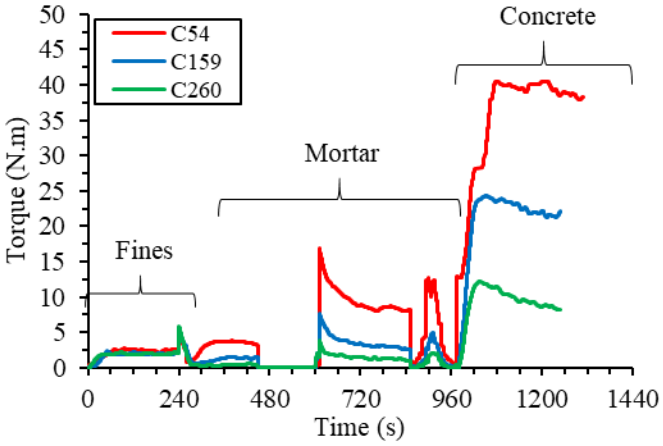

Figure 4.4. Rheological analysis of mortar and concrete mixture.

Figure 4.5 displays the torque vs rotation results of the three concrete mixtures studied. C54, C159 and C260 presented an initial torque approximately equal to zero, as expected since they presented a slump-flow of 615 ± 5 mm. Furthermore, C54 and C159 presented a shear thinning behaviour (i.e. decrease of viscosity as a function of torque) whereas C260 showed a linear relationship between torque and rotation and thus its viscosity did not change as a function of the torque applied.

The time dependence of all concrete mixtures was also evaluated. Normally, the time dependence behaviour of suspensions can be divided into two categories: thixotropy and rheopexy. Thixotropy is defined as the viscosity decrease as a function of a torque applied over time, while rheopexy is defined as the viscosity increase as a function of the torque applied over time (Han and Ferron, 2016; Ferraris *et al.*, 2017). Considering Table 4.6 results and evaluating the hysteresis loops observed in the torque-rotation curves, all concrete mixtures presented a rheopexy behaviour due to their positive hysteresis area (HA) values obtained (Filho *et al.*, 2016; Chauhan *et al.*, 2018). Finally, the apparent viscosity (i.e. ration between torque and rotation and the first deceleration point) was also appraised and showed to be directly proportional to PC content in the mix, as expected.

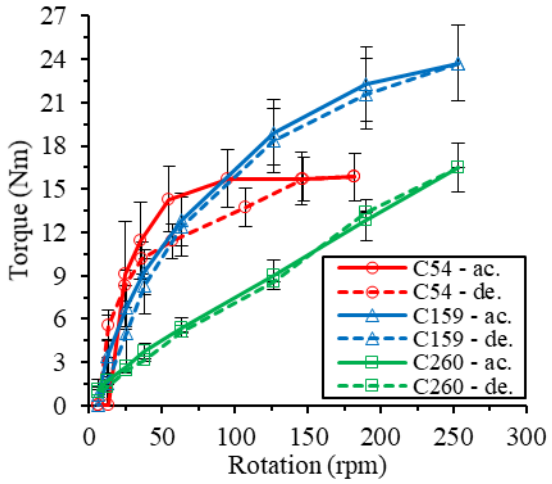

Figure 4.5. Hysteresis loop: ac. stands for acceleration and de. stands for deceleration.

Table 4.6. Rheological properties of eco-efficient concrete mixtures

Concrete	C54	C159	C260
Hysteresis Area (N.m.rpm)	238.56	160.10	27.74
Minimum Torque (N.m)	0.05	0.00	0.92
Apparent Viscosity (N.m/rpm)	0.11	0.11	0.07

4.6.2. Porosity

First of all, one may notice that the total porosity (TP) from a concrete sample is the summation of the capillary and gel pores found in the specimen, whereas the apparent porosity (AP) represents only the capillary pores. Both porosity types decrease as a function of PC hydration over time. From Figure 4.6, it can be seen that the 14-day TP does not change as a function of the cement content of the mixtures. Thus, a value of 9.88% (on average) was obtained regardless of the amount of cement. However, at 28 days, TP decreased with the increase of cement content, presenting a straight downward trend. The range of total porosity measured varied from 10.0 to 12.5, 9.6 to 9.1 and 10.0 to 8.5 for the C54, C159 and C260 mixtures, respectively at 14 and 28 days. It is worth noting that C54 showed a higher TP at 28 days which is somewhat unexpected and may be attributed to segregation and capillaries formation due to the high water to cement ratio.

Similarly to the TP at 28 days, the AP dropped steadily with the increase of CP content at 14 and 28 days. The 28-day AP is slightly lower than 14-day AP, as expected and as a result of the hydration process. C54, C159 and C260 decreased from 9.7 to 8.9%, 5.0 to 3.7%, and from 3.5 to 2.8%, respectively.

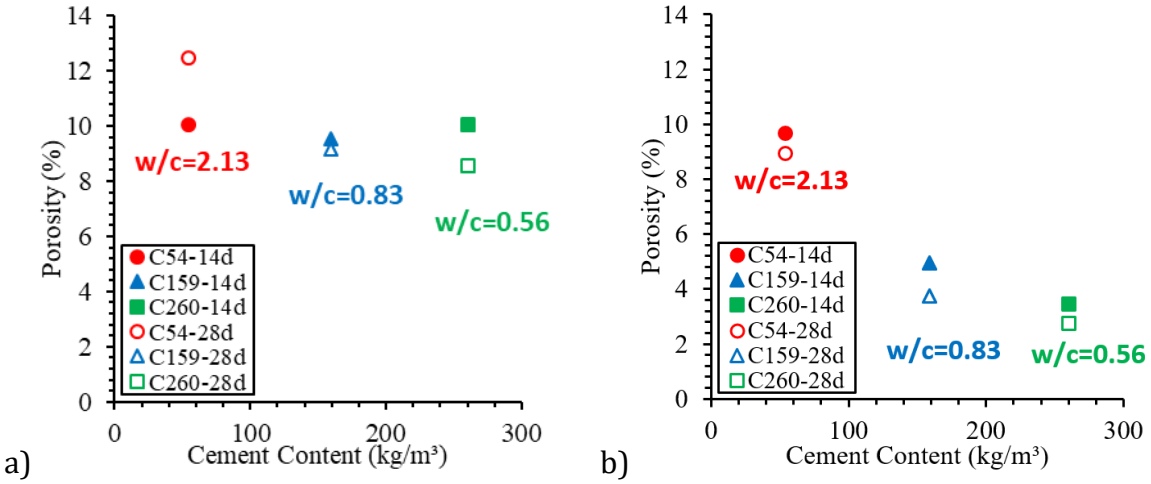

Figure 4.6. Average a) total porosity (TP) and b) apparent porosity (AP).

4.6.3. Compressive Strength

The 14 and 28-day compressive strength of the three concrete mixtures evaluated were correlated with their PC content and paste volume (Figure 4.7a and b respectively). Analyzing the data below, one notices that the higher the PC content and paste volume, and the lower the water to cement ratio, the higher the compressive strength. The compressive strength values ranged from 15 MPa for the C54 mix to 70 MPa for the C260

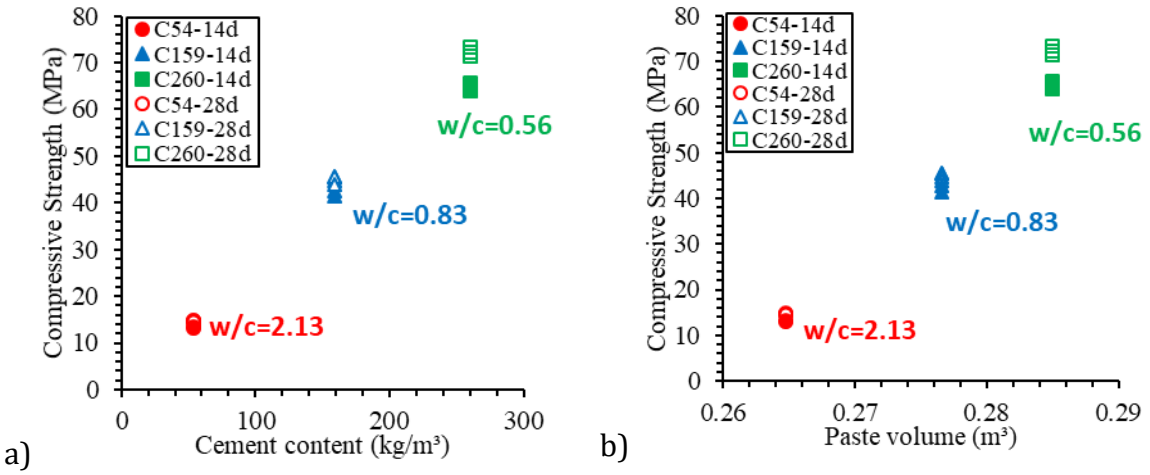

Figure 4.7. Correlation of compressive strength with a) cement content and b) paste volume.

4.6.4. Dynamic and static modulus of elasticity

First, the dynamic modulus of elasticity was performed at 14 and 28 days as described in the section 4.3.2. The correlation of dynamic modulus of elasticity with PC content and paste volume and the water to cement ratio is illustrated in Figure 4.8a and b, respectively. As for the compressive strength results, the stiffness of the mixtures measured by the dynamic modulus of elasticity increased with the increase of PC and paste content. The values gathered ranged from 33 GPa (C54) to 50 GPa (C260) according to their cement and paste content. Conversely, the higher the water to cement ratio the lower the dynamic modulus of elasticity of the mixes, as expected. The static modulus of elasticity was performed only at 28 days. The correlation between static modulus of elasticity and w/c ratio is shown in Figure 4.8c.

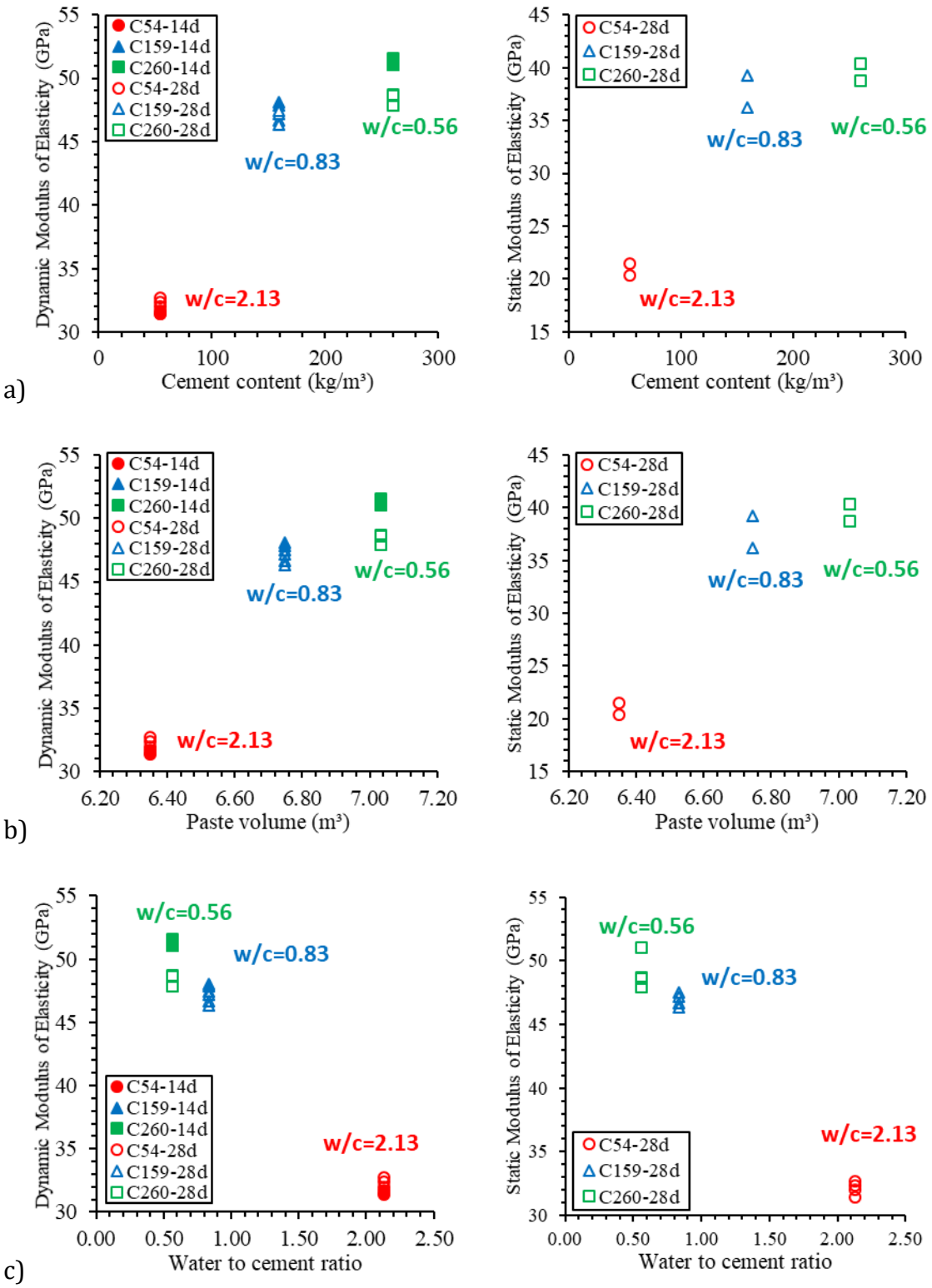

Figure 4.8. Correlation of Modulus of Elasticity with a) cement content b) paste volume, and c) w/c.

4.6.5. Air-Permeability

Figure 4.9 gives a plot on the influence of the permeability of the specimens at the top (Figure 4.9a) and bottom (Figure 4.9b) as a function of their cement content. It can be seen that concrete mixtures with 159 and 260 kg/m^3 of cement have approximately the same permeability response, while the concrete with 54 kg/m^3 (C54) is more permeable and thus presents a higher value both at the top and bottom; the latter is much more significant at the top. Moreover, C54 mix presented important permeability scatter between 14 and 28 days, especially at the top of the specimen, which likely indicates some segregation. Otherwise, this has not been found in the C159 and C260 mixes.

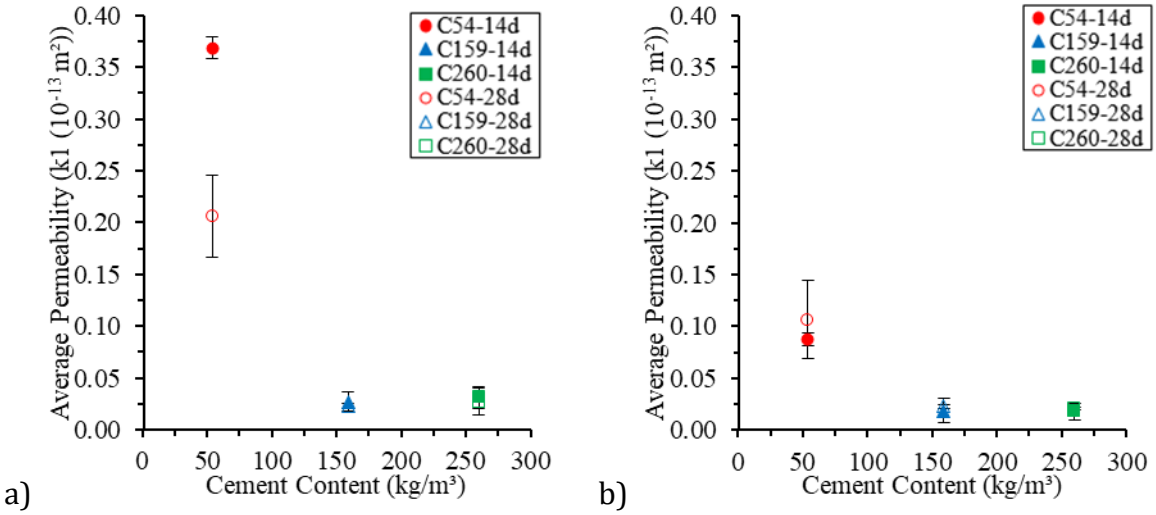

Figure 4.9. Effect of cement content on permeability a) specimen top and b) specimen bottom.

4.7. DISCUSSION

4.7.1. Fresh state behaviour

Most concrete mixtures are described in the literature following a Bingham rheological model (Equation 4.10), in which the relationship between shear stress and shear rate is linear (Bao, Lavrov and Møll Nilsen, 2017; Ferraris *et al.*, 2017).

$$\tau = \tau_0 + k_B\gamma \qquad \textit{Equation 4.10}$$

Where: τ is the torque, τ_o is the yield torque, k_B is the viscosity constant of Bingham, γ is the rotation.

However, Figure 4.10 clearly shows that C54 and C159 cannot be considered a Bingham suspension since the viscosity changes with the increase of torque applied. Both mixtures presented a shear-thinning behaviour which is normally recommended for concrete mixtures poured under high torque levels; e.g. pumped and or vibrated concrete (Pileggi and Pandolfelli, 2002).

In order to evaluate nonlinear suspension behaviours of cementitious materials, two models are generally used in the literature: Herschel-Bulkley (*Equation 4.11*) (Szilas, 1985; Nguyen *et al.*, 2006) and Ostwald-de Waele, also known as the power-law model (*Equation 4.12*) (Szilas, 1985; Alfani *et al.*, 2007).

$$\tau = \tau_0 + k_{HB}\gamma^n \qquad \textit{Equation 4.11}$$

Where: k_{HB} is the viscosity constant of Herschel-Bulkley and n is flow behaviour factor.

$$\tau = \tau_0 + \gamma^n \qquad \textit{Equation 4.12}$$

In the above models, suspensions with a shear thinning (pseudoplastic) behaviour must have $n < 1$, while suspensions with a shear thickening (dilatant) behaviour must have $n > 1$ (Bao, Lavrov and Møll Nilsen, 2017). Figure 4.10 illustrates the comparison between the three presented models previously mentioned and the deceleration segment of the three concrete mixtures studied. Assessing the scatter between the plots from the models and the data measured at the lab, one verifies that the Herschel-Bulkley model is the most accurate representation of the three concrete mixtures analyzed and thus may be used to describe LCC mixtures in the fresh state.

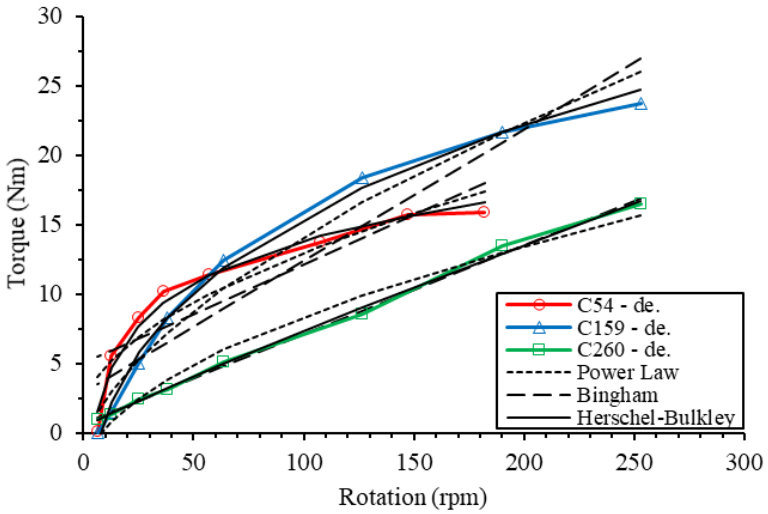

Figure 4.10. Rheological behaviour of the three concrete mixtures compared to distinct models.

Additionally, it is important to further discuss the mixing energy of the mixtures as a function of the mobility parameters adopted while their mix-designs. Interestingly, although the flow was set the same for all mixtures, different mixing energies were needed to reach the maximum torque and thus to enable flow to the distinct mixtures. Moreover, the energy required is directly associated with the IPS and MPT parameters calculated (Figure 4.11); i.e. the higher the IPS and MPT, the lower the viscosity and the energy required to the maximum torque.

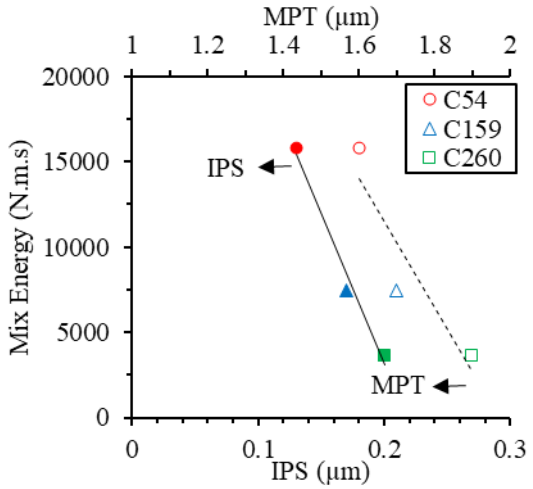

Note: Solid dots = IPS; empty dots = MPT

Figure 4.11. Correlation of mix energy and mobility parameters.

4.7.2. Hardened state behaviour

4.7.2.1. Porosity

It has been shown in Figure 4.6 that the apparent (capillary pores) and total (capillary + gel pores) porosity decrease at a function of PC content at 28 days, whereas PC amount does not seem to influence the total porosity at 14 days. Therefore, the difference between 14 and 28 days in apparent porosity was deemed to be further assessed. In order to do that, cylinders were fabricated from each of the LCC mixtures studied and sliced in three parts (top, middle, and bottom) so that visual observations along with apparent porosity measurements might be conducted (Figure 4.12 and Figure 4.13, respectively). Analyzing Figure 4.13, one attests that important segregation was found for C54 mix when compared to C159 and 260 at both 14 and 28 days. The latter could be easily verified while the AP measurements at both 14 and 28 days, especially for the top C54 specimen.

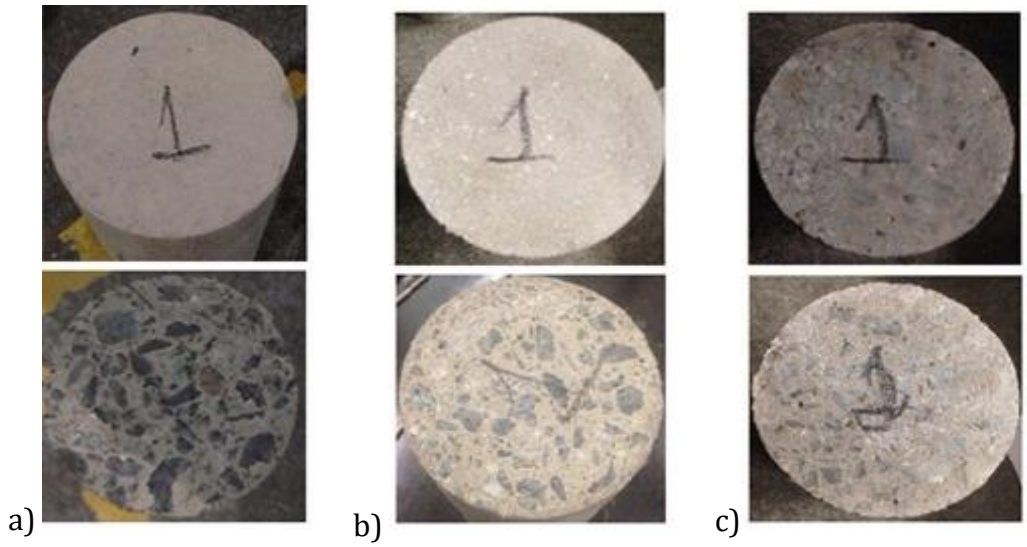

Figure 4.12. Segregation of specimens with different cement content a) C54, b) C159, and c) C260

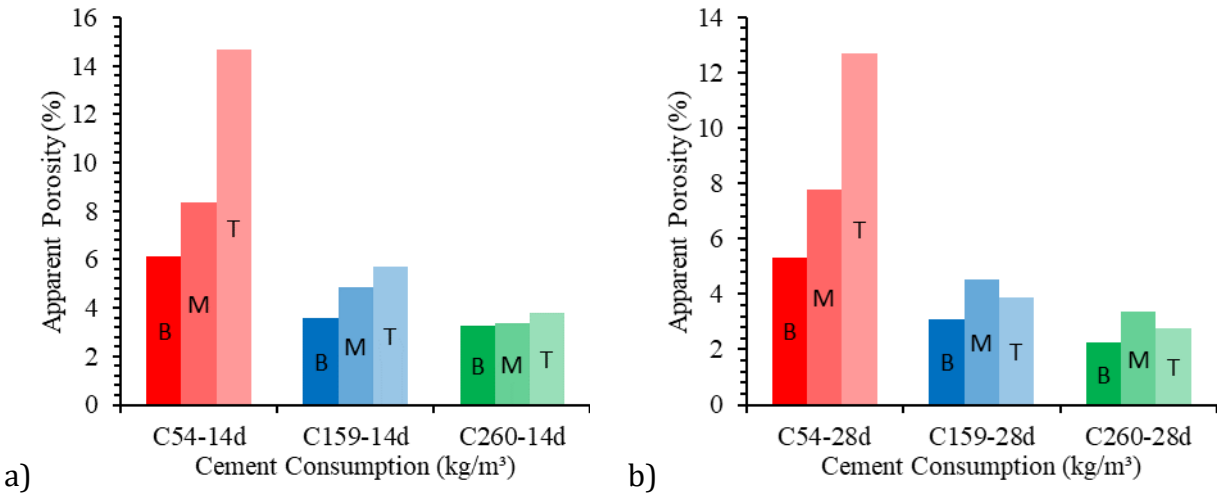

Figure 4.13. Relationship between apparent porosity and cement content a) 14-day and b) 28-day.

Moreover, as prior highlighted in 4.2., higher PC mixtures presented lower AP. The latter may be explained due to better compaction of lower viscosity system but also on the lower water to cement ratio of the higher PC content mixes.

4.7.2.2. Mechanical properties

It is well established that compressive strength of concrete mixtures is inversely proportional to their water to cement ratio (i.e. indirectly a measure of porosity) (Mehta and Paulo J. M. Monteiro, 2006; Helene and Tutikian, 2011; Han and Ferron, 2016; Ferraris *et al.*, 2017; Shadkam *et al.*, 2017). This relationship, known as Abrams' law (Abrams, 1918), is widely known for conventional concrete; however, it has been found that sometimes in highly packed systems with reduced amount of PC (e.g. lower than 200 kg/m^3), Abrams law is not the only parameter affecting the mechanical properties and should not be considered as the sole main parameter. Figure 4.14 evaluates the relationship between the hardened state properties assessed (e.g. compressive strength and modulus of elasticity) and other parameters linked to the materials microstructure such as permeability, total porosity, w/c, etc.

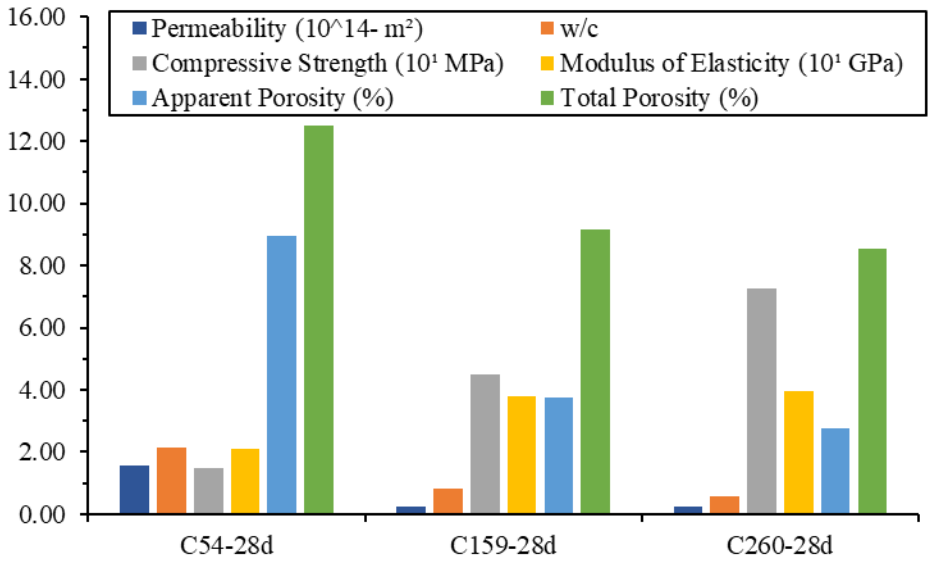

Figure 4.14. Comparison between compressive strength, modulus of elasticity, w/c, permeability, and porosity.

Analyzing Figure 4.14, one observes that although Abrams may not be considered the sole main factor affecting the behaviour of LCC systems, it still seems to control the mechanical properties performance and microstructure features of all mixes, since the higher the water to cement ratio, the lower the stiffness and compressive strength and the higher the porosity (total and apparent) and permeability of the mixtures. Furthermore, some of the microstructure features of the mixtures could also be attributed to the mobility parameters, especially the MPT, that although being greater for mixes with higher PC contents, has led to lower overall porosity than mixes containing much lower amounts of PC which should enhance their durability-related properties, especially the ones governed by transport mechanisms.

4.7.3. Eco-efficiency of concrete

Damineli (Damineli *et al.*, 2010; Damineli and John, 2012) proposed the use of the bi factor to assess the eco-efficiency of concrete mixes. The authors attested that worldwide, conventional concrete mixtures (e.g. 20 to 40 MPa) are normally produced with high amounts of PC and thus produce bi factors greater than 10.0 kg/m^3. MPa^{-1}. Evaluating the

mixes designed in this work and plotting those in the global record provided by Damineli *et al.* (2010), one verifies that the three mixtures studied in this research may be considered eco-efficient concrete and are located below the bottom line of 250 kg/m^3. Furthermore, the bi factors obtained were close to 3.6 kg.m^3.MPa^{-1} for all mixes (Figure 4.15), which attests the possibility of producing high-performance mixtures with reduced environmental impact.

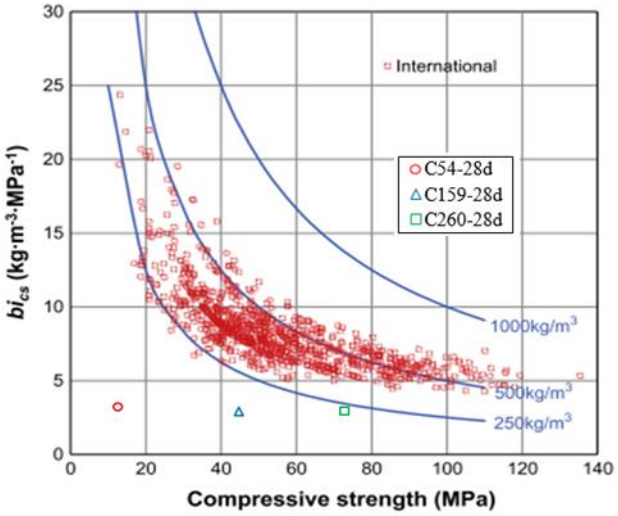

Figure 4.15. Relationship between binder intensity and compressive strength at 28-days (international records) *(Damineli* et al*., 2010)*.

4.8. CONCLUSION

The main goal of the present research program was to better understand the effect of PC content on the fresh and hardened properties of LCC systems. The primary conclusions of the work are presented hereafter:

- The use of the mobility parameters to mix-design LCC mixes without considering any PPM technique seems to be promising and should be further evaluated in the future.
- All the LCC mixtures studied in this work presented a shear thinning behaviour and thus might be used in applications under high torque regimes such as pumped and/or vibrated concrete. Yet, their rheological behaviour and mixing energy were fairly

distinct which emphasizes the inefficiency of the slump test to forecast the rheological behaviour of concrete under different torque regimes.

- Previous studies have highlighted that the sole use of Abrams law is not enough to explain the hardened state behaviour of densely packed mixtures with reduced PC amount. Therefore, Abrams law empirical parameters should be different than conventional concrete to evaluate and forecast highly packed concrete mixtures.
- The fresh state, mechanical properties and eco-efficiency of PPMs mix-designed concrete seems quite interesting. However, the long-term behaviour of LCC systems with high amounts of filler and reduced PC content is still unknown and should be further investigated.

4.9. ACKNOWLEDGMENTS

The authors gratefully acknowledge the financial support from the University of Ottawa for the international experience scholarship, Mitacs for the Mitacs Globalink Research Award, CGS – Master's – NSERC, Laboratory of Microstructure and Material Eco-efficiency – LME and CNPq - National Council for Scientific and Technological Development (research grant - 155357/2016-6). Special thanks to Heitor Montefusco and Jose Mesquita for the help.

4.10. REFERENCES

Abrams, D. A. (1918) Design of Concrete Mixtures. Chicago.

Adamczyk, Z. (2017) Particles at interfaces: interactions, deposition, structure. Second, Potential Interactions Among Particles. Second. London : Academic Press.

Aïssoun, B. M., Hwang, S. D. and Khayat, K. H. (2016) 'Influence of aggregate characteristics on workability of superworkable concrete', Materials and Structures/Materiaux et Constructions, 49(1–2), pp. 597–609.

Alfani, R. et al. (2007) 'The use of the capillary rheometer for the rheological evaluation of extrudable cement-based materials'.

ASTM C150 (2018) 'Standard Specification for Portland Cement'. West Conshohocken.

ASTM C39 (1999) ‘Standard Test Method for Compressive Strength of Cylindrical Concrete Specimens’, ASTM C39, American Society for Testing and Materials.

ASTM C469 (2017) ‘Standard Test Method for Static Modulus of Elasticity and Poisson’s Ratio of Concrete in Compression’. West Conshohocken.

Bao, K., Lavrov, A. and Møll Nilsen, H. (2017) ‘Numerical modeling of non-Newtonian fluid flow in fractures and porous media’, Comput Geosci, 21, pp. 1313–1324.

Bonadia, P. et al. (1999) ‘Maximum paste thickness (MPT) principle applied to high alumina refractory castables’, Cerâmica. Associação Brasileira de Cerâmica, 45(291), pp. 24–28.

Brouwers, H. J. H. and Radix, H. J. (2005) ‘Self-compacting concrete: the role of the particle size distribution’, in First International Symposium on Design, Performance and Use of Self-Consolidating Concrete SCC’2005. Changsha, China, pp. 109–118.

Castro, A. K. and Pandolfelli, V. C. (2009) ‘Review: Concepts of particle dispersion and packing for special concretes production’, 18 Cerâmica, 55, pp. 18–32.

Cesar De Oliveira Romano, R. et al. (2015) ‘Impact of aggregate grading and air-entrainment on the properties of fresh and hardened mortars’.

Chauhan, G. et al. (2018) ‘Rheological studies and optimization of Herschel-Bulkley flow parameters of viscous karaya polymer suspensions using GA and PSO algorithms’, Rheologica Acta, 57, pp. 267–285.

Damineli, B. L. et al. (2010) ‘Measuring the eco-efficiency of cement use’, Cement and Concrete Composites, 32, pp. 555–562.

Damineli, B. L. et al. (2016) ‘Viscosity prediction of cement-filler suspensions using interference model: A route for binder efficiency enhancement’, Cement and Concrete Research, 84, pp. 8–19.

Damineli, B. L. and John, V. M. (2012) ‘Developing Low CO2 Concretes: Is Clinker Replacement Sufficient? The Need of Cement Use Efficiency Improvement’, in Key Engineering Materials. Trans Tech Publications, pp. 342–351.

Dinger, D. and Funk, J. (1994) Predictive process control of crowded particulate suspensions. 1st edn. Edited by S. S. + B. M. LLC. New York.

Ferraris, C. F. et al. (2017) ‘Role of Rheology in Achieving Successful Concrete Performance’, (June), pp. 43–51.

Filho, R. S. A. et al. (2016) ‘Evaluating the applicability of rheometry in steel fiber reinforced self-compacting concretes’, Ibracon structures and materials journal, 9(6), pp. 969–988.

Han, D. and Ferron, R. D. (2016) 'Influence of high mixing intensity on rheology, hydration, and microstructure of fresh state cement paste', Cement and Concrete Research, 84, pp. 95–106.

Helene, P. and Tutikian, B. F. (2011) 'Dosagem dos Concretos de Cimento Portland', in Cechella Isaia, G. (ed.) Concreto: Ciência e Tecnologia. 1st edn. São Paulo: Ibracon, pp. 415–451.

Innocentini, M. et al. (2001) 'Effect of particle size distribution on the drying behavior of refractory castables', Ceramica, 47(304).

Innocentini, M. D. et al. (2009) 'Permeability optimization and performance evaluation of hot aerosol filters made using foam incorporated alumina suspension', Journal of Hazardous Materials, 162, pp. 212–221.

Innocentini, M. D. M. et al. (2003) 'PSD-Designed refractory castables', Am. Ceram. Soc. Bull., 82(7), p. 9401–9406.

Juenger, M. C. G. and Siddique, R. (2015) 'Recent advances in understanding the role of supplementary cementitious materials in concrete', Cement and Concrete Research, 78, pp. 71–80.

Kawashima, S. et al. (2012) 'Study of the mechanisms underlying the fresh-state response of cementitious materials modified with nanoclays'.

Knop, Y. and Peled, A. (2016a) 'Packing density modeling of blended cement with limestone having different particle sizes', Construction and Building Materials. Elsevier Ltd, 102, pp. 44–50.

Knop, Y. and Peled, A. (2016b) 'Setting behavior of blended cement with limestone: influence of particle size and content', Materials and Structures, 49, pp. 439–452.

Kwan, A. K. H., Chan, K. W. and Wong, V. (2013) 'A 3-parameter particle packing model incorporating the wedging effect', Powder Technology, 237, pp. 172–179.

Kwan, A. K. H. and Li, L. G. (2012) 'Combined effects of water film thickness and paste film thickness on rheology of mortar', Materials and Structures, 45, pp. 1359–1374.

De Larrard, F. and Belloc, A. (1997) 'The influence of aggregate on the compressive strength of normal and high-strength concrete', ACI Materials Journal, 94(5), pp. 417–426.

Limbachiya, M., Bostanci, S. C. and Kew, H. (2014) 'Suitability of BS EN 197-1 CEM II and CEM V cement for production of low carbon concrete', Construction and Building Materials, 71, pp. 397–405.

Lothenbach, B., Scrivener, K. and Hooton, R. D. (2011) 'Supplementary cementitious materials', Cement and Concrete Research, 41, pp. 217–229.

Makul, N. and Sua-Iam, G. (2018) 'Effect of granular urea on the properties of self-consolidating concrete incorporating untreated rice husk ash: Flowability,

compressive strength and temperature rise', Construction and Building Materials, 162, pp. 489–502.

Mangulkar, M. N. and Jamkar, S. S. (2013) 'Review of Particle Packing Theories Used For Concrete Mix Proportioning', International Journal Of Scientific & Engineering Research, 4(5).

Mehdipour, I. and Khayat, K. H. (2017) 'Effect of particle-size distribution and specific surface area of different binder systems on packing density and flow characteristics of cement paste', Cement and Concrete Composites. Elsevier Ltd, 78, pp. 120–131.

Mehta, P. K. and Monteiro, P. J. M. (2006) Concrete: Microstructure, Properties, and Materials. McGraw-Hill.

Nguyen, V. H. et al. (2006) 'Flow of Herschel–Bulkley fluids through the Marsh cone', J. Non-Newtonian Fluid Mech, 139, pp. 128–134.

Noël, M., Sanchez, L. and Fathifazl, G. (2016) 'Recent Advances in Sustainable Concrete for Structural Applications', in Sustainable Construction Materials & Technologies 4, p. 10.

Oliveira, I. R. et al. (2000) Dispersão e Empacotamento de Partículas. São Paulo: Fazendo Arte Editorial.

Pileggi, R. G. and Pandolfelli, V. C. (2002) 'Rheology and particle size distribution of pumpable refractory castables', Cerâmica, 48(305), pp. 11–16.

Romano, R. C. O. et al. (2008) 'Influence of the dispersion process in the silica fume properties', Cerâmica, 54, pp. 456–461.

Sebaibi, N. et al. (2013) 'Composition of self compacting concrete (SCC) using the compressible packing model, the Chinese method and the European standard', Construction and Building Materials, 43, pp. 382–388.

Shabab, M. E. et al. (2016) 'Synergistic Effect of Fly Ash and Bentonite as Partial Replacement of Cement in Mass Concrete', Korean Society of Civil Engineers, 20(5), pp. 1987–1995.

Shadkam, H. R. et al. (2017a) 'An investigation of the effects of limestone powder and Viscosity Modifying Agent in durability related parameters of self-consolidating concrete (SCC)'.

Shadkam, H. R. et al. (2017b) 'An investigation of the effects of limestone powder and Viscosity Modifying Agent in durability related parameters of self-consolidating concrete (SCC)', Construction and Building Materials, 156, pp. 152–160.

Su, N., Hsu, K.-C. and Chai, H.-W. (2001) 'A simple mix design method for self-compacting concrete', Cement and Concrete Research, 31, pp. 1799–1807.

Szilas, A. P. (ed.) (1985) Developments in Petroleum Science.

Varhen, C. et al. (2016) ‘Effect of the substitution of cement by limestone filler on the rheological behaviour and shrinkage of microconcretes’, Construction and Building Materials, 125, pp. 375–386.

Wen, Z. et al. (2016) ‘Design and Preparation of High Elastic Modulus Self-compacting Concrete for Pre-stressed Mass Concrete Structures’, Journal of Wuhan University of Technology.

Zachar, J. and Asce, M. (2011) ‘Sustainable and Economical Precast and Prestressed Concrete Using Fly Ash as a Cement Replacement’, J. Mat. in Civil Engineering, 23(6), pp. 789–792.

Chapter Five: Summary and Conclusion

There is currently a misconception in the concrete industry which states that the amount of binder, often measured by the Portland cement (PC) content, is directly proportional to the material's strength. Furthermore, PC is the most expensive concrete constituent and presents the largest carbon footprint of the material. Over the last decades, numerous strategies were developed to decrease PC content and thus the environmental impact of concrete. Amongst those, the use of scientific mix-design techniques, the so-called particle packing models (PPMs) and mobility parameters (MP) showed promising results.

In this research, high packing density LCC concrete mixtures were mix-proportioned through advanced mix-design techniques (i.e. PPMs – Chapter 3 and MP – Chapter 4) and evaluated in the fresh (i.e. slump, flow, mixing energy and rheological behaviour) and hardened (i.e. compressive strength, modulus of elasticity, porosity, and permeability) states. Chapter 3 shows the evaluation of six eco-efficient concrete mixtures proportioned through the use of PPMs (i.e. Alfred model – using 1 or 2 q factors) and presenting PC contents of about 150, 200, and 270 kg/m^3. Chapter 4 presents the appraisal of three eco-friendly mixes designed with the use of MP and presenting PC contents of 54, 159, and 260 kg/m^3. Although the above research projects were developed with distinct mix-design techniques, the main objective was to design eco-efficient mixes without compromising the material's fresh and hardened states. The main findings of this research program are presented hereafter:

- Eco-efficiency

  Although literature shows that very few concrete mixtures are produced worldwide with PC contents lower than 250 kg/m^3, this research program has proved that it is possible to produce concrete with reduced amount of PC and suitable fresh and

hardened state properties. All concrete mixes developed throughout this project can be considered eco-efficient since the bi factors obtained from all of them were lower than 5kg/m^3. MPa^{-1} and approximately equal to 3.4 kg/m^3. MPa^{-1} on Chapter 3 and 4, respectively.

- Mix-design techniques

  High densely packed and eco-efficient concrete mixtures may be achieved through the use of PPMs (Chapter 3) and/or using mobility parameters (Chapter 4). Yet, the latter should be further assessed in the future in order to develop a standardized mix-design approach.

- Rheological behaviour

  The results obtained in this research showed that all LCC mixtures appraised presented a shear thinning behaviour (i.e. decrease of viscosity as a function of torque), independently of the PC content and the w/c. Shear thinning (or pseudoplastic) is the recommended behaviour for concrete mixtures poured under high torque levels (e.g. pumped and or vibrated concrete). Although for many of them the slump measurement was exactly the same, analyzing their mixing energy, one may notice that the mixing energy was substantially distinct among the mixes due to the change of PC content (i.e. the lower PC content, the higher mixing energy). Moreover, the inefficiency of the slump test to estimate the overall rheological behaviour of concrete mixtures under different torque regimes was highlighted.

- Compressive strength

  The results demonstrated that the amount of PC does not directly influence the compressive strength of LCC concrete. Moreover, it has been found that only the use of Abrams law is not enough to forecast the mechanical properties of LCC and densely packed mixtures, as highlighted in previous research. Yet, the water to fines ration (w/f) was deemed to be a promising parameter to support w/c in the evaluation of hardened state properties of LCC systems.

Chapter Six: Recommendations for future research

After conducting this research, further investigations can be drafted, as presented hereafter:

- Microscopic analysis must be performed on LCC concrete mixtures with distinct mix-proportions to understand the mechanism of failure of high-density LCC systems. Moreover, the impact of the MPT_{coarse} on the mechanical properties of concrete mixtures with reduced amount of PC still needs to be further evaluated;
- An in-depth evaluation of the durability-related properties of densely packed LCC systems should be performed. Moreover, the long-term behaviour of LCC systems with high amounts of inert filler is still unknown and should be assessed;
- An evaluation of the impact of aggregate features (i.e. shape, texture and hardness) on the porosity fresh state properties or LCC is still lacking.
- Appraisal of the structural behaviour of LCC concrete, especially under shear loads to evaluate the influence of high densely packed systems on aggregate interlock behaviour.
- Develop a quality control protocol for PPMs and/or high densely packed systems.